Multi-parametric Cardiac Magnetic Resonance Imaging and Arrhythmic Risk Stratification in Fabry Disease

---

by

Ravi Vijapurapu

BMed Sci (Hons), MBChB, MRCP (UK)

Student ID: [redacted]

A thesis submitted to the University of Birmingham for the degree of

DOCTOR OF PHILOSOPHY

Institute of Cardiovascular Sciences

School of Medical and Dental Sciences

University of Birmingham

June, 2022

Abstract

Fabry disease is an X-linked lysosomal storage disorder, with cardiovascular manifestations including progressive LVH, chronic myocardial inflammation, fibrosis, congestive cardiac failure, arrhythmia and sudden death. Despite widely available Fabry specific therapies, cardiac involvement has a significant prognostic impact and is still the leading cause of morbidity and mortality in FD. Thus early identification of cardiovascular involvement is key to enable initiation of therapy at the earliest opportunity and prevent progressive cardiomyopathy. The main aims of this thesis are:

1) To characterise the stages of cardiovascular disease and potential mechanisms for arrhythmia in FD;
2) To quantify the burden of arrhythmia and consequent therapy usage in FD e.g. cardiac device implantation.

This thesis has provided a significant insight into Fabry cardiomyopathy. The use of CMR tissue characterisation, feature tracking techniques and advanced ECG analysis has shown great promise not only in the detection of early cardiac involvement, but also in potentially predicting adverse clinical outcomes. Risk stratification and early therapy is crucial in reducing morbidity and mortality in Fabry disease and this thesis has provided a platform to provide this information and gain a better understanding of the complex pathophysiology in this rare disease.

Dedication

To my extraordinary wife, Mitra, and my late father, Lakshman.

Acknowledgements

The work presented in this thesis has been achieved under the supervision of Professor Richard Steeds (Consultant Cardiologist), Dr Tarekegn Geberhiwot (Consultant in Inherited Metabolic Disorders) and Professor Dipak Kotecha (Consultant Cardiologist) at the University Hospital Birmingham NHS Foundation Trust. I am extremely grateful for the invaluable support and exceptional mentorship of my lead supervisor Professor Richard Steeds. His guidance and intellectual input with each component of this thesis has enabled me achieve all targets throughout my research and to ensure that these studies have been a success.

I would also like to thank the collaborators I worked with during this thesis: Dr Rebecca Kozor, Dr Maren Maanja, Dr Todd Schlegel and Dr Martin Ugander, whose expertise facilitated my understanding of the complex concepts of advanced electrocardiography; and Dr Sabrina Nordin and Dr Joao Augusto, who supported with recruitment of patients within London. I would like to express my appreciation to Mr James Hodson and Dr Peter Nightingale for their statistical advice throughout this thesis. Further thanks to my friends, colleagues and co-researcher's Dr Anna Price, Ms Heather Small, Dr Shanat Baig and Dr Boyang Liu for their continued support and friendship. I would like to recognise the support of the Society for Mucopolysaccharide Diseases for awarding me a grant during my first year and also to the Fabry patients for their voluntary involvement in further our understanding of Fabry cardiomyopathy.

Finally, I would like to thank my wife Mitra for her infinite support, guidance and understanding during this research. She has encouraged me to persevere despite personal challenges and without her encouragement and stability none of my achievements would have been possible.

Extent of personal contributions

The work presented within this thesis is my own with the following exceptions described below. The original project hypothesis incorporating the RaILRoAD study was designed by Professor Richard Steeds and Dr Tarekegn Geberhiwot. The overall thesis outline and individual component studies were further developed together with my supervisors over the course of this research period. Ethical approval for the RaILRoAD study was obtained by myself from the Research Ethics Committee and Health Research Authority. Recruitment and consent of all patients to this study was carried out by myself with the support of the departmental lead research nurse, Heather Small. I collected all retrospective data from clinical service for all aspects of this thesis and obtained local research and development registration for the individual component studies. Ethical and sponsor approval for the Fabry400 study was obtained by the chief investigator and lead research fellow in London, Professor James Moon and Dr Sabrina Nordin. Local study set up and registration at UHB was carried by myself with the support and guidance of Dr Shanat Baig. I recruited and consented patients to Fabry400 within UHB.

Cardiac magnetic resonance imaging (CMR) was performed by myself as part of clinical service, with the support of clinical radiographers and Professor Richard Steeds. I performed the study transthoracic echocardiography scans during routine clinic attendance. Recruitment of healthy volunteers was from a separate study set up by Dr Stefania Rosmini at the Bart's Heart Centre in London. Demographic and CMR DICOM data were provided for inclusion within this thesis. All CMR and echo analysis was performed by myself, with reproducibility assessments carried out by Dr Anna Price and Dr Boyang Liu. Advanced ECG data analysis was carried out by myself under the supervision of Dr Todd Schlegel at the Space EKG headquarters in Switzerland. I performed all statistical analysis with support from Dr Peter

Nightingale and Mr James Hodson. Dr Maren Maanja provided guidance for statistical analysis of the advanced ECG data.

All manuscripts were drafted and edited by myself with guidance and input from my supervisors Professor Richard Steeds and Dr Tarekegn Geberhiwot.

Table of Contents

List of Figures

List of Tables

List of Abbreviations

2D	Two dimensional
3D	Three dimensional
95% CI	95% confidence intervals
A-ECG	Advanced ECG
AF	Atrial fibrillation
AGAL-A	α-Galactosidase A
AHA	American Heart Association
AI	Artificial intelligence
Anti-TLR4	Anti-toll-like receptor-4
ATP	Anti-tachycardia pacing
AUC	Area under the receiver operating characteristic curve
AV	Atrioventricular
AVNRT	Atrioventricular nodal re-entry tachycardia
BMI	Body mass index
BSA	Body surface area
CCS	Canadian Cardiovascular Society
CD	Cardiac device
CKD	Chronic kidney disease
CoV	Coefficient of variance
CMR	Cardiac magnetic resonance imaging
CMR-FT	CMR feature-tracking
CRT	Cardiac resynchronisation therapy
ECG	Electrocardiogram

ECV	Extracellular volume
eGFR	Estimated glomerular filtration rate
ERT	Enzyme replacement therapy
ESC	European Society of Cardiology
FA	Flip angle
FD	Fabry disease
FLASH	Fast low angle shot
FoV	Field of view
FT	Feature-tracking
Ga3	Galabiosylceramide
Gb3	Globotriaosylceramide
GLA	Galactosidase-alpha
GLS	Global longitudinal strain
GTI	Indexed global wall thickness
GWT	Global wall thickness
HCM	Hypertrophic cardiomyopathy
HF	Heart failure
HLA	Horizontal long axis
Hs-Troponin	High sensitive troponin
HV	Healthy volunteers
ICC	Intra-class correlation
ICD	Implantable cardioverter defibrillator
IHD	Ischaemic heart disease
ILR	Implantable loop recorder
IQR	Interquartile range

LGE	Late gadolinium enhancement
LVEF	Left ventricular ejection fraction
LVH	Left ventricular hypertrophy
LVMi	Indexed left ventricular mass
LVPW	Left ventricular posterior wall
LysoGB3	Globotriaosylsphingosine
MOLLI	Modified Look-Locker Inversion
MSSI	Mainz Severity Score Index
MVA	Malignant ventricular arrhythmia
MWT	Maximum wall thickness
NSVT	Non-sustained ventricular tachycardia
NYHA	New York Heart Association
OCT	Oral chaperone therapy
PPM	Permanent pacemaker
PSIR	Phase sensitive inversion recovery
QRSd	QRS duration
RaILRoAD	Role of Implantable Loop Recorders in Anderson-Fabry Disease
ROI	Regions of interest
RV	Right ventricular
RWT	Relative wall thickness
S1P	Sphingosine-1-phosphatase
SAM	Systolic anterior motion
SAPPHIRE	Saturation Pulse Prepared Heart rate independent Inversion Recovery

SASHA	Saturation recovery Single Shot Acquisition
SAX	Short axis
SC	Standard care
SCD	Sudden cardiac death
SD	Standard deviation
ShMOLLI	Shortened Modified Look-Locker Inversion
SSFP	Steady-state free precession
STE	Speckle-tracking echocardiography
SVD	Singular value decomposition
SVT	Supraventricular tachycardia
TIAs	Transient ischaemic attacks
TE	Echo time
TR	Repetition time
TTE	Transthoracic echocardiography
VCG	Vectorcardiogram
VLA	Vertical long axis
VT	Ventricular tachycardia
VUS	Variant of unknown significance
XCI	X-chromosome inactivation

1. Introduction

Fabry disease (FD) is an X-linked lysosomal storage disorder that was first described by Johann Fabry and William Anderson in 1898. The primary genetic defect, however, was only identified in 1963 with over 1000 mutations now described (1-3). These pathogenic variants in the galactosidase-alpha (GLA) gene, located on the Xq22.1 chromosome locus, result in a deficiency or absence of the enzyme α-Galactosidase A (AGAL-A) (4). This causes progressive accumulation of sphingolipids in a number of tissues across the body (5), resulting in widespread cellular dysfunction and life-threatening cardiovascular, renal and neurological complications (6).

1.1 Epidemiology

The incidence of FD is thought to be estimated around 1:40,000 in men and 1:117,000 across the general population (5,7). This however, is likely to be an under-estimate as the presenting symptoms vary in severity and are non-specific, leading to difficulties in diagnosis. Targeted screening has shown that a higher prevalence of FD can be found in patients with unexplained cardiovascular, renal or cerebrovascular disease. For example, 3-4% of patients with sarcomeric hypertrophic cardiomyopathy (HCM), 1% of patients with unexplained left ventricular hypertrophy (LVH) (8-10) and, up to 5% of patients with cryptogenic stroke (11) have been found to have genetically confirmed FD. Newborn screening in some areas has also suggested a prevalence of up to 1 in 8,800 newborns (12).

Improved awareness of the disease together with cheaper diagnostic tests that are more widely available has also led to increased investigation of symptomatic and asymptomatic individuals and more frequent cascade screening of family members. Consequently, the prevalence of FD in the Western World has been reported as high as 1 in 2500, with a

significant rise occurring in the United Kingdom (UK) population (13). There has also been a shift in the natural course of the disease over recent years and as a result of increased availability of renal replacement therapy, mortality due to renal failure has drastically reduced and cardiovascular disease has now replaced chronic kidney disease as the leading cause of morbidity and mortality (4).

1.1 Pathophysiology

AGAL-A is a lysosomal exoglycohydrolase, which facilitates the hydrolytic cleavage of galactose residues occurring within glycosphingolipids. An absence or deficiency in this enzyme leads to an intracellular accumulation of un-metabolised glycosphingolipids with a terminal alpha-galactosyl moiety, in particular globotriaosylceramide (Gb3), galabiosylceramide (Ga2) and the deacylated form of Gb3, globotriaosylsphingosine (lysoGb3), *Figure 1.1* (14-18). Consequently, these un-metabolised substrates accumulate in microvascular endothelial cells, smooth muscle cells and fibroblasts of various organs across the body (19). Intracellular accumulation is known to begin in utero and is believed to be the pathogenic trigger for clinical manifestations (20,21).

Figure 1.1. Metabolic pathway for Gb3: a schematic illustration of the degradation pathway for globotriaosylceramide (Gb3) (14,15)

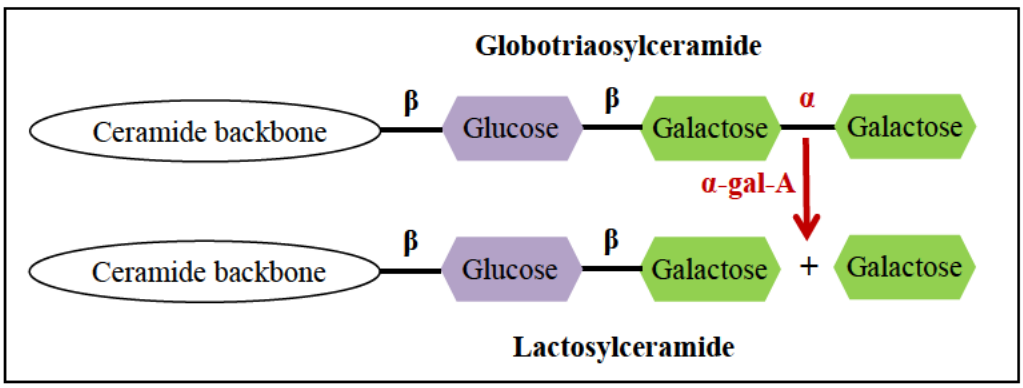

Over 1000 genetic variants have been identified within the GLA gene and have been classified as: 1) pathogenic, 2) benign variants without clinically significant manifestations, or 3) benign variants of unknown significance. Nonsense and missense mutations resulting in low or absent AGAL-A activity usually lead to the classic early-onset FD, which is typically characterised by onset of symptoms during childhood, with multi-organ involvement and rapid disease progression (22,23). Missense mutations, in which there is a degree of residual AGAL-A enzyme activity present, tend to result in a later onset FD that is often organ specific and thus termed non-classical. These classical and non-classical variations will be discussed in greater detail later.

From a cardiovascular perspective Gb3 accumulates in all cell types, including myocytes, endothelial and smooth muscle cells of myocardial vasculature, endocardium, valvular fibroblasts and the conduction tissues (22,24). Direct effects of Gb3 accumulation can lead to localised tissue effects, but this does not explain the whole spectrum of FD pathophysiology (25). In combination with the mechanical primary processes caused by sphingolipid deposition, activation of secondary pathways can lead to widespread biological and functional impairment (26,27). *Figure 1.2* demonstrates these secondary processes.

Figure 1.2. Secondary molecular pathways that occur in FD. Taken from Pieroni et al (22).

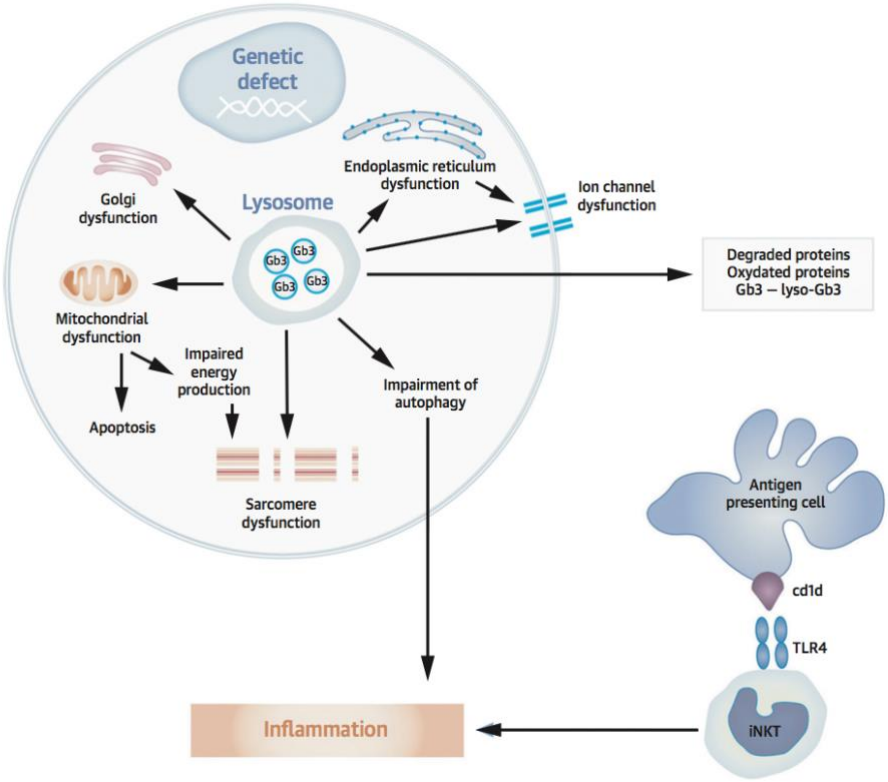

Lysosomes have multiple roles within the cellular microenvironment. These include storing and releasing apoptotic enzymes, trafficking organelles, sensing nutrients and repairing mitochondria. Studies have shown that an increased intra-lysosomal Gb3 can reduce endocytosis and autophagy, induce apoptosis and affect mitochondrial activity (28). The accumulation of Gb3 within lysosomes can directly affect cellular lipid metabolism, which in turn will have a direct effect on the composition the cell membranes, including the inner mitochondrial membrane (28). This can interfere with mitochondrial energy production and thus mitochondrial energy depletion in combination with trophic factors, such as sphingosine, can trigger the activation of myocyte hypertrophic response pathways (22,29). Additionally, in vitro studies of cardiomyocytes have shown that intracellular glycosphingolipid can also directly cause sarcomeric myofilament dysfunction and myofibrillolysis (30). Sphingosine-1-phosphatase (S1P) is an active growth factor found within the plasma of Fabry patients and

due to its involvement in proliferative mechanisms has been hypothesised to be involved in cardiac remodelling within FD (31). In vitro studies have shown that introduction of S1P can initiate myocyte hypertrophy (31) and in clinical studies S1P correlated significantly with progression of left ventricular hypertrophy (LVH) (32).

It is widely suggested that fibrosis and Gb3 deposition within the myocardial conduction tissues can lead to electrical abnormalities (33,34) An in vitro study by Birkett et al (35) found enhanced sodium and calcium ion channel activity in cardiomyocytes derived from pluripotent stem cells, which led to higher and shorter spontaneous action potentials in FD. They further hypothesised that lipid deposition within lysosomes may cause changes in this cellular ion channel expression and cell membrane trafficking, thus affecting the electrochemical properties of the cardiac conduction tissue. This has, to some degree, been suggested as a potential causative factor for early changes seen on the resting 12-lead electrocardiogram such as a shortened PR interval without the presence of a pre-excitation conduction pathway (19,33).

Recent research utilising novel cardiac magnetic resonance imaging techniques has supported previous in vitro work highlighting the central role of inflammation in the pathogenesis of FD (36,37). Rozenfeld et al (38) hypothesised that Gb3 and lyso-Gb3 themselves may act as lipid based antigens activating invariant natural killer T cells, leading to a chronic inflammatory phase and ensuing autoimmunity. They also demonstrated a reduction in this sphingolipid mediated effect, following the introduction of anti-toll-like receptor-4 (anti-TLR4) antibodies, which act to block this inflammatory activation, thus highlighting the key role of inflammation in FD (38,39).

There does not seem to be an established causal link between the degree of residual enzyme activity, measured plasma levels of Gb3 and lyso-Gb3 and the occurrence of clinical outcomes. For example, despite heterozygote females having a significant level of residual enzyme, their clinical presentation can vary from asymptomatic to severe organ involvement (40). On the other hand, hemizygotes (carrier of one mutant allele) who have complete absence of enzyme activity can have evidence of Gb3 at birth or even in utero but do not develop phenotypic features of FD until later in life, suggesting that Gb3 either does not cause immediate adverse effects or may not even be pathogenic. This may help to explain why enzyme replacement therapy (ERT) can normalise Gb3 levels within cardiac endothelium but may not necessarily prevent serious adverse consequences, such as sudden cardiac death (41,42).

Although specific mutations have been identified within the AGAL-A gene, there are a multitude of genetic variants, all of which have varying effects on enzyme activity (13). This has complicated any attempt to establish a clear genotype-phenotype relationship and when combined with potential modifier genes and environmental influences, can lead to an extremely variable clinical presentation, even within the same family.

1.2 Clinical Presentation

Patients can present with a wide range of clinical manifestations, varying between severe organ involvement in males to asymptomatic disease in female patients, with a spectrum of disease presentations in between. Although the age of onset can be variable, males appear to show greater consistency in the age at which phenotypic changes can develop, with dermatological and gastrointestinal symptoms starting as early as the first decade of life (43). Although once thought to only be heterozygote carriers of the disease with no significant

disease activity, X-chromosome inactivation (XCI) occurs in females, where there is random transcriptional silencing of the unaffected X-chromosome leading to hemizygotic females having a similar profile of symptoms as male patients, with major organ involvement and associated morbidity/mortality (44,45). This XCI can be random or skewed and recent literature has shown that women with random XCI tend to have symptoms that are milder in severity with a slower rate of progression (46), but do go on to develop the full phenotype of symptoms with progressive cardiac disease, arrhythmia and renal failure. The symptom presentation in women with skewed XCI is largely dependent on the expressed allele, where early symptom onset, rapid progression of disease and adverse outcomes are associated with a predominant expression of the mutant GLA allele (44,47).

1.2.1 Classical vs. non-classical variations

As described earlier, the level of residual enzyme activity varies depending on the specific mutation, and this subsequently determines the clinical presentation of individual patients. Terms such as classical phenotype and non-classical or late-onset phenotypes are widely used as the pattern of disease progression and prognosis between these two groups does differ significantly (48).

Patients with classical FD tend to have more widespread and severe clinical signs and often have very low or complete absence of AGAL-A activity (less than 1% enzyme activity) (49), thus usually presenting earlier during childhood. Early manifestations include acroparesthesia, heat intolerance, angiokeratomas (*Figure 1.3a*), cornea verticillata (*Figure 1.3b and c*), gastrointestinal symptoms and microalbuminuria. Acroparesthesia, an extremely common early clinical finding, presents as episodic pain, pins and needles or a burning sensation, occurring particularly within the hands and feet (50). Hypohidrosis (inability to

appropriately sweat) and heat intolerance are also frequent early symptoms of classical FD (51). Major organ involvement develops over time, often as early as 20-30 years of age, and includes renal, cardiac and cerebrovascular complications often leading to premature death (52-54). *Table 1.1* describes the presenting features of classical FD.

Renal involvement is extremely common and this often manifests as microalbuminuria, often occurring as early as childhood in classical FD (55,56). By the second or third decade of life overt proteinuria is usually present and is associated with a predictable decline in glomerular filtration rate, with male patients developing overt renal failure by 40-50 years of age (55,57). Neurological involvement can include acute cerebrovascular events, such as transient ischaemic attacks (TIAs) and strokes, vestibulocochlear dysfunction, cerebral white matter lesions and peripheral neuropathy (58,59). Ischaemic strokes occur in early and advanced FD, with a prevalence as high as 48% in men and 32% in women (60). Although the precise pathophysiology is not known, vascular endothelial Gb3 accumulation has traditionally been thought to play a role in its aetiology (61). Recent literature, however, has shown that the rate of asymptomatic paroxysmal atrial fibrillation in advanced FD is high, suggesting that thromboembolic disease may be a more significant factor that previously thought (62). Cardiac manifestations of FD will be discussed in detail later.

Figure 1.3. Clinical manifestations of classical Fabry disease. Taken from Zampetti et al (63) and van der Tol et al (64).

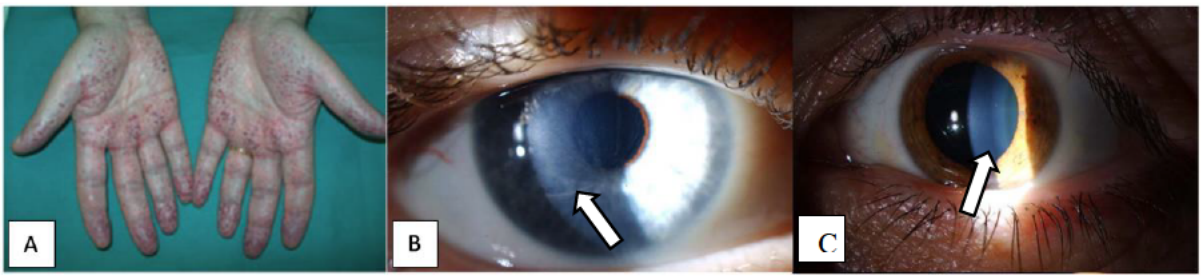

Panel A – Angiokeratomas: *an accumulation of Gb3 in dermal endothelial cells leads to incompetence and consequent dilation of the vasculature (63). This causes bulging lesions to form on the skin, which commonly occur in clusters on the torso, upper thighs and genital area.*

Panel B and C – Cornea verticillata: *also termed vortex keratopathy, occurs when there are deposits within the basal epithelium of the cornea (demonstrated by arrow on images). These form a faint vortex pattern of whitish lines, which usually occur within the inferior cornea. The precise cause is unclear, but some histological specimens have suggested diffuse accumulation of sphingolipid within the cornea may lead to this ocular manifestation (64,65).*

Table 1.1. Clinical features of Fabry disease. Adapted from Linhart et al (43)

System	Clinical Manifestation
Dermatological	Angiokeratoma Hypohidrosis Lymphoedema Coarse facial features
Cardiac	LVH Diastolic dysfunction Arrhythmia Heart failure
Renal	Microalbuminuria/proteinuria Renal failure
Gastrointestinal	Diarrhoea Early satiety Abdominal discomfort
Pulmonary	Airway obstruction

	Decreased diffusion capacity
Neurological	Neuropathic pain (acroparesthesia) Painful febrile crises Autonomic and small fibre dysfunction TIA/stroke Vertigo/tinnitus/hyperacusis, sudden deafness
Ophthalmic	Cornea verticillata Tortuous retinal vessels
Other	Anaemia Decreased bone density

Some Fabry patients have residual enzyme activity and thus only tend to have reduced plasma AGAL-A levels, which can vary between 2 and 30%. Due to this residual enzyme, this group of patients tends to have few or none of the classical features associated with FD and have been described as having a 'non-classical' phenotype (49). Disease presentation is often more indolent and symptoms occur much later in life (often between 40-50 years of age), usually affecting only one organ system. Terms such as 'cardiac variant' or 'renal variant' are commonly used depending on the organ involved, with specific gene mutations associated with each subtype. *Table 1.2* shows the cardiac variant group of gene mutations (22,66). Diagnosis of non-classical variants is often made incidentally during investigation for unexplained organ disease e.g. LVH, arrhythmia, proteinuria and renal impairment.

Table 1.2. GLA mutations commonly associated with the cardiac variant of FD. Adapted from Patel et al (66).

Location	Nucleotide Change	Protein Sequence Change
Exon 5	c.644 A>G	N215S
Exon 6	c. 886 A>G	M296V
Exon 6	c.835 C>G	Q279E
Exon 6	c.902 G>A	R301Q
Exon 6	c.888 G>A	M296I
Exon 1	c.58 G>C	A20P
Exon 2	c.5171 T>C	I91T
Exon 2	c.5236 T>C	F113L
Exon 2	c.334 G>A	R112H

Exon 6	c.982 G>A	G328R
Intron 4	IVS4+919 G>A	-

1.2.2 Cardiovascular involvement in Fabry disease

Myocardial tissue can be susceptible to low plasma AGAL-A levels and consequently the cardiac variant is the most common of the non-classical phenotypes. Cardiac involvement occurs in up to 78% of patients (67) with a mean age of onset of 29 years in males and 34 years in females (52). Cardiac manifestations have been documented as the presenting feature leading to a diagnosis of FD in 13% of males and 10% of females (68,69) and include progressive LVH, chronic myocardial inflammation (36), fibrosis, congestive cardiac failure, arrhythmia and sudden death (52). Despite Fabry specific and symptomatic cardiac therapies being widely available, cardiac involvement has a significant prognostic impact and is still the leading cause of morbidity and mortality in FD (69).

1.2.2.1 Cardiac symptoms

Cardiovascular symptoms occur often in FD patients, but they are non-specific. Shortness of breath has been reported early on in the disease process even before overt cardiac involvement is present. It can be a result of increasing myocardial mass, impaired ventricular filling and a dilated left atrium, all of which are signs of ventricular diastolic dysfunction.

Fatigue and exercise intolerance are also highly prevalent but poorly understood. Impairment in exercise capacity has been described even in the absence of severe cardiac disease. A number of studies utilising cardiopulmonary exercise testing and 6-minute walk tests, have shown significant impairment in $VO2_{max}$ or peak oxygen uptake during exercise (70-72). They also describe a reduced duration and distance of exercise in FD patients when compared to healthy volunteers. The precise mechanisms for their exercise intolerance remains unclear. Sphingolipid deposition within the cardiac and systemic conduction systems, leading to

autonomic dysfunction and a blunted heart rate/blood pressure response, however, have been hypothesised as a potential cause of the limited exercise tolerance observed in FD (70).

Palpitations and syncope are common symptoms occurring in up to 50% of women and 75% of men on ERT (52,73). In the general population, ambulatory Holter monitoring (usually over 24, 48 or 72 hours) can be used to identify those needing further investigation. Given the frequency of these symptoms in FD however, symptomatic status can lose specificity for identifying those at risk of arrhythmia, although the presence of red flag symptoms should prompt further investigation. However, given the risk of malignant ventricular arrhythmia and sudden death in FD (73), alternative rhythm monitoring modalities must be considered, and will be discussed in more detail throughout this thesis.

Chest pain is a frequently occurring symptom in Fabry patients and angina has been described to occur in up to 25% of Fabry patients (74), with a similar prevalence in men and women. Typical atherosclerotic coronary disease, however, is uncommon and the myocardial ischaemia leading to anginal symptoms in Fabry patients is often multifactorial (*Figure 1.4*) (74,75).

Figure 1.4. Mechanisms of impaired coronary blood flow in Fabry disease. Adapted from Roy et al (74).

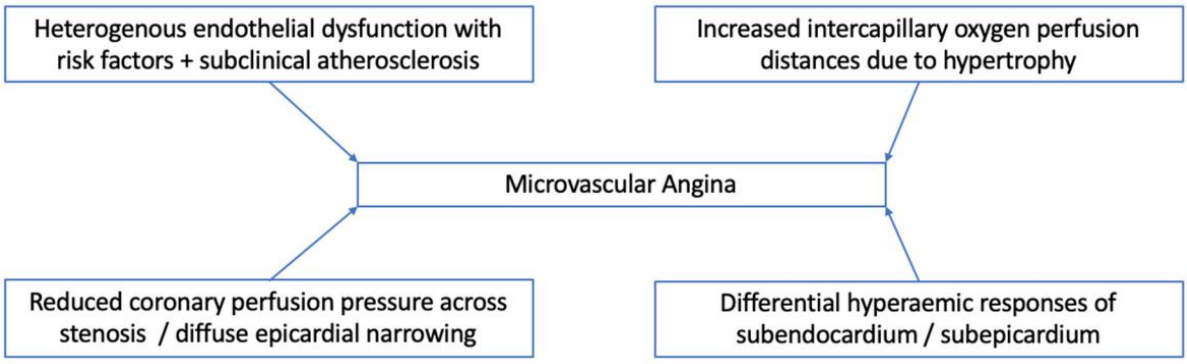

Symptoms of heart failure are less common and tend to occur with more advanced Fabry cardiomyopathy, where an advanced 'burnt-out' dilated cardiomyopathy phenotype develops. At this point symptoms such as orthopnoea, paroxysmal nocturnal dyspnoea and peripheral oedema are managed with standard heart failure therapies.

1.2.2.2 Clinical signs of cardiac involvement

1. Left Ventricular Hypertrophy

LVH is the primary clinical feature typically associated with cardiac involvement in FD and has been reported in 43% of male patients and 26% of females (69,76). Men tend to present earlier and progress more rapidly than women, however the prevalence of LVH is known to increase with advancing age (23). LVH is defined as increased total cardiac mass or elevated wall thickness greater than 12mm as measured by transthoracic echocardiography (TTE) or cardiac magnetic resonance imaging (CMR). Typically the pattern of LVH seen in FD is symmetrical with concentric hypertrophy, but in a small proportion of cases (usually females) eccentric and apical myocardial thickening can also be seen (*Figure 1.5*).

Figure 1.5. Transthoracic echocardiography images demonstrating various patterns of LVH. Images taken from Kromen et al (77), Mihl et al (78) and Hughes et al (79).

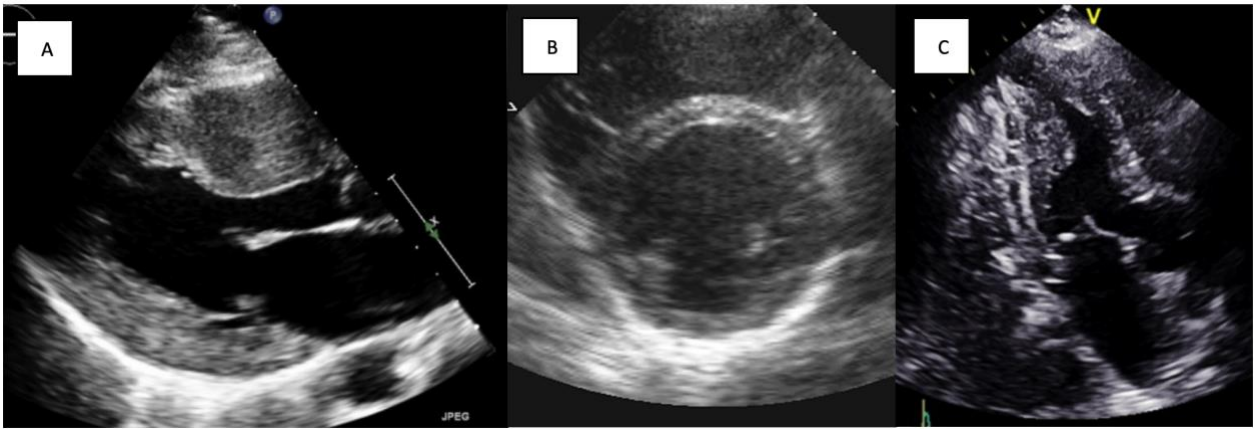

Panel A – *Parasternal long axis image demonstrating concentric LVH with increased septal and posterior wall thickness.*

Panel B – *Parasternal short axis image showing eccentric hypertrophy.*

Panel C – *Apical three chamber view demonstrating apical hypertrophy.*

Although common, LVH is not specific for Fabry cardiomyopathy and a number of systemic acquired and inherited causes exist (*Table 1.3*) (7). After LVH has been identified, a structured assessment with detailed clinical review and targeted investigations are crucial in identifying the precise cause of hypertrophy. Clinical history may quickly exclude more common causes such as hypertension and increased body mass index (BMI), and further evaluation with cardiac imaging and biochemical blood markers can help identify rarer inherited causes.

Table 1.3. Acquired and inherited causes of LVH. Adapted from Yousef et al (7).

ACQUIRED	
Disease process	**Mechanism**
1) Mechanical	
Hypertension	Increased afterload
Aortic stenosis	Increased afterload
LV outflow tract obstruction	Increased afterload
Obesity	
2) Physiological	
Athletic heart	Normal physiological response
3) Myocardial infiltration	
Haemochromatosis	Iron overload, infiltrative
Myocarditis	Inflammation, myocardial oedema
Sarcoidosis	Systemic inflammatory disease
INHERITED	
Disease process	**Mechanism**
1) Myocardial infiltration/abnormalities	
Amyloidosis (familial ATTR)	Systemic deposition of amyloid fibrils
AL amyloidosis	Systemic deposition of amyloid fibrils
Hypertrophic cardiomyopathy	Sarcomere protein disease
2) Metabolic disorders	
Fabry disease	Lysosomal storage disorder, sphingolipid deposition
Pompe disease	Glycogen storage disorder
Danon disease	Lysosomal glycogen storage disease
PRKAG2 cardiomyopathy	Lysosomal glycogen storage disease
Primary carnitine deficiency	Fatty acid oxidation disorder
3) Mitochondrial disorders	
MELAS	
MERFF	
4) Syndromic conditions	
Noonan's syndrome	Growth hormone mutation
Freidrich's ataxia	Autosomal recessive, mutation of protein involved in mitochondrial iron metabolism

With FD, sphingolipid deposition occurs in all cardiac cell types and myocyte hypertrophy and vacuolation occurs, with subsequent triggering of the hypertrophic response. This can be seen in *Figure 1.6*.

Figure 1.6. Sphingolipid deposition within valvular fibroblast and myocytes.

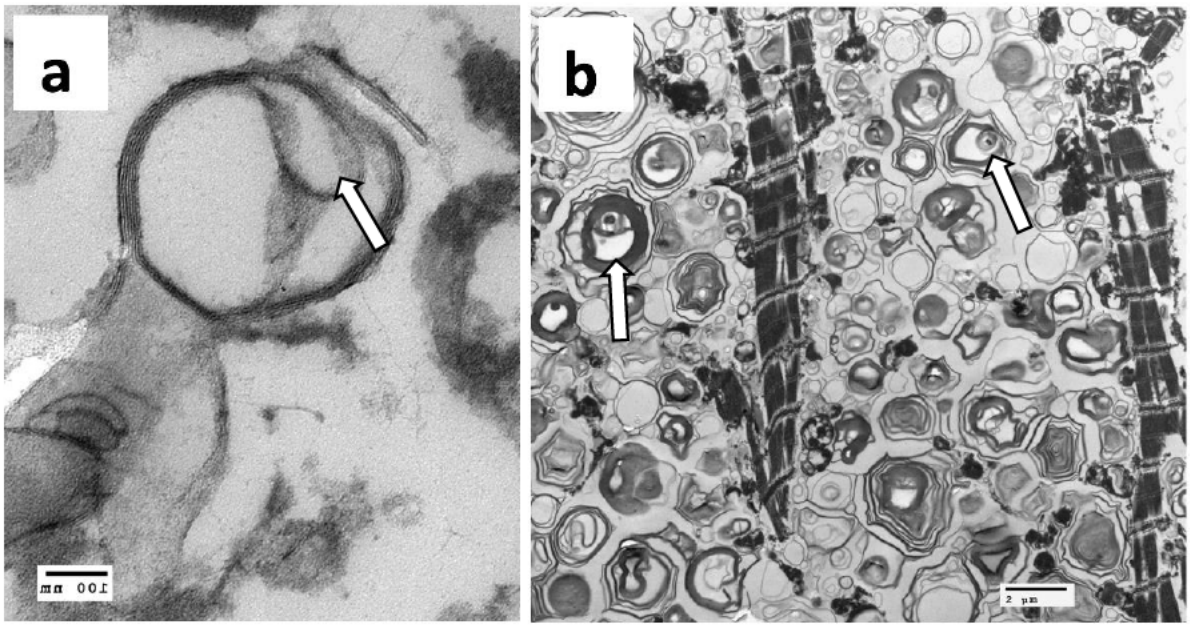

Panel A. Whorl in cell in valve fibroblast. *The residual part of a concentrically lamellated structure (zebra body) seen within a valvular fibroblast. [Transmission electron micrograph; original magnification x 68,000]. See arrow.*

Panel B. Cardiac muscle (low magnification). *Cardiomyocyte containing numerous cytoplasmic lamellated structures (zebra bodies), separating and displacing myofibrils, which is characteristic of Fabry disease. [Transmission electron micrograph; original magnification x 4,800]. See arrow.*

Images provided by Dr T Geberhiwot and Dr A Warfield, University Hospital Birmingham.

Even though LVH is a common finding in cardiac FD, in vitro chemical extraction studies have demonstrated that the amount of sphingolipid deposited is unrelated to the extent of myocardial hypertrophy, with only 1-3% of the total myocardial mass demonstrating Gb3 deposition (80). This suggests that Gb3 accumulation does not immediately cause phenotypic effects and that multiple pathways may be involved in the hypertrophy found in FD. As described earlier, as well as Gb3, other trophic and growth stimulating factors such as lyso-

Gb3 and S1P have been identified as key components in cardiac remodelling and activation of the hypertrophic response (31,81). The various mechanisms suggested can be seen in *Figure 1.2 and 1.7.* Although the precise pathophysiology of LVH is unclear, a number of theories have been described as potential causative mechanisms: 1) direct toxic effect of Gb3 causing oxidative stress and upregulation of cell adhesion molecules leading to small vessel coronary ischaemia (29) or disruption of mitochondrial energy metabolism (82,83); and 2) inflammatory and neurohormonal dysregulation (84,85).

Figure 1.7. Metabolic pathways involved in the hypertrophic response in the development of cardiovascular complications in FD. Taken from Baig et al. (13).

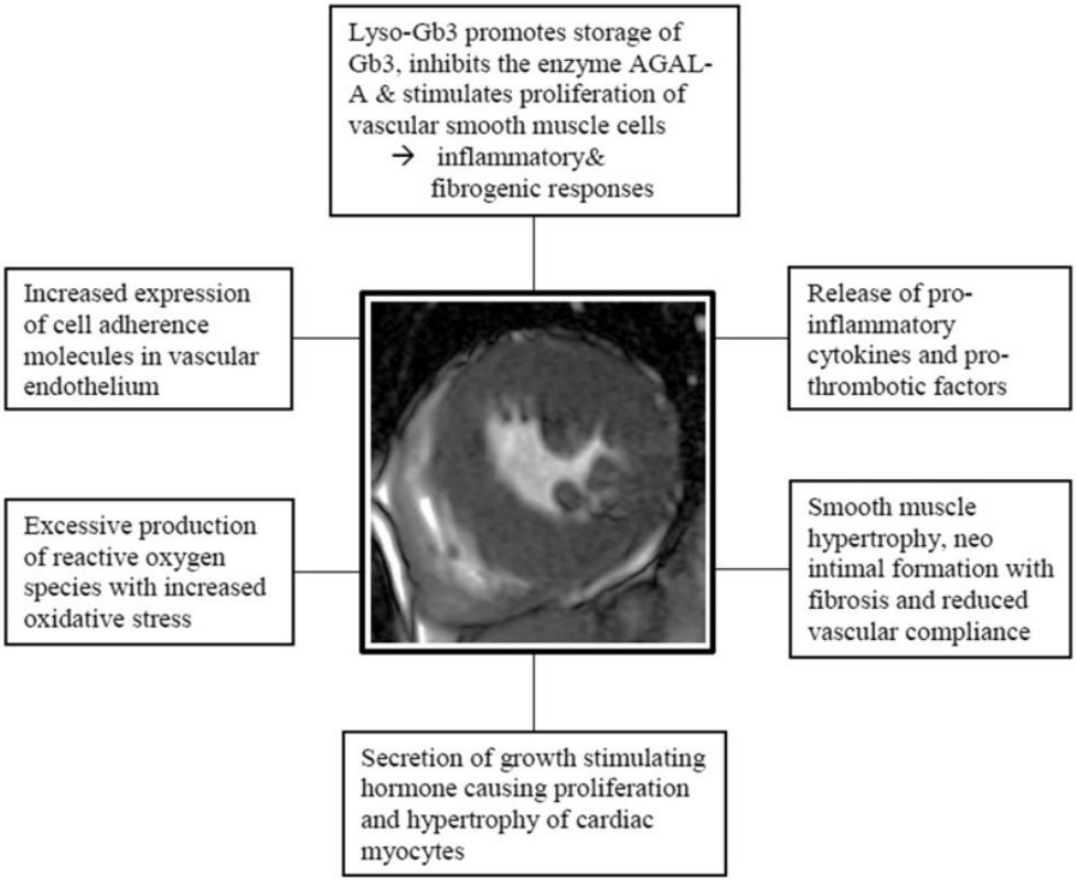

2. Cardiac Arrhythmia

Sphingolipids accumulate in all cardiac cells including the conduction system (86). A typical early electrocardiogram feature of FD is PR shortening without pre-excitation (34). It is likely that this occurs as a result of Gb3 accumulation within and around the atrioventricular (AV) node causing shortening of the PR interval and subsequent acceleration of AV conduction (33). With advancing age and progression of cardiac disease, there is often prolongation of the PR interval, broadening of the QRS duration, repolarisation abnormalities and varying degrees of AV block (33). Both LVH by Sokolow-Lyon criteria and QRS prolongation correlate closely with the presence of sphingolipid storage assessed using T1 mapping and LVH measured on CMR imaging (87). ST/T wave inversion in V5-6 is common in those with inferolateral fibrosis and rare in those without (37). Detailed changes that occur on CMR will be discussed later. It is believed that the Gb3 deposition within the conduction system triggers a cascade of cellular reactions leading to a pro-inflammatory microenvironment with local tissue injury and apoptosis (88). The ensuing damage to conductive tissue contributes to electrical instability and subsequent development of arrhythmia (62).

Although symptoms such as palpitations and syncope are common in FD, little is known regarding the true frequency of arrhythmia (89). A systematic review by Baig et al demonstrated that up to 75% of deaths in Fabry patients are cardiovascular with the majority of these being sudden cardiac events (62%) (13). There is however, very little association between symptoms and occurrence of life-threatening rhythm abnormalities. Registry data and small single centre studies suggest that the rate of atrial arrhythmia (commonly atrial fibrillation [AF]) could be as high as 13% (66), whilst the reported incidence of ventricular arrhythmia varies widely from 5 to 30% (42,90,91), increasing progressively with advancing age (92). This varying incidence of cardiac arrhythmia in FD is likely to reflect limitations in

current standard monitoring techniques, such as ambulatory Holter monitoring. These include, firstly, that this monitoring is usually performed over a 24-hour period and thus only captures a relatively brief period of rhythm monitoring, making the diagnostic yield very low (93). Additionally, there is significant difficulty in transmitting real-time data to clinical teams which delays identification of arrhythmia. Collaboration between patients and clinicians is crucial to facilitate definitive correlation of any arrhythmic burden with accurately reported symptoms (93). More recent data, however, suggests that more prolonged cardiac monitoring using implantable loop recorder (ILR) devices or wearable devices may provide greater detail and a more accurate incidence of arrhythmia in FD (91,94). Although this supports the hypothesis that the true burden of arrhythmia is higher than currently described, this data was from a single centre with only 16 patients (91) and thus further work is required to characterise this in more detail.

Limited data have identified the following potential arrhythmic risk factors in FD that would warrant more detailed investigation: LVH, the presence of late gadolinium enhancement (LGE) as a marker of scar on CMR, left atrial dilatation, a QRS duration greater than 120ms, previously documented non-sustained ventricular tachycardia (NSVT) and, an elevated Mainz Severity Score Index (MSSI) above 20 (73). Additionally, 12-lead ECG abnormalities such as a prolonged PR interval and QRS duration have been identified as independent predictors of permanent pacemaker (PPM) implantation in FD (95). All of these clinical features, however, have been identified from small single centre cohorts and require validation. At present, no definitive criteria exist to guide implantation of cardiac devices for primary prevention and FD is specifically excluded from the sudden cardiac death risk prediction tool used for HCM (96), despite similarities in risk factors between FD and sarcomeric HCM (97). Consequently, in current practice, implantation of devices is

predominantly based on secondary prevention indications following a clinically significant bradyarrhythmia, symptomatic ventricular arrhythmia or aborted sudden cardiac death, or non-guideline-based physician concern, but definitive data are lacking (98,99). Given the potentially higher arrhythmic burden that is suspected in FD, arrhythmic risk stratification is crucial in identifying patients who would benefit from early intervention with medical therapy or a cardiac device.

3. Valve disease

Valvular heart disease is increasingly described, with aortic and mitral valves commonly affected (100,101). Post-mortem histological studies have demonstrated extensive sphingolipid accumulation within the fibroblasts of valve leaflets themselves (*Figure 1.6a*) as well as the associated valvular apparatus (102). Mild-moderate mitral and aortic regurgitation are common in Fabry patients with advanced cardiac disease and LVH (54,100). Valve disease in earlier stages of Fabry cardiomyopathy, however, has not been evaluated. Existing echo studies, based on small numbers, suggest progression of valve disease is slow (101). Haemodynamic factors have been hypothesised as playing a role in the propensity for left sided valve disease in Fabry but association with haemodynamic parameters on echocardiography has been weak (101).

1.2.2.3 Assessment of cardiac involvement

1.2.2.3.1 Electrocardiogram and prolonged rhythm monitoring

The 12-lead electrocardiogram (ECG) is a simple, non-invasive diagnostic test, providing valuable structural information. Abnormalities in the resting ECG have been described during childhood and adolescence, with PR and PQ interval shortening being one of the earliest electrical abnormalities to occur, prior to the onset of cardiac disease (23,33). Subsequent

abnormalities can occur as cardiovascular disease progresses with PR prolongation, interventricular conduction abnormalities, and, advancing AV block. Voltage criteria suggestive of LVH, repolarisation changes and T wave abnormalities are often present when Fabry cardiomyopathy is advanced (23,34). The frequency of interventricular conduction delay and AV block increase with age and can be a marker of adverse prognosis (95). ST segment abnormalities together with T wave changes can indicate myocardial ischaemia or underlying myocardial fibrosis (95,103). *Figure* 1.8 demonstrates the ECG of advanced FD cardiomyopathy.

Figure 1.8. Typical ECG changes in Fabry cardiomyopathy.

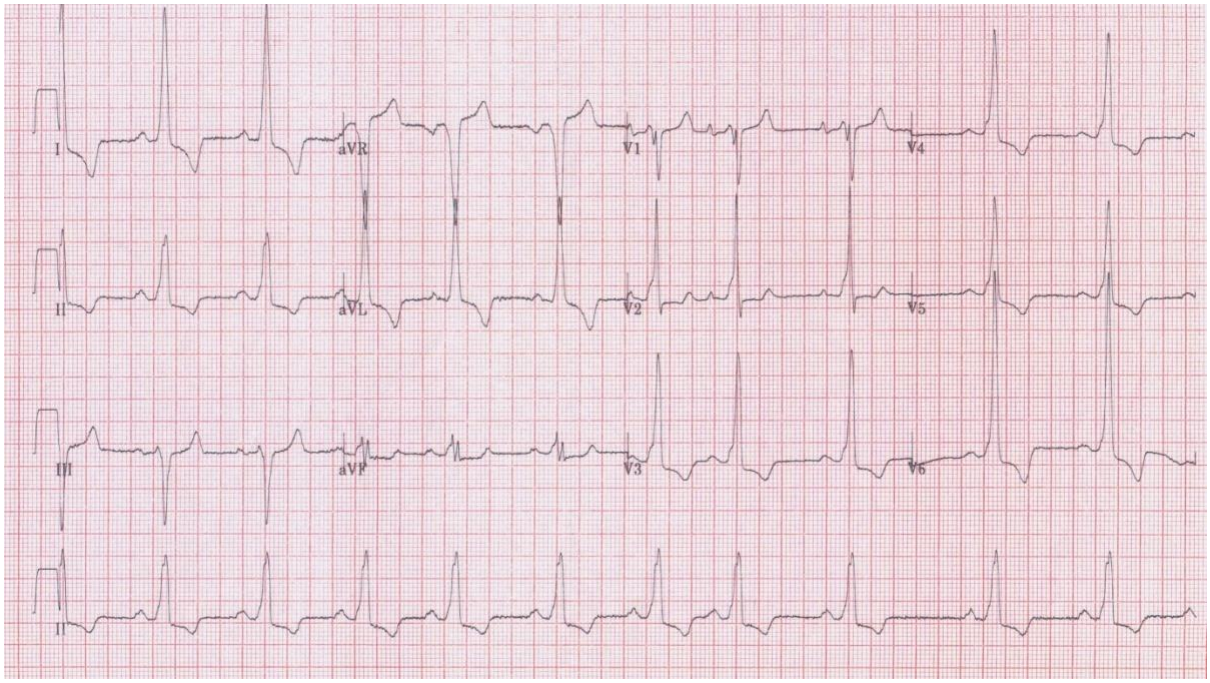

This ECG shows conduction abnormalities (broad QRS, shortened or prolonged PR interval), T-wave changes and ECG criteria for LVH (by Sokolow-Lyon criteria).

Image provided by Professor R Steeds, University Hospital Birmingham. Taken from clinical care, anonymised with consent.

Annual 24hr ambulatory ECG monitoring is recommended for surveillance of progressive electrical disease. Previous studies, however, have noted the limited sensitivity of 24hr ECG monitoring in general cardiovascular disease (104). The use of subcutaneously implanted rhythm monitors, known as ILRs, providing continuous cardiac rhythm monitoring for 3 years, have significantly greater sensitivity for arrhythmia detection in FD. All studies evaluating these in FD, however, are only single-centre, retrospective cohort studies and further prospective work is needed to validate their use (105).

1.2.2.3.2 Transthoracic echocardiography

TTE is the first line cardiac imaging modality used to assess cardiovascular disease, in particular LVH, systolic and diastolic function, valvular abnormalities and proximal aortic disease (13). Typically, concentric LVH is seen, but eccentric and apical hypertrophy similar to that found in hypertrophic cardiomyopathy can also occur. If marked septal hypertrophy is present, systolic anterior motion (SAM) of the mitral valve can commonly occur, leading to a left ventricular outflow tract obstruction. Although CMR has replaced TTE as the gold standard for assessment of LVH, TTE is useful in the evaluation of diastolic dysfunction, which can occur prior to the onset of LVH. Typically a reduction in early myocardial relaxation velocity (e') and late diastolic relaxation velocity (a') on tissue Doppler imaging (TDI), combined with an elevated early mitral filling velocity are markers of LV stiffening and diastolic dysfunction. These changes lead to an increase in E/e' ratio, which is a marker of high left ventricular end-diastolic filling pressures. *Figure 1.9* demonstrates these changes.

Figure 1.9. Echocardiographic assessment of diastolic function.

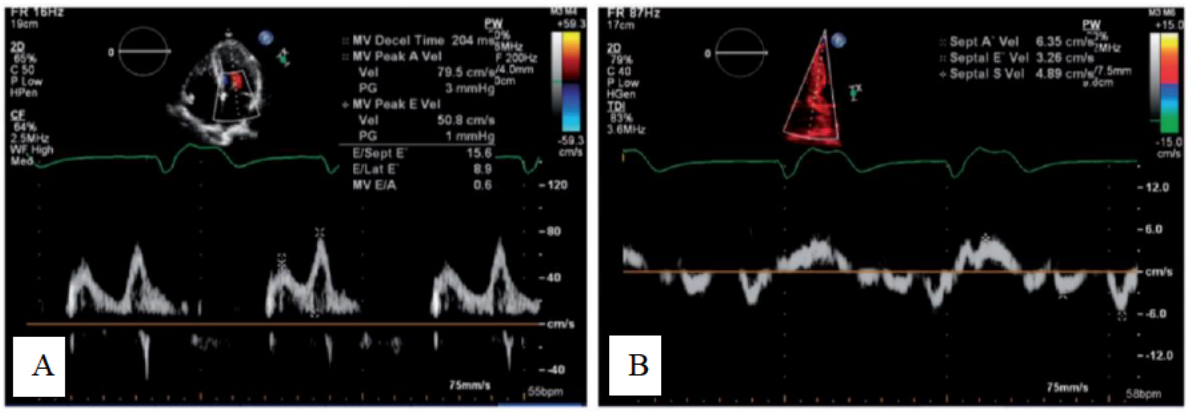

Panel A – *Pulsed wave Doppler at the tips of the mitral valve demonstrating a reduction in early filling velocity (E wave) and a relative increase in the dependence of atrial filling (A wave).*

Panel B – *Tissue Doppler imaging showing a reduction in early myocardial relaxation at the septal mitral annulus.*

Provided by Professor R Steeds, University Hospital Birmingham. Taken from clinical imaging, anonymised with consent.

Two dimensional (2D) speckle tracking on TTE measures longitudinal myocardial strain and can be abnormal prior to the onset of LVH (106). A bull's eye plot is generated, demonstrating myocardial strain using the American Heart Association (AHA) segmentation. Typical changes have been shown to occur in FD and thus can be useful in differentiating from alternative causes of LVH (*Figure 1.10*).

Figure 1.10. Longitudinal strain bull's eye plots from various stages of Fabry cardiomyopathy. Taken from Liu et al (106).

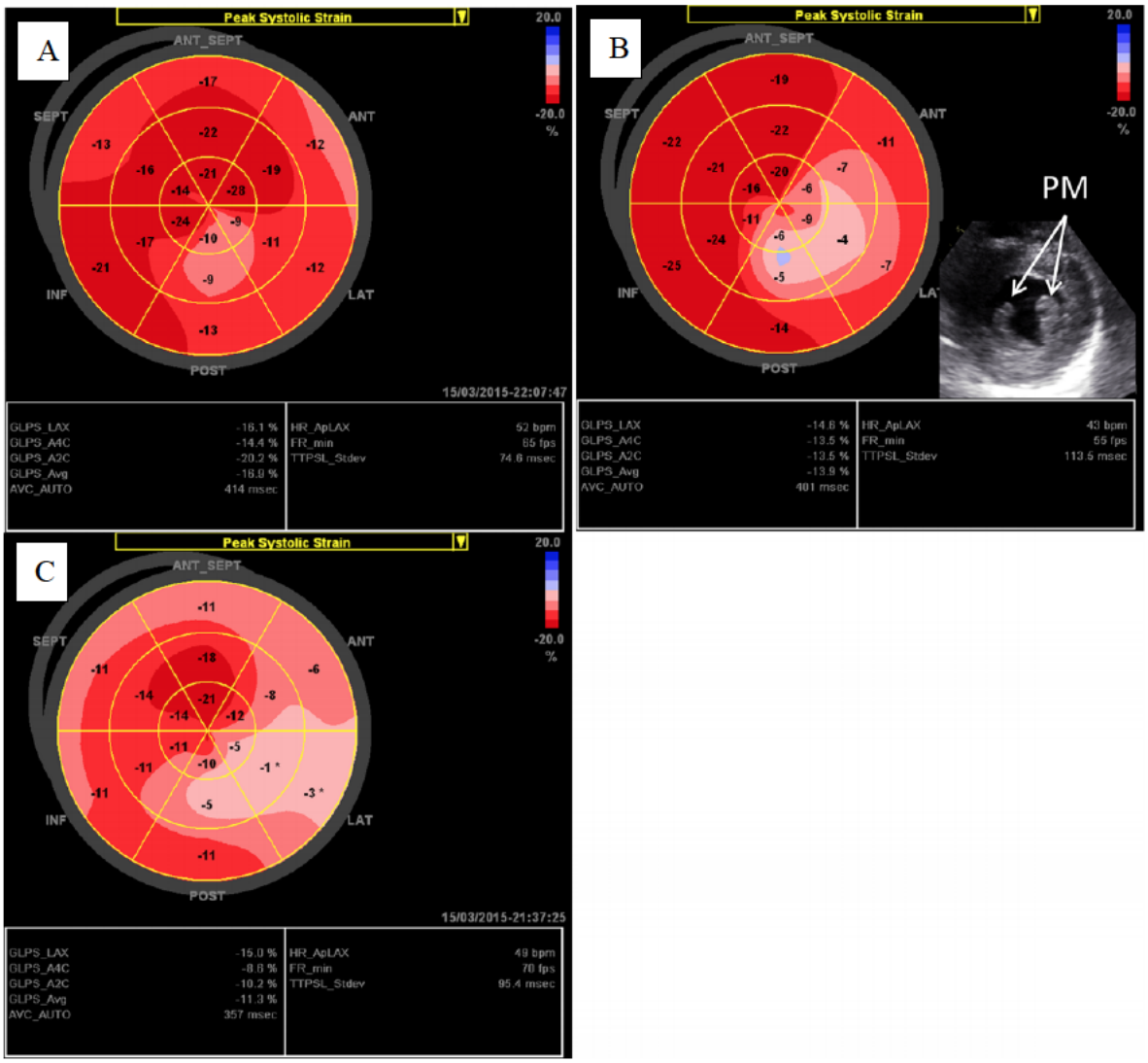

Panel A – *Concentric LVH in a 48 year old male (maximum wall thickness [MWT] of 13mm).*

Panel B – *Prominent papillary muscles in a 44 year old female (MWT 14mm).*

Panel C – *Advanced Fabry cardiomyopathy in a 74 year old female (MWT 18mm), with LGE in the basal inferolateral wall.*

1.2.2.3.2 Cardiac magnetic resonance imaging

CMR is the gold standard imaging technique for myocardial assessment, providing highly reproducible data on ventricular size and volume, myocardial mass and function using steady

state free precession (SSFP) cine imaging (37). A significant benefit of CMR is its ability for detailed non-invasive soft tissue characterisation through measurement of T1 relaxation time. This is the time taken for protons within a tissue to return to equilibrium after excitation by a radio-frequency pulse (107,108). When applied across the magnet, the radio-frequency pulse acts to invert the magnetic field and when removed the T1 relaxes in an exponential manner to a state of equilibrium (108). The rate of recovery is dependent on the specific properties and component molecules of the tissue.

Late Gadolinium Enhancement

The use of Gadolinium-based contrast agents has revolutionised tissue characterisation in CMR enabling the detection of specific myocardial abnormalities. Gadolinium is always chelated with a larger molecule, which prevents it from entering the intracellular volume through an intact cell membrane (37). When the extracellular matrix is disrupted and there is expansion of the extracellular space, there is an alteration in the kinetics of the Gadolinium volume of distribution leading to a slower accumulation and subsequently slower dissipation of Gadolinium within the extracellular space (109). This residual Gadolinium contrast within the extracellular space leads to shortening of the T1 time. A subsequent inversion recovery sequence is used to null the normal myocardium, producing a black signal where the Gadolinium has washed out and areas of bright white signal where Gadolinium contrast remains in the extracellular space (37). Thus, imaging the myocardium after a specified time point from Gadolinium injection (usually greater than 10 minutes), will show a greater degree of Gadolinium contrast in the enlarged extracellular space compared with the normal myocardial tissue (110).

CMR in Fabry Disease: Late Gadolinium Enhancement

Early data has shown that LGE is common within the basal inferolateral wall and histology has demonstrated that this reflects focal fibrosis in up to 50% of patients (111). *Figure 1.11* demonstrates the typical pattern of LGE within the basal inferolateral wall. There is also a significant correlation between the degree of myocardial hypertrophy and LGE, suggesting that the onset and progression of LVH may cause myocyte fibrosis. Over time, the pattern of LGE can progress, become more diffuse, and affects a larger proportion of myocardium (112). More recent data however, has shown that not all Fabry patients follow this trajectory of progressive LGE and fibrosis, with focal LGE being identified in a large proportion of females without LVH (36,87). The presence and extent of LGE, however, is a marker of prognosis, in particular with arrhythmic risk stratification and as a predictor of sudden cardiac death (73). Its presence also predicts non-response to ERT, suggesting the importance of early intervention prior to its onset but also indicating that this scar may not be a marker of early disease (113).

Figure 1.11. Late Gadolinium enhancement in Fabry disease.

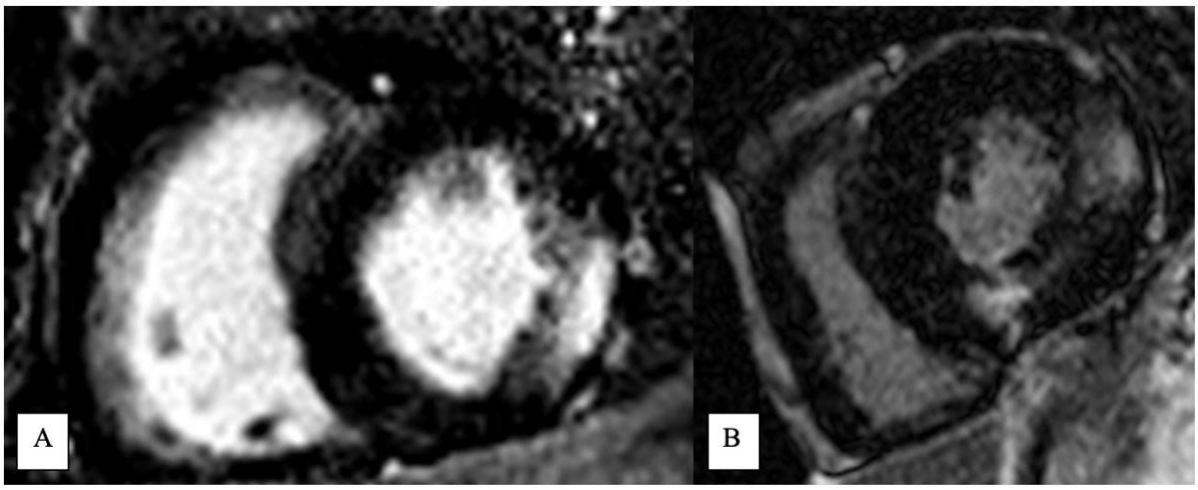

Panel A – *LGE within the basal inferolateral wall, which is the typical initial location.*

Panel B – *extensive LGE affecting a larger area of the myocardium in advanced FD (basal inferolateral and inferior walls, inferoseptum and small area of the anteroseptum).*

Provided by Professor R Steeds, University Hospital Birmingham. Taken from clinical imaging, anonymised with consent.

Native T1 and T2 mapping

The developments of novel CMR tissue characterisation techniques, including T1 and T2 mapping, have enabled greater insight into myocardial composition and structure. There are two main benefits of these mapping techniques over traditional LGE imaging. Firstly, Gadolinium contrast is contraindicated in patients with an estimated glomerular filtration rate (eGFR) <30 ml/min/1.73m^2, but is not required for native T1 mapping. This can therefore provide valuable data on a large proportion of patients who have advanced renal disease, but would have previously been excluded. Secondly, LGE imaging is semi-quantitative comparing 'normal' to 'abnormal', in describing either the presence or absence of LGE (114). It can be quantified as a percentage of the total myocardium, but precise quantification of extracellular volume (ECV) cannot be done using this methodology (115). With T1 mapping however, each individual voxel is presented as a specific pixel, which is subsequently allocated a specific colour based on signal intensity (116,117). Thus, a colour-coded map for the total myocardium is produced based on T1 time, enabling detailed microscopic changes in myocardial tissue to be assessed (117).

T1 mapping involves the acquisition of a series of images taken at varying times following inversion or nulling of the equilibrium magnetisation, generating images with different inversion times and T1 weighting (116). The signal intensities of each individual T1 weighted image are subsequently fit to an equation for T1 relaxation. Initial methodology for T1 measurement was developed by Look and Locker in the 1970s, but this has since been

adapted as the Modified Look-Locker Inversion (MOLLI) recovery sequence, which is widely used (118). This sampling technique acquires a series of 17 images over successive heartbeats, but at the same cardiac phase during a single breath hold. The original sampling method was a 3(3)3(3)5 technique, where 11 images were taken with a total of 3 inversions, *Figure 1.12*. Complete breath hold is essential for this technique to reduce any respiratory artefact, but image quality can be improved through use of post image acquisition motion correction.

Figure 1.12. Modified Look-Locker Inversion (MOLLI) recovery sequence for myocardial T1 mapping. Taken from Kellman et al (118).

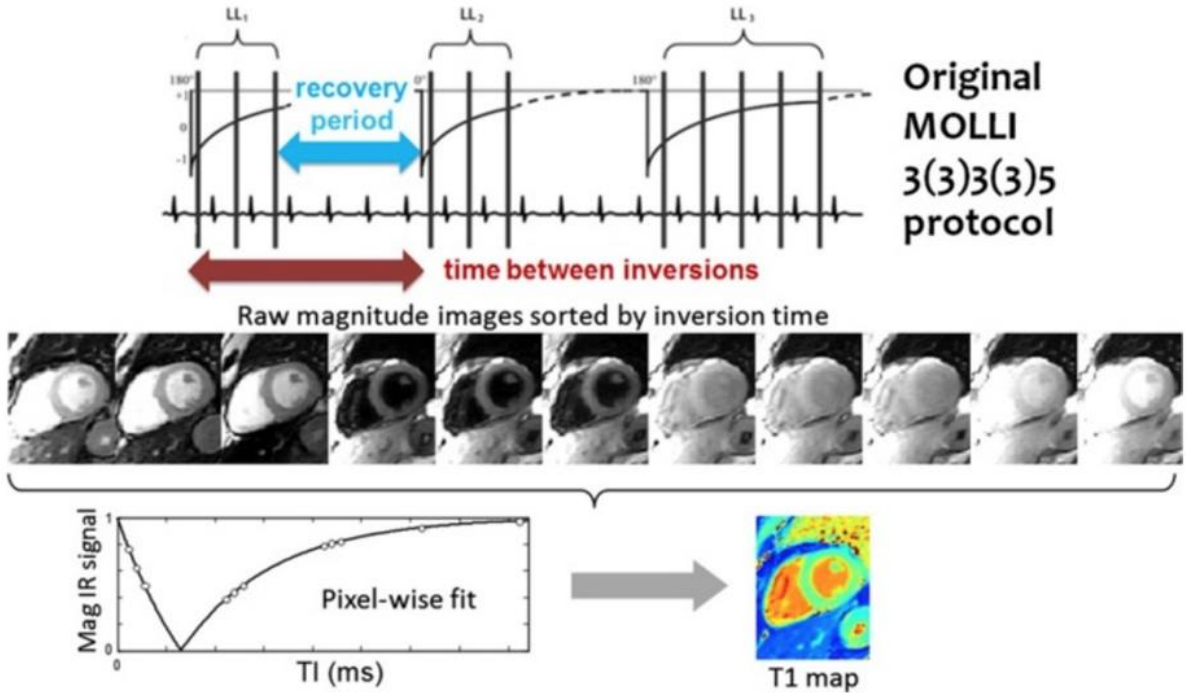

The original methodology involved 3, 3 and 5 images taken in heartbeats following inversion, with 3 heartbeat recovery periods between inversions. T1 inversion times from these images are then fit to the T1 equation curve to generate a colour-coded T1 pixel map.

Other T1 mapping sequences have since been developed, including the Shortened Modified Look-Locker Inversion (ShMOLLI) recovery, the Saturation recovery Single Shot Acquisition (SASHA) and the Saturation Pulse Prepared Heart rate independent Inversion Recovery (SAPPHIRE) (117,119).

Figure 1.13 demonstrates the causes of differing native T1 values in relation to ECV. Generally, elevated native T1 occurs as a result of myocardial oedema or interstitial changes secondary to infiltration. Low native T1 values occur as a result of myocardial infiltration (e.g. Fabry disease, iron overload). It is important to note that T1 values are variable between T1 mapping sequences and CMR field strengths and as such each centre undertaking T1 mapping, must ensure the availability of healthy volunteer reference ranges and regular phantom quality control (explained in detail within Chapter 4).

Figure 1.13. Tissue composition of different diseases using native T1 mapping and ECV. Image provided from Martin Ugander, SCMR Conference 2014 (117).

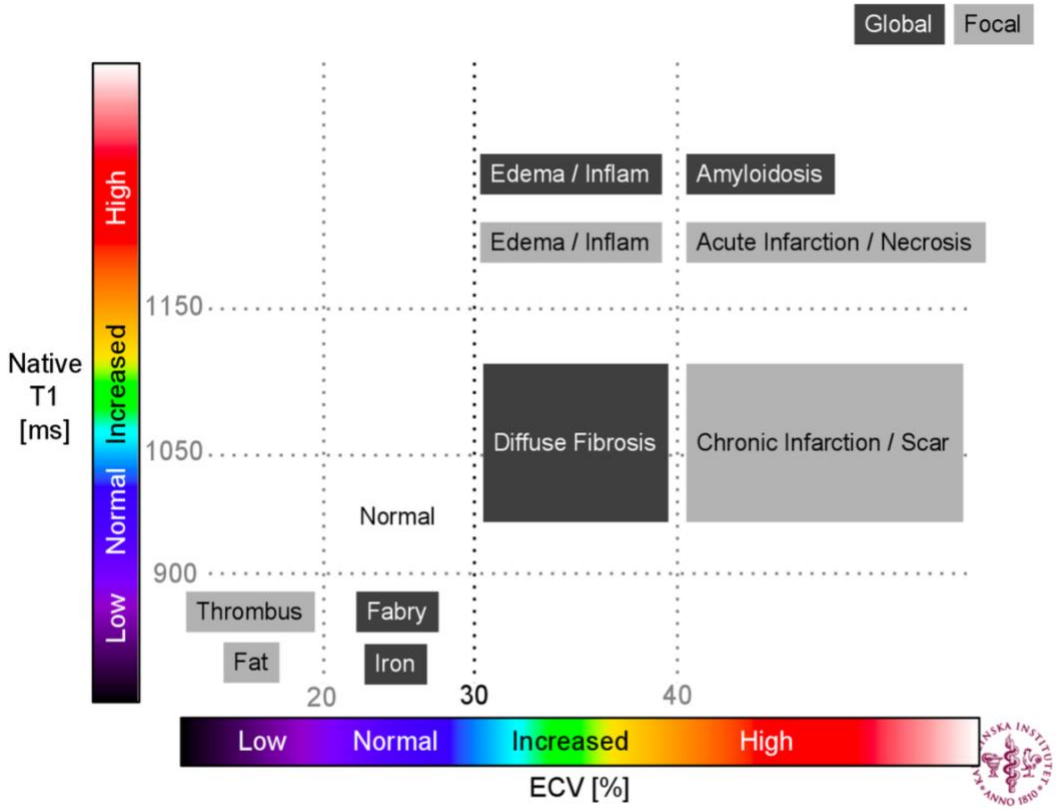

T2 mapping is an additional CMR tissue characterisation technique that measures the transverse relaxation time (120) and is dependent on water content. In contrast to T1 mapping, T2 elevation only occurs in the presence of myocardial oedema, thus its use in combination with T1 mapping can help delineate the precise composition of the myocardium. Additionally, ECV measures the extracellular interstitial fluid within the heart and is calculated using both pre- and post-contrast T1 imaging data of the myocardium and blood-pool. This can provide detailed information on the presence of diffuse fibrosis in a number of cardiac pathologies (117,120).

CMR in Fabry Disease: Native T1 and T2 Mapping

Recent advances in CMR tissue characterisation using T1 and T2 mapping have further developed understanding of Fabry cardiomyopathy. Lipid is known to have a low native T1 value and histological studies of endomyocardial biopsy samples in FD have correlated T1 values and the degree of sphingolipid accumulation (121). Thus, T1 mapping can be used to measure myocardial sphingolipid storage and differentiate between FD and other causes of LVH. It is known that 85% of FD patients with LVH have a low T1 value (122), demonstrating sphingolipid deposition in those with progressive cardiac disease. More importantly however, half of all patients without LVH (previously the main characteristic feature of cardiovascular involvement in FD) also have a low T1 – suggesting this may be an early marker of disease (123). The relationship between low native T1 and changes in electrical activity on a resting 12-lead ECG has also been of great interest. Recent literature has identified that ECG changes can co-segregate with low native T1 in FD patients without LVH (87). This interaction however, has not yet been clearly defined and whether low native T1 (early sphingolipid deposition) is a potential marker of future electrical abnormalities and arrhythmia is yet to be determined.

The value of T2 mapping has also become apparent in recent years and provided further insight into potential causative mechanisms of the cardiac phenotype. Recent literature has described that LGE in FD is not always due to replacement fibrosis, but in certain individuals can be associated with a high T2 and a rise in troponin, suggesting that the extravascular, extracellular deposition of Gadolinium may be due in part to chronic inflammation (36).

These new insights using novel CMR techniques described have led to the formulation of a possible model of disease development, suggesting that there may be distinct phases within

the natural progression of FD (37). These include: (i) an accumulation phase, with subclinical sphingolipid storage within the myocardium; (ii) an inflammatory and myocyte hypertrophy phase, with progressive increase in myocardial mass and extent of LGE; and (iii) late fibrosis and impairment phase, with fibrosis, thinning and LV dysfunction (37). The inflammation and fibrosis that occurs during these phases are likely to be the substrate for cardiovascular events and in particular for arrhythmia.

1.3 Diagnostic testing for Fabry disease

When suspected in males, a diagnosis of FD can be made by a reduced or absent plasma or leucocyte AGALA activity, with additional confirmation by genetic testing (124). AGALA activity <1% is highly suggestive of a diagnosis of classical FD (124). In female heterozygotes or atypical variants however, AGALA activity can be extremely variable and often within the normal range, even in the presence of an overt phenotype. Hence AGALA activity can be a poor predictor of the clinical course and has limited diagnostic utility (40,125) and confirmatory gene testing is mandatory in all patients and GLA gene mutations identified may be associated with classical FD, a variant phenotype (e.g. cardiac or renal) or a variant of unknown significance (VUS) (126). An important step of the diagnostic process is evaluating genetic amenability for pharmacological oral chaperone therapy, which will be discussed later. Measurement of plasma and urinary lyso-Gb3 can be particularly useful in patients with variable AGALA activity and those with a VUS.

1.4 Treatment for Fabry disease

1.4.1 Fabry-specific disease modifying therapy

Treatment of FD is primarily directed at replacing the deficient or absent enzyme, AGAL-A. ERT is the primary therapy for FD and involves two weekly intravenous infusion of either

recombinant or gene-activated preparations of the deficient AGAL-A (agalsidase beta, Fabrazyme, Sanofi-Genzyme, USA and agalsidase alpha, Replagal, Shire, USA). Both of these forms of ERT were developed using the same samples of human DNA containing the GLA gene, however they are produced using different protein expression systems (agalsidase beta is made in a Chinese hamster ovary cell line and agalsidase alpha is made in a human cell line) and have been approved with varying dosing regimens (127). Currently, ERT is indicated in all patients with symptomatic classical FD and can also be commenced when organ specific involvement (cardiac, renal or neurological) from FD becomes evident. The indications and contra-indications for therapy are described in *Table 1.4* (31). Guidance stipulates that initial ERT infusions are performed within a hospital environment, to allow monitoring for any evidence of anaphylaxis. Subsequent administration of ERT can be performed by community district nursing teams at the patient's residence, thus minimising frequent day case hospital admissions.

Table 1.4. Indications and contraindications for enzyme replacement therapy initiation. Adapted from NHS standard operating procedure for Lysosomal Storage Disorders (128).

Indications for ERT		
General	Uncontrolled pain interfering with quality of life	
Renal disease	Clinically significant reduction in eGFR (<80 ml/min)	
	Males with proteinuria >300mg/24 hrs	
	Males with microalbuminuria and renal biopsy showed endothelial deposits	
	Children with persistent microalbuminuria	
Cardiac disease	ECG	LVH by Romhilt-Estes or Cornell
		Isolates repolarisation abnormalities
		Conduction abnormalities
	Echo	Increased LVMi (Devereux method)
		Increased LV MWT (>13mm)
		Left atrial enlargement
		Valve thickening./regurgitation
		LV systolic impairment
		Diastolic dysfunction

		Arrhythmia
		IHD
Neurological disease	Previous stroke/TIA in absence of risk factors	
	Progression of abnormal MRI brain	
Gastrointestinal disease	Pain, vomiting or altered bowel habit affecting quality of life	
Contraindications for ERT		
Presence of another illness, where ERT will not benefit		
Fabry patients deemed too unwell to benefit from ERT		
ESRF requiring dialysis		
Severe cardiac disease in the absence of any other indications		

Efficacy in Fabry cardiomyopathy is mixed, with benefit from early initiation but limited impact in advanced disease (129). The presence of overt LVH and fibrosis on CMR have been shown to limit benefits of ERT and are associated with ongoing cardiovascular progression, suggesting that early ERT initiation is essential for symptomatic and morphological improvements (113,130).

One of the earlier studies by Kampmann et al (131) evaluated the efficacy of ERT (agalsidase alpha) in 45 Fabry patients over a 10-year follow-up period and demonstrated a significant reduction in LV mass and anginal symptoms. In patients with LVH at baseline (classified as an indexed left ventricular mass [LVMi] >50g/m^2), there was a significant reduction in LVMi by 13.55 g/m^2 over the 10-year follow-up duration (p=0.0061). Improvements occurred in the New York Heart Association (NYHA) class in 52% of the cohort and the Canadian Cardiovascular Society (CCS) angina score in 98% following initiation of ERT (81). Other studies of the impact on mass have been conflicting (132-134). Rombach et al (135) assessed the response to ERT (agalsidase alpha and beta) in 57 patients. Disease stability was found in females at 1 year (reduction in LVMi by 0.3g/m^2, p=0.52) but ongoing disease progression occurred in males despite ERT (increased LVMi by 1.2g/m^2, p<0.001). It was also demonstrated that although individual organ involvement was not halted, the risk of developing a second organ system complication was lower in those with a longer duration of ERT (OR 0.52, p=0.014) (135).

This variation in current evidence may suggest a potential step-change effect of treatment, where ERT leads to an initial reduction in LVMi, but does not prevent progression of cardiac disease in the longer term. Additionally, most studies have measured LV mass using echocardiography, although limits of agreement of both M-mode and 2D quantification are much wider between echo studies compared to CMR (TTE: average mean difference between scans varied between 4.5g/m^2 [95% limits of agreement -24.9, 33.9] to 6.4g/m^2 [-23.0, 35.8] and CMR: 0.32g [-20.1, 21.7]) (136).

Migalastat (Amicus Therapeutics, USA) is a newer small molecule pharmacological chaperone (OCT) that reversibly binds to the active site of AGAL-A. It stabilises specific forms of mutant enzyme and facilitates appropriate trafficking to lysosomes where AGAL-A catabolises sphingolipid (137). All FD patients over the age of 16 years who have an amenable mutation can be considered for migalastat as a potential alternative to intravenous ERT. Its use is contraindicated in renal impairment however, with an eGFR less than 30ml/min, and during pregnancy or breast-feeding. Use of OCT has been associated with improvements in cardiovascular disease, with small studies showing a reduction in LV mass and wall thickness on TTE (138,139).

1.4.2 Novel and emerging therapies

An additional oral therapy for FD is substrate reduction therapy. N-butyldeoxygalaconojirimycin (Lucerastat, Idorsia Pharmaceutical, Switzerland) is an iminosugar that acts as a glucosylceramide synthase inhibitor. It acts by preventing the accumulation of Gb3 through limiting the quantity of ceramide that is converted to glycosphingolipid. A recent study (140) of 10 patients found that administration of Lucerastat

1000mg twice daily led to a reduction in circulating Gb3 after only 12 weeks. It is currently undergoing phase 3 clinical trials for use as a monotherapy in FD, but work is also under way for further sub study investigation into combination therapy with ERT (141).

Gene therapy is another strategy that is currently undergoing its first human clinical trial (the FACT study, ClinicalTrials.gov NCT02800070). It involves autologous stem cell transplantation with CD34+ cells transduced with the lentivirus vector, which encodes the human AGAL-A gene. Transduced stem cells may deliver the functional enzyme to areas that may not be well targeted by ERT. Early safety and toxicity evaluations are showing promising results with the first patient nearly three years post stem cell transplantation, having normal AGAL-A levels (142).

1.4.3 Concomitant cardiac therapy

Despite a lack of studies showing benefit, smoking cessation, increase in physical activity and optimal management of conventional risk factors, including dyslipidaemia, hypertension and diabetes, is recommended (2). There is evidence to suggest that strict blood pressure control may be beneficial in delaying progression of LVH, with angiotensin converting enzyme inhibitors used first line in view of co-existing renal dysfunction (143). Symptoms of heart failure, angina and arrhythmia are common in advanced FD and can be difficult to manage, with medical therapy following current standard practice.

Compromise of conduction tissue early in the disease process can lead to multiple cardiac arrhythmias, including supraventricular tachycardia, atrial tachycardia, atrial fibrillation (AF) and ventricular tachycardia (VT). Treatment for AF is often managed with a rhythm control strategy in the first instance, since the arrhythmia is tolerated poorly in those with LVH and

impaired diastolic filling. Rate-limiting medications, such as beta-blockers or calcium-channel blockers, should be administered with caution and close monitoring due to the increased risk of conduction disease and bradycardia in these patients. The CHA_2DS_2-VAS_c scoring system was developed to evaluate the annualised risk of stroke in patients with AF. It is a composite score incorporating the presence of congestive cardiac failure, hypertension, diabetes mellitus, a previous history of ischaemic stroke/TIA, vascular disease and gender (144). Its use in FD however is not recommended for initiation of anticoagulation (145). Given the high incidence and risk of stroke in FD, lifelong anticoagulation is recommended in those with AF, even if sinus rhythm has been achieved. There is currently no FD specific guidance for choice of anticoagulant.

Those with advanced FD are known to have an increased risk of bradyarrhythmia requiring pacing and ventricular arrhythmia requiring implantable cardioverter defibrillators (ICDs) (146). There are however, no criteria to guide implantation of cardiac devices for primary prevention like those available in HCM, with FD specifically excluded from the risk prediction tool for sudden cardiac death (SCD). Consequently, implantation of such devices in FD tends to occur on a secondary prevention basis, following clinically significant bradyarrhythmia, symptomatic ventricular arrhythmia or aborted SCD.

Cardiac transplantation is a viable option for those with severe, life limiting cardiovascular involvement. Patients who remain symptomatic (NYHA class 4) despite optimal medical and device (biventricular pacemaker) therapy may be considered for potential transplantation, although the presence of renal dysfunction can be a frequent limitation to acceptance. FD does not appear to develop in the allograft, presumably due to residual enzyme activity in the donor organ (147).

2. Research aims

Fabry disease continues to be a diagnostic challenge and there is still a significant lack of knowledge regarding arrhythmia burden in Fabry cardiomyopathy. There remains significant scope to further our understanding of cardiac pathophysiology in FD, in particular the biology of arrhythmia generation, burden and subsequent therapeutic interventions.

The main aims of this thesis are:

1) To characterise the stages of cardiovascular disease and potential mechanisms for arrhythmia in FD;
2) To quantify the burden of arrhythmia and consequent therapy usage in FD e.g. cardiac device implantation.

There are three primary hypotheses within this thesis:

1) low T1 represents early cardiac involvement in patients without LVH, and precedes electrical (ECG), structural (LVH) and functional (deformation) change;
2) arrhythmia burden is higher than existing data indicate;
3) prediction of arrhythmia can be improved using clinical, metabolic and multiparametric CMR markers of risk.

This chapter will demonstrate an outline of my thesis structure, with a summary of data that will be presented. The results described in this thesis will delineate the various stages of cardiovascular disease in FD, exploring the possible mechanisms and risk predictors leading to cardiac arrhythmia.

2.1 The natural evolution of the cardiac phenotype and the impact of enzyme replacement therapy

Background:

The interaction between progressive myocardial storage/the development of the cardiac phenotype on CMR and the development of electrical abnormalities has not been previously evaluated. Additionally, the effect of enzyme replacement therapy on this progression of cardiac disease remains unclear.

Hypothesis:

Progressive sphingolipid deposition and structural cardiac disease will occur in untreated patients with associated progression in electrical abnormalities. The use of ERT may demonstrate a protective effect on cardiac disease, delaying the onset of structural and electrical change.

2.2 Early markers of Fabry heart disease: The interaction between myocardial mechanics and sphingolipid deposition

Background:

Up to 59% of LVH negative patients have been shown to have low T1, suggesting that sphingolipid storage occurs earlier prior to the onset of myocardial hypertrophy. ECG changes and abnormalities in blood biomarkers are also known to precede structural change and recent literature has shown that ECG abnormalities co-segregate with low native T1. Early mechanical dysfunction has also been demonstrated in Fabry disease by impairment of global longitudinal strain on echo, however, this has not been explored in relation to sphingolipid storage on CMR or conduction abnormalities. This chapter aims to demonstrate that mechanical dysfunction on CMR is associated with early sphingolipid storage.

Hypothesis:

Mechanical dysfunction on CMR is associated with early sphingolipid storage prior to the onset of structural change.

2.3 The use of digital advanced electrocardiogram analysis in detection of cardiovascular disease

Background:

The conventional 12-lead ECG is a simple diagnostic tool that has a significant role in FD management. Incorporation of advanced computer technology has enabled novel ECG analysis techniques to emerge, based on detailed analysis such as advanced signal averaging, noise reducing vectorcardiographic reconstruction and analysis, frequency content analysis, and beat-to-beat variability studies. A number of advanced ECG (A-ECG) markers have been shown to have both a higher sensitivity and specificity than conventional ECG parameters in prediction of arrhythmic risk and in the assessment of conditions such as LVH, HCM and ischaemic heart disease. Certain markers have also been suggested as potential predictors of cardiac involvement in FD, but these are only from small datasets.

Hypothesis:

A-ECG parameters can be used to create a composite risk prediction score identifying FD patients with early cardiac involvement, as defined by low native T1 on CMR. A-ECG can also be used to predict outcome arrhythmic and clinical markers.

2.4 Cardiac device implantation in advanced Fabry cardiomyopathy

Background:

Registry data have described the rate of atrial arrhythmias such as AF to be as high as 13%, whilst the rate of ventricular arrhythmia is variable between 5 and 30%. When and how to treat these arrhythmia remains unclear and no guidance exists for the use of cardiac devices, with FD specifically excluded from the sudden death risk stratification tool used in HCM. Although cardiac devices such as PPMs and ICDs are implanted in FD, data are lacking on specific indications for primary prevention device implantation and on the incidence of arrhythmia requiring device utilisation.

Hypothesis:

The prevalence of arrhythmia in advanced Fabry cardiomyopathy is higher than the literature suggests. The use of cardiac devices in FD is unclear and may not follow current guidance. In particular implantation of ICDs may occur based on clinician suspicion of arrhythmic risk, which will need further evaluation through prospective studies.

3. General Methodology

3.1 Study population

This thesis incorporates patients with genetically confirmed FD taken from three different cohorts. All patients are followed up at national specialist centres within the UK and Australia: University Hospital Birmingham NHS Foundation Trust, Birmingham; Salford Royal Hospital, Salford; Royal Free Hospital, London; Addenbrookes Hospital, Cambridge; Royal North Shore Hospital, Sydney. Patients included in this thesis will be recruited from the following areas:

1) The Fabry400 study (ClinicalTrials.gov: NCT03199001).

   This is a prospective multicentre, multinational collaboration sharing CMR data acquired at centres in Birmingham, London and Sydney. All imaging was performed using shared multiparametric imaging protocols (as detailed in section 3.4). The study closed for recruitment in 2019, with over 280 patients recruited and 450 CMR scans available (37).

2) Clinical service.

   Retrospective data analysis will be carried out using historical cardiac investigations performed as part of clinical service at Birmingham, Salford, London and Cambridge. Standard clinical care of Fabry patients with cardiac involvement includes regular assessment with CMR, echocardiography and ECG. All data utilised in parts of this thesis was previously collected for primary use as part of clinical service and its use in research is secondary.

3) The Role of Implantable Loop Recorders in Anderson-Fabry Disease: RaILRoAD randomised controlled study (ClinicalTrials.gov, NCT03305250).

This is a prospective multicentre, international study proposing to use ILRs to define arrhythmic risk predictors and improve cardiovascular outcomes.

Figure 3.1 demonstrates how the individual cohorts will contribute patient data to each aspect of this thesis.

Figure 3.1. Diagram demonstrating the various patient cohorts used to recruit patients and their relationship with each chapter of this thesis.

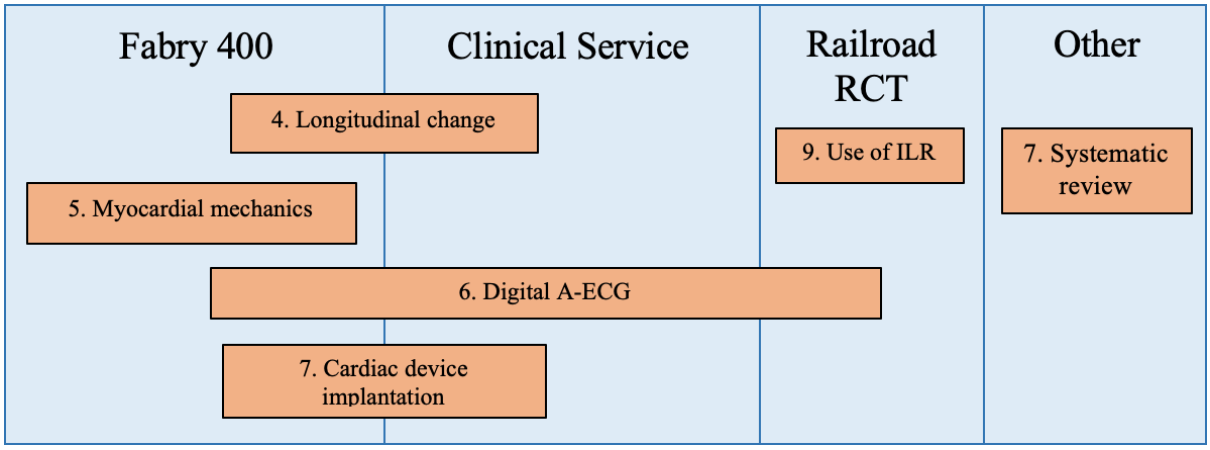

3.2 Ethical and clinical governance approval

Ethical approval was obtained for the two prospective studies: Fabry400 and Railroad. This was obtained from the UK National Research Service for the UK cohort and the Northern Sydney Local Health District Ethics Committee for the Australian FD patients. National ethical approval was obtained for the Railroad study as part of this thesis (17/WM/0421) and for the Fabry400 study by the study chief investigator within the London site (14/LO/1948), with independent local recruitment for Fabry400 in Birmingham. All patients were prospectively recruited with informed consent. For the retrospective components of this thesis, which utilised data from Inherited Metabolic Disease clinical service, local clinical governance approval was obtained. In accordance with UK National Research Service

guidelines, ethical approval was not required for use of these patient's data as their use in research was a secondary intention of the data. All studies conformed to the Health Research Authority (HRA) Good Clinical Practice guidelines.

3.3 Clinical assessment/Demographic parameters collected

Routine demographic data were obtained for all FD patients, both prospectively recruited and retrospectively taken from clinical service data. Detailed medication history, with particular focus on ERT (historical and current), was obtained. Height and weight data were recorded for calculation of BMI and total body surface area (BSA) by Mosteller equation (BSA (m^2) = √ height (cm) x weight (kg) / 3600), which were used during CMR analysis.

Blood tests results recorded included: renal function, full blood count, N-terminal-pro B type natriuretic peptide (NT-pro BNP), high sensitive troponin T or I (hs-Troponin T/I), Fabry genetic mutation analysis, and AGAL-A/lyso-Gb3 levels (where available).

3.4 Cardiac Magnetic Resonance Imaging

3.4.1 Scanner details

All CMR studies were performed on a 1.5 Tesla scanner using a 32-channel phased array coil – Avanto, Siemans, Erlangen, Germany: Birmingham (University Hospital Birmingham NHS Foundation Trust), London (Bart's Heart Centre), Salford (Manchester Royal Infirmary), Cambridge (Addenbrooke's Hospital) and Aera, Siemans, Erlangen, Germany: Sydney, Australia (Royal North Shore Hospital). 1.5 Tesla scanners commonly achieve high quality, reproducible SSFP cine images, without flow related artefact that can occur at higher field strengths (148).

3.4.2 Overview of general CMR imaging protocol

The CMR protocol used in all aspects of this thesis with specific timing of sequences is shown in *Figure 3.2*.

Figure 3.2. Summary of CMR protocol

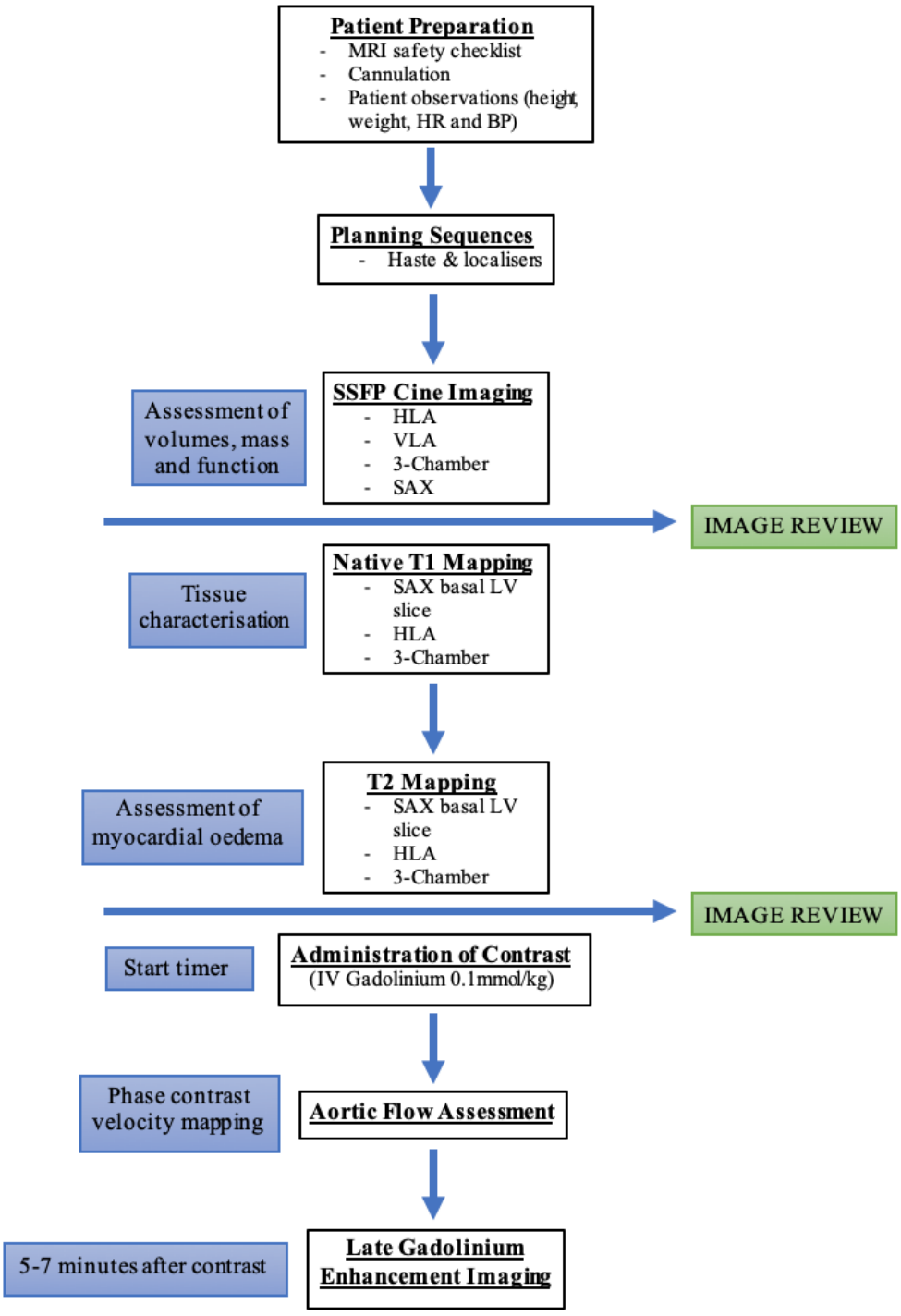

3.4.3 Sequences and protocols

3.4.3.1 Patient preparation, localisers and SSFP imaging

MRI safety checks were performed in all patients. ECG electrodes were applied on to three bony prominences on the chest wall, ensuring a good quality 3-lead electrocardiogram. Standard localiser images were taken during breath hold in sagittal, axial and coronal planes, to aid sequence planning and ensure that the heart was at the magnet isocentre. SSFP cine imaging was then performed on the horizontal (HLA) and vertical long axis (VLA) of the left and right ventricles. Serial imaging of the short axis (SAX) of the left ventricle was performed commencing at the atrioventricular junction, moving towards the apex in parallel to the mitral annulus. A slice thickness of 7mm was taken with 3mm interval gaps between SAX cine images. Retrospective ECG gating was used over 25 phases of the cardiac cycle, with breath hold imaging performed at end expiration. The CMR scan parameters included: repetition time (TR) 66ms, echo time (TE) 1.22ms, flip angle (FA) 80°, field of view (FoV) 360mm.

3.4.3.2 MOLLI for T1 mapping

SSFP motion corrected MOLLI sequence imaging was used for native T1 mapping. Breath hold images were taken at end-diastole in the following views: 1) LV long axis: HLA and VLA and 2) LV short axis: basal, mid and apical LV slice, with a 2 slice interval between each. The basal slice was the first slice with LV myocardium covering 100% of the circumference of the ventricle. Sampling for T1 recovery was performed using a 3(3)3(3)5 scheme, with 11 T1 weighted images acquired over a breath hold of 17 R-R intervals (117). Parameters for MOLLI imaging were as follows: TR 568ms, TE 1.01ms, FA 35°, FoV 320mm. After motion correction and T1 equation curve fitting of all 11 images, a pixel-wise colour map was generated for each view.

3.4.3.3 T2 mapping

T2 maps were also obtained in a single breath hold prior to contrast administration (Work In Progress package 448B, Siemens Healthcare, Erlangen, Germany). As part of this sequence, three single images were taken at varying T2 preparation times (0ms, 24ms and 55ms). The same slice positions as used with MOLLI imaging were taken. The following scanner parameters were used: TR 225ms, TE 1.12ms, FA 70°, FoV 340mm. Similar to T1 imaging, the T2 weighted images were motion corrected and following curve fitting, a pixel-wise T2 colour map was generated.

3.4.3.4 Aortic flow assessment

In the time immediately following intravenous contrast administration, a phase contrast velocity mapping sequence was taken perpendicular to the ascending aorta to evaluate aortic flow. This sequence was taken during a single breath hold with retrospective ECG gating. Parameters for this sequence were: TR 47.15ms, TE 2ms, FA 30°, FoV 227mm. The images were manually reviewed for artefact, background noise or aliasing and repeated if required.

3.4.3.5 Late gadolinium enhancement protocol

An intravenous bolus dose of gadolinium contrast (0.1mmol/kg) was administered following T2 mapping sequences. After 5-7 minutes, the initial scout image was positioned at mid ventricular slice and the normal myocardium was nulled and the inversion time chosen was based on the image taken where the myocardium was black. LGE images were acquired in the standard long axis and short axis views of the LV using either a fast low angle shot (FLASH) sequence with phase sensitive inversion recovery (PSIR) (149) or a respiratory motion corrected free breathing single shot SSFP averaged PSIR sequence. During subsequent images the inversion time was manually adjusted to ensure appropriate nulling of

the myocardium. Images were reviewed real-time and if LGE was suspected, the same image was repeated with an alternative phase encoded direction, to confirm that the LGE seen was not artefactual.

3.4.4 CMR analysis

3.4.4.1 Anonymisation methodology and software

All CMR scans were anonymised with unique study codes. Subsequent analysis was carried out over a 3 month time period to ensure uniformity of analysis technique. All MRI analysis was performed in accordance with standardised guidelines and analysis techniques (150), using Cvi42® post processing software (version 5.3.4, Circle Cardiovascular Imaging, Calgary, Canada).

3.4.4.2 Mass and volumetric assessment

CMR is the gold standard imaging modality for assessment of ventricular mass and volume and offers more accurate and reproducible measures, resulting from superior spatial resolution and more precise tissue interface definition (151). Blinded analysis of ventricular volumes and mass was performed from the SAX cine images. The basal slice was confirmed if greater than 50% of the LV myocardium was present and the end-diastolic and end-systolic phases were selected by visually determining the largest and smallest LV cavity size respectively (*Figure 3.3*). The epicardial border was manually drawn and rounded at the interface of the myocardium and extra-cardiac space. Delineation of the endocardial border was performed using the thresholding technique, with papillary muscles included within evaluation of myocardial mass, as described in the literature, *Figure 3.4* (152). This was done as papillary muscle hypertrophy has been shown to occur early in FD and often prior to the onset of typical muscle hypertrophy (153). Epi- and endocardial volumes were calculated

from combining contouring on SAX slices and detailed LV volumetric calculations performed. Myocardial mass was evaluated using the epi- and endocardial volumes in combination with myocardial density, which is a fixed and known value.

Figure 3.3. Analysis of ventricular mass and volumes using post-processing software.

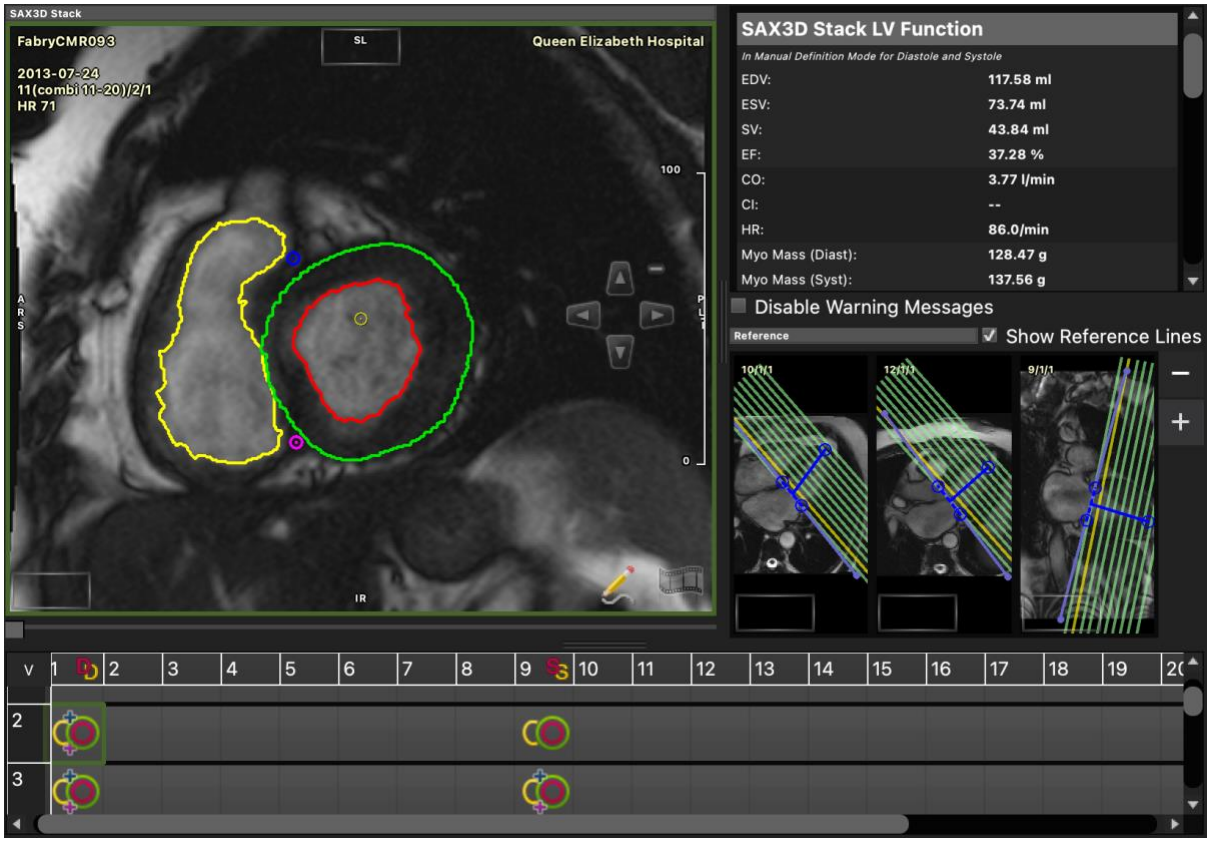

This image shows the work interface from Circle Cvi42©, used for assessment of LV mass and volumes. The LV stack is shown at the bottom of the workspace starting with diastole at phase 1. The systolic phase is defined manually by visually assessing the smallest LV cavity size. Endo- and epicardial LV borders are drawn as red and green contours, respectively. The right ventricular (RV) endocardial border is represented by the yellow contour. Contours are drawn for end-diastole (phase 1) and end-systole (phase 9) in order to evaluate LV volumes and mass.

Figure 3.4. Detailed analysis of the LV and RV.

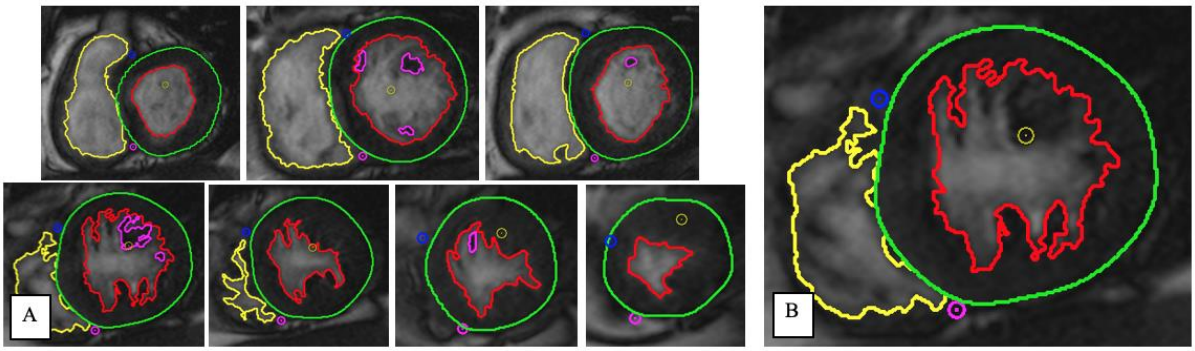

Panel A *– This shows epi- and endocardial LV borders with papillary muscle included within the myocardial mass. Only endocardial borders are drawn on the RV to enable volumetric analysis.*

Panel B *– LV myocardial mass assessment without inclusion of papillary muscle mass. Consequently, a large amount of LV mass is not included in overall assessment.*

End-diastolic LV wall thickness was evaluated using the AHA 17-segment model (154), where the myocardium is split into individual segments at each level of the short axis LV stack. The pattern of hypertrophy is classified by evaluation of LV mass as described above, and relative wall thickness (RWT), by the following equation: RWT = (2 x LV posterior wall in diastole) / diastolic LV internal diameter. This will enable differentiation between eccentric and concentric patterns of LVH, *Figure 3.5* (155).

Figure 3.5. Left ventricular geometric patterns determined by assessment of relative wall thickness and LV mass index. Adapted from Oktay et al (155).

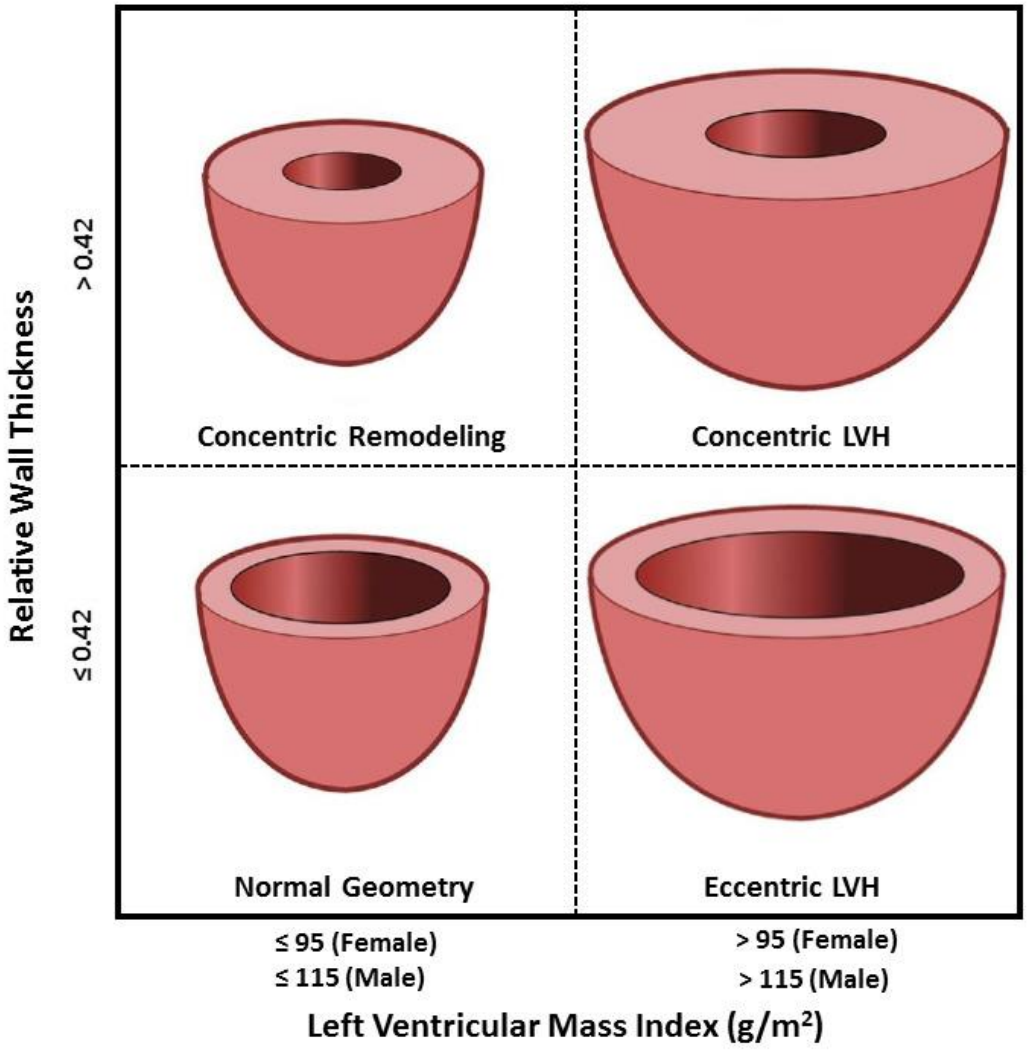

This demonstrates differing patterns of LVH dependent on relative wall thickness and LVMi. The bottom left panel represents a normal LV with a RWT <0.42 and a normal LVMi.

3.4.4.3 T1 and T2 mapping analysis

Prior to analysis of the colour maps generated, the uncorrected T1 raw images, the motion corrected raw images and the LGE images were reviewed for any evidence of artefact or fibrosis, as this would affect the calculated T1 time. Any artefactual segments were excluded from final analysis. T1 times were calculated by two methods: 1) assessing specific regions

of interest (ROIs) and 2) AHA segmentation of SAX LV images. ROIs were taken from the inferoseptum (HLA), inferolateral wall (3Ch) and septum and lateral wall of basal and mid LV SAX slices (*Figure 3.6*). Epi- and endocardial borders were manually drawn on the T1 colour map ensuring avoidance of the blood pool and extracardiac structures. A 20% offset from the epi- and endocardium was applied to both contours to confirm avoidance of these structures, as this has previously been shown to be the most reproducible offset methodology (156). *Figure 3.7* demonstrates AHA segmentation of the T1 colour map. The same methodology was performed for assessment of T2 colour maps.

Figure 3.6. An example of a ROI taken from different LV views of a MOLLI colour map.

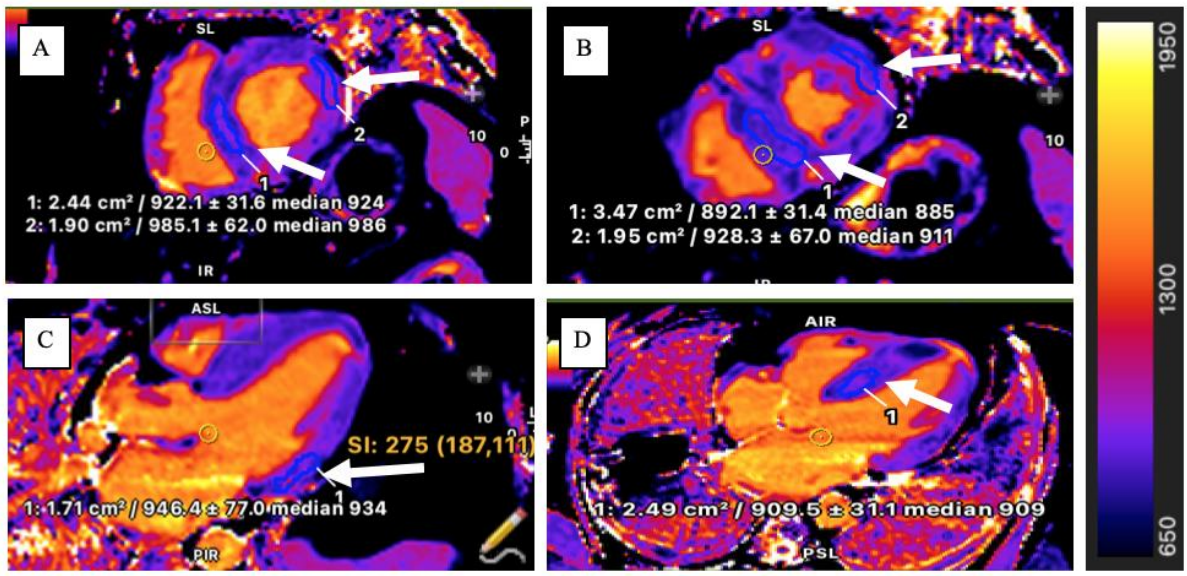

These panels demonstrate motion corrected native T1 colour maps, where lower values (blue/purple) represents sphingolipid deposition and higher values (orange/yellow) represents fluid. ROIs are taken from different areas of the myocardium from different LV views: septum and lateral wall of basal LV SAX (panel A), septum and lateral wall of mid LV SAX (panel B), inferolateral wall of the 3-chamber image (panel C) and inferoseptal wall of the HLA image (panel D). The ROIs are demonstrated by the white arrows.

Figure 3.7. Assessment of T1 times using AHA segmentation of LV SAX.

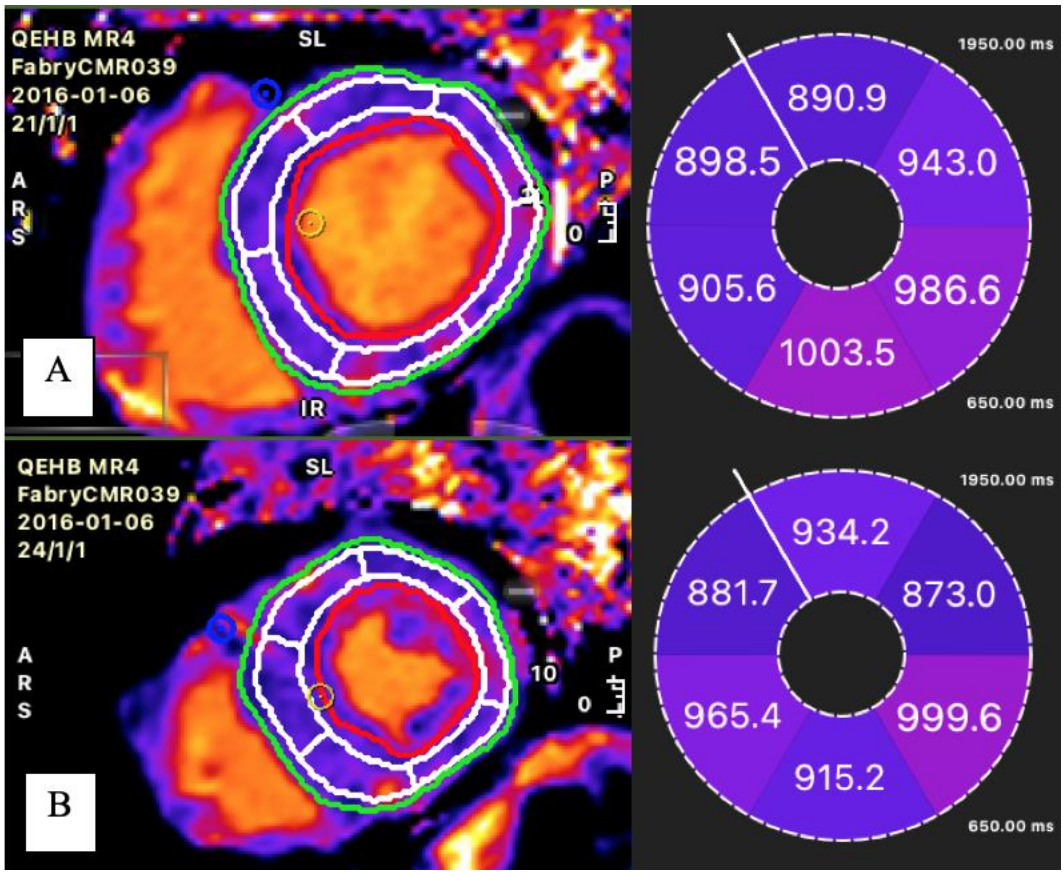

Endo- (red) and epicardial (green) contours have been drawn on the basal LV SAX slice (panel A) and the mid LV SAX slice (panel B). After placing the anterior RV insertion point marker, the myocardium is split into 6 AHA segments at each level with a 20:20% offset from the epi- and endocardial border, as described above. This provides a polar map of segmented native T1 times, as shown on the right.

3.4.4.4 LGE quantification

LGE was evaluated initially by visual assessment and was defined as being present if it was present in an LV SAX slice and in a corresponding long axis view of the heart. It was also assessed and confirmed using repeat imaging performed following an alteration in phase encoding direction. LGE was also quantified using previously described techniques, with a

threshold of six standard deviations above the mean signal intensity of reference myocardium (150). This methodology will be described in detail within Chapter 4.

3.5 Standard 12-lead electrocardiogram assessment

All patients underwent resting 12-lead ECG, with standard lead placement using six precordial leads and four limb leads (*Figure 3.8*). Parameters recorded included: heart rate, rhythm, PR interval, QRS complex duration and morphology, QTc interval duration, the presence of T wave inversion in at least two contiguous leads and the presence of multi-focal ventricular ectopy. The presence of LVH by ECG voltage criteria was also assessed using the Sokolow-Lyon and Cornell methodology (157).

1. Sokolow-Lyon – S wave depth in V1 + tallest R wave height in V5-6

   Value greater than 35mm suggests LVH by voltage criteria.

2. Cornell criteria – R wave height in aVL + S wave depth in V3

   Value greater than 28mm in males or 20mm in females suggestive of LVH.

Details of digital advanced ECG methodology will be described in Chapter 6.

Figure 3.8. Standard placement of precordial leads. An additional four limbs are placed on both wrists and ankles. Taken from Khan G (158).

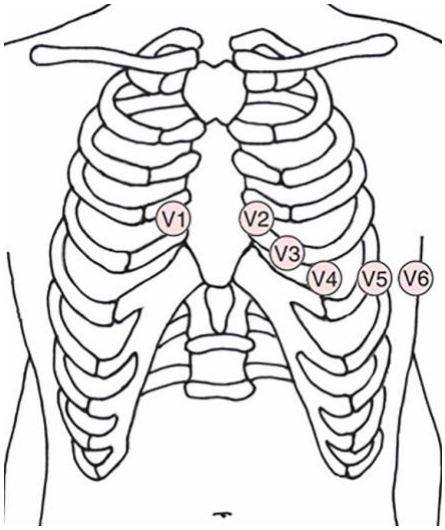

3.6 Statistical analysis

Statistical analyses were carried out using SPSS 23 (IBM, Armonk, NY). All continuous variables are expressed as mean ± standard deviation and all non-continuous data are expressed as frequencies or percentages. Normality was evaluated using the Shapiro-Wilk test and by visual evaluation of histogram plots. Groups were compared with independent t-testing for parametric data and Mann-Whitney U testing for non-parametric data. Chi-squared or Fishers-exact testing was used to compare proportions within two independent groups. Comparisons between multiple groups were performed using ANOVA testing with post-hoc Tukey correction. A p-value of <0.05 was considered statistically significant throughout.

4. Results: The natural evolution of the cardiac phenotype and the impact of enzyme replacement therapy

The work in this chapter is based on the published first author original article, where this data was first presented:

Vijapurapu R, Baig S, Nordin S et al. Longitudinal assessment of cardiac involvement in Fabry disease using cardiovascular magnetic resonance imaging. *JACC: Cardiovascular imaging*. 2020 Aug; 13(8): 1850-1852. DOI: 10.1016/j.jcmg.2020.03.004.

Extent of personal contribution

This study was a multi-centre study and I was responsible for recruitment of all patients seen as part of clinical care, which contributed to 60% of the total cohort. The remaining patients were taken from the Fabry400 study, of which UHB was the second largest contributor and whose patients I recruited. I performed the CMR studies, 12-lead ECGs and TTE for the patients recruited through the Fabry400 study.

Following completion of recruitment, I analysed all of the data with guidance from the UHB R&D statistical team. The first draft of the above manuscript was written by myself and I was responsible for all editing and subsequent revisions.

4.1 Introduction

Cardiac involvement is an increasingly common clinical manifestation in FD and the prevalence of LVH is known to increase with advancing age. Registry studies have reported the presence of LVH in 53% of men and 33% of women by the third decade of life (89), and in 76.9% of all Fabry patients aged ≥75 years (159). Progression tends to be more rapid in

men however, with a mean age of onset of 39±10 years in men and 50±11 years in women (69) and complete genetic penetrance occurring 10 years after in both (*Figure 4.1*).

Figure 4.1. Cumulative onset of LVH in Fabry disease according to age. Taken from Nordin et al (37).

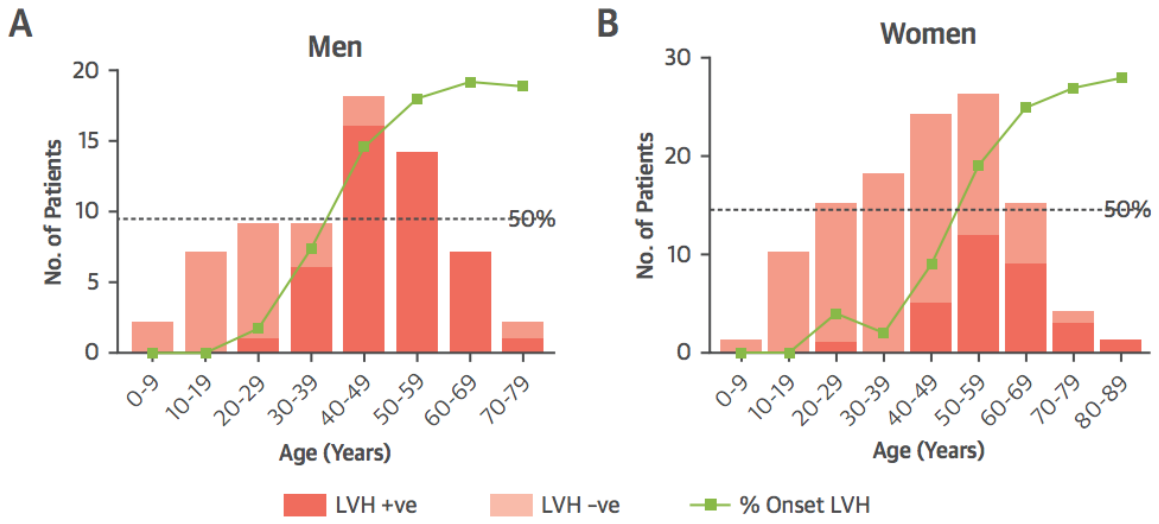

Panel A *– demonstrates an earlier onset of LVH in male patients, with a greater proportion of LVH positive patients in the third decade of life.*

Panel B *– women develop LVH much later with a predominance of LVH positive patients in the sixth decade.*

The green dotted line demonstrates cumulative number of patients with complete genetic penetrance of LVH.

In addition to earlier onset of LVH, men tend to have accelerated and more severe hypertrophy when present. The LVMi in male patients has been described to range up to 2.6 times the upper limit of normal, with females only reaching as high as 1.7 times the upper limit (37). Progression of cardiac disease has also been shown to be greater in patients with classical FD when compared to those with non-classical organ specific variants. A

multicentre study by Arends et al (48) of 596 Fabry patients using echocardiography showed that men with classical FD tended to have the highest LVMi and most significant progression of hypertrophy (percentage of classical FD with LVH: men 32%, women 22%, $p<0.001$ for both). *Figure 4.2* demonstrates the spread of LVMi across the different age groups, with significant differences seen between classical and non-classical disease in both genders.

Figure 4.2. Left ventricular mass as determined by echocardiography compared to age, in males and females. Taken from Arends et al (48).

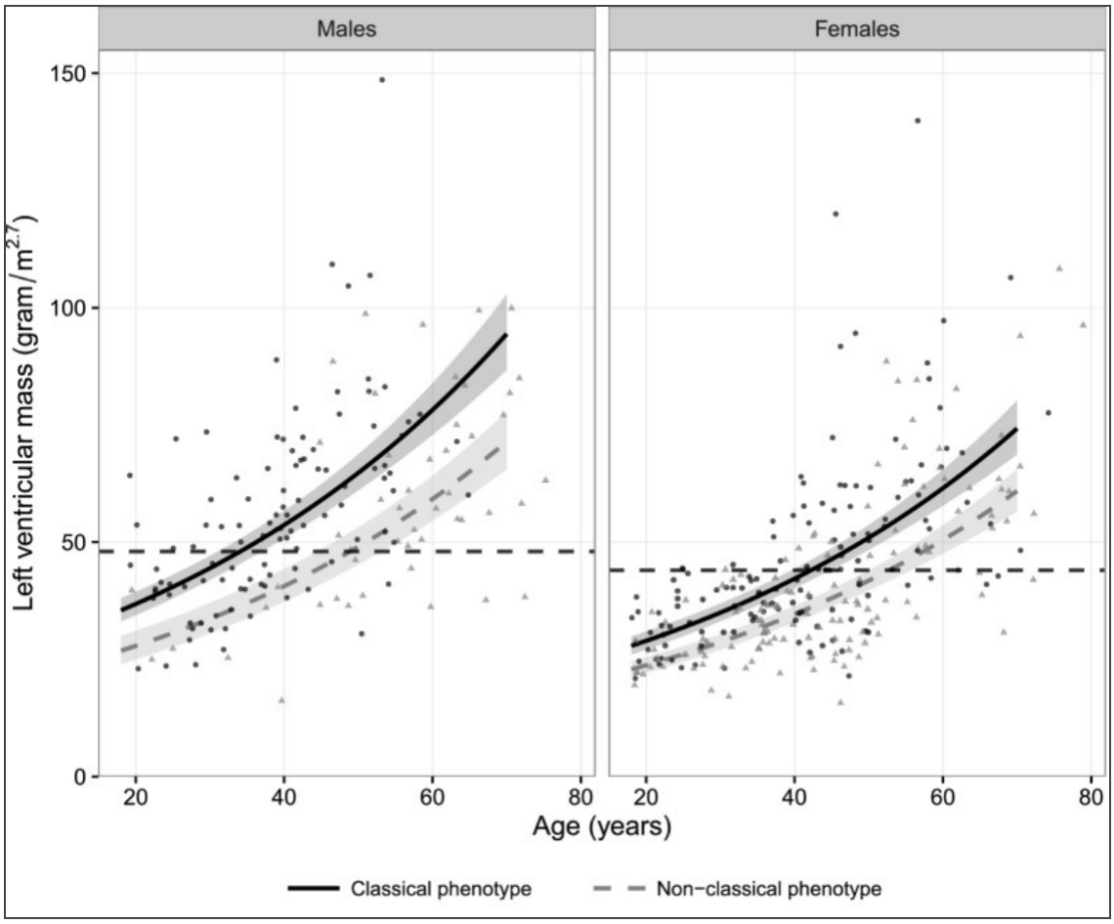

Each gender is split according to classical and non-classical Fabry disease. The dashed line represents the upper limit of normal LVMi (men: 48g/m^2 and women: 44g/m^2).

The effect of ERT on the natural progression of Fabry cardiomyopathy has been of significant interest and although ERT has been widely used since 2001, a number of queries exist regarding optimal timing to initiate therapy, when dose adjustment is needed and what the specific goals of therapy should be. The existing literature is mixed with some studies demonstrating significant improvement or stability in cardiac disease, but others showing progressive LVH despite ERT.

One of the earlier trials evaluating progression of cardiac disease using TTE in FD was by Weidemann et al (113), where the effect of ERT (agalsidase alpha) in 32 patients was assessed over a 3 year follow-up period. This study described a potential benefit of ERT in patients with earlier cardiac disease (no fibrosis on CMR and mild LVH), where normalisation of LV wall thickness and mass with improved radial and longitudinal function was observed (LV mass: baseline 238±42 vs 3 year 202±46g, $p<0.01$). Those with advanced disease (extensive fibrosis in multiple AHA segments) showed minimal reduction in LVH and minimal benefit in terms of functional improvement (LV mass: baseline 303±84 vs 3 year 247±45g, $p=0.24$). A sub-study of a cohort taken from the Fabry Outcome Survey registry evaluating the effect of agalsidase alpha in 250 patients (69% male), demonstrated a significant reduction of LVMi in females only over a 48 month follow-up period (baseline to 48month: females 48.2±17 to 43.7±16.2 g/m^2, $p=0.0031$ and males 54.7 to 52.2 g/m^2, $p=0.247$) (160). A retrospective chart review by Motwani et al (133) supported these early findings, describing a small but significant reduction in LV mass assessed by TTE over a 3 year follow-up period (LV mass before ERT 116±28 vs after ERT 113±26g/m^2, $p<0.001$). When analysed by baseline phenotype, those with LVH at baseline showed an improvement in LV mass and function (LV mass: before ERT 135±13 vs after ERT 133±13, $p<0.01$; LV ejection fraction [LVEF]: before ERT 62±5 vs after ERT 64±3, $p<0.001$) and in those

without LVH at baseline, mass and functional parameters remained unchanged, suggesting that ERT may prevent cardiac disease progression and the onset of LVH. Smaller studies such as those by Liu et al (n=18, follow-up range 13-46 months) (161) and Tsuboi et al (n=11, median follow-up 36 months) (162) have also shown a reduction in LV mass following introduction of ERT and a switch from agalsidase beta to alpha, respectively. Tsuboi et al also noted a reduction in MWT over the follow-up period (LV posterior wall [LVPW] at end diastole: 12.3 to 10.1mm, p=0.002) (162). Later studies by Kampman et al (131) have also shown similar trends, with a reduction in LVMi in both men and women 1 year following initiation of ERT (percentage reduction in LVMi: men -16.46 g/m^2 [95% CI -23.81, -9.11] and women -16.69 g/m^2 [-23.62, -9.75], $p<0.0001$ for both). They did however, suggest a possible sex dimorphism with a sustained reduction in LV mass up to 10 years after introduction of ERT occurring in men only (reduction in LV mass at 10 years: men -13.55 g/m^2, p=0.0061). The reduction in LVMi was also greater in patients with a higher LV mass at baseline ($\geq$50 g/m^2). In summary, these six studies using TTE described a reduction in LVM in patients with an earlier disease phenotype, following the introduction of ERT. With advanced disease, however, no discernible improvements in cardiac disease were observed.

More recently, the effect of ERT on progression of cardiac disease has been brought into question by Beck et al (163). This study of 317 patients followed up over 5 years showed a smaller but significant annual increase in LVMi in treated patients (ERT: males +0.33, females +0.48 g/m^2/year, no ERT: males +4.07, females +2.31 g/m^2/year). A smaller prospective study of 57 patients over similar follow-up demonstrated a significant increase in LV mass despite treatment with ERT in males only (+1.2 g/m^2 per year, $p<0.001$ vs -0.3g/m^2 in females, p=0.52) (135).

All of these existing trials however, are all small, single-centre observational studies. Only small changes in LV mass have been described with very wide standard deviations and all generally have a short follow-up duration. Additionally, they all use TTE to evaluate LV mass and wall thickness, which is well known to have limitations (164). Methods of assessing myocardial geometry include use of M-mode linear measurements with the two-dimensional (2D) cube function and the area-length method with measurements taken from 2D apical images (165,166). Both of these assume a fixed geometric shape, which is a common source of error in LV mass estimation, especially in Fabry hearts where a change in geometry is almost standard. The use of cube-function methodology has demonstrated a consistent underestimation in LV mass of 14.3g, with wide limits of agreement between reporting clinicians (±57.6g for cube-function and ±46.3g for area-length method), when comparing to three dimensional (3D) measurement using CMR (164). The use of these methods for evaluation of LV mass is also heavily dependent on endocardial border definition, which can often be challenging in echocardiography, leading to under or over-estimation of ventricular mass. For M-mode imaging cursor positioning perpendicular to the septum is crucial to ensure accuracy of measurements obtained, which may not always be possible (167). All of the studies described above utilised M-mode echocardiography with the cube function methodology in evaluating LV mass. The changes identified vary between one to 20g/m^2, all of which lie within the margin of error for measurement and thus should be viewed with caution.

Captur et al (168) have also recently shown that despite the use of high quality echo images and expert operators, the measurement of MWT in patients with HCM demonstrates a variability of ±20%. As a result of the high inter-reader variability (-59% to 117% [SD±20%]), it has been suggested that MWT should not be utilised as part of any risk

stratification tools in HCM, reinforcing the need for caution when using these parameters in hypertrophic muscles disorders such as HCM and FD.

Furthermore all of the studies to date, with the exception of two registry datasets (160,163), are small observational studies arising from single centres with a cohort size between four and 45. Thus any assessment of the causal relationship between use of ERT and cardiovascular outcomes is difficult and highly unreliable, as there is very little scope to correct for any degree of bias or confounding variables in small cohorts.

CMR imaging however, offers greater potential and is the gold standard modality for assessment of ventricular volumes and mass. Its high resolution enables a clearly defined tissue interface to facilitate cardiac analysis with greater accuracy (95% limits of agreement 0.32g [-20.1, 21.7]) (136). Changes in LV mass have been described using CMR, but all have been cross-sectional data demonstrating how mass differs across age groups, with no longitudinal component evaluating the natural progression of Fabry cardiomyopathy. Furthermore, it has been well described that papillary muscle hypertrophy and trabecular thickening often occur prior to myocardial hypertrophy, and thus contribute a significant amount towards overall LV mass, often reclassifying patients LVH status when included in LV mass assessment (152,169). The greater resolution and overall image quality with CMR, enables more accurate assessment of these structures compared to standard 2D echocardiography (152,153). CMR tissue characterisation has also revolutionised assessment of cardiovascular involvement in FD, enabling earlier diagnosis and greater potential for tracking disease progression. The relationship of native T1 to LVH has been described, but only at a single time point (37). Prior to the onset of LVH, native T1 falls in both genders, but more significantly in men ($r=-0.54$, $p<0.001$ compared to $r=-0.28$, $p=0.01$ in women). After

the onset of LVH however, the correlation reverses in men demonstrating a pseudonormalisation of native T1 ($r=0.63$, $p<0.001$) and women show no relationship between LVMi and native T1.

The lack of robust echo data and longitudinal CMR studies in Fabry highlights the need for further detailed CMR-based assessment of cardiac disease, with a larger cohort over a longer follow-up period.

4.1.1 Hypothesis

Progressive sphingolipid deposition and structural cardiac disease will occur in untreated patients with associated progression in electrical abnormalities. The use of ERT may demonstrate a protective effect on cardiac disease, delaying the onset of structural and electrical change.

4.1.2 Aims

The aim of this chapter was to define changes in cardiac structure and function that occur in FD over time using CMR, considering any alteration of the natural progression of cardiac disease by the use of ERT.

4.2 Brief methodology

4.2.1 Study population and design

This was a multi-centre study and patients were recruited from two separate cohorts, as shown in Figure 3.1. Firstly, consecutive adults with genetically proven FD attending the Rare Diseases Centre at the University Hospital Birmingham NHS Foundation Trust (UHB) as part of standard clinical care. Secondly, patients recruited to the prospective, observational

international Fabry400 study (NCT03199001) from UHB, the Royal Free Hospital London and the National Hospital for Neurology and Neurosurgery London were also included. All patients were investigated following the same protocol as that used within the UHB clinical service. Patients were eligible for the Fabry400 study if they were ≥ 18 years of age and had a genetically confirmed diagnosis of FD. Patients were excluded if they had an absolute or a relative contra-indication to CMR or if they had only undergone a single CMR scan. The first baseline visit for this study was on 14th March 2009 and final follow-up visit was on 10th April 2019.

The primary outcome measures were: LV mass and MWT. Secondary outcome measures collected included: native T1 at mid LV cavity, mass of LGE, T2 values, left atrial volumes, TTE parameters of diastolic function (septal e' and Septal E:e' ratio), PR interval and QRS duration on resting 12-lead ECGs and serum hs-Troponin levels.

4.2.2 Ethical and clinical governance approval

Health Research Authority (HRA) and ethical approval was obtained for the prospective Fabry400 study by the chief investigator (14/LO/1948), with local UHB Research and Development (R&D) registration (RRK5361). In accordance with HRA guidance, ethical approval was not required for use of data historically collected as part of clinical service, where its inclusion in research is secondary. This study was registered with UHB R&D (RRK6621) and conformed to the principles of the Helsinki Declaration.

4.2.2 Additional CMR analysis: LGE quantification

All CMR scans were reanalysed as described in Chapter 3, blinded to temporal order and patient demographics to enable accurate comparison of outcome measures from baseline to follow-up (cvi42 ®, version 5.3.4, Circle Cardiovascular Imaging, Calgary). In addition to

the methodologies described in Chapter 3, the degree of LGE was quantified using previously described techniques, with a threshold of six standard deviations above the mean signal intensity of reference myocardium (150). Endo- and epicardial contours were drawn on the SAX stack of LGE images obtained. A myocardial reference ROI was drawn and areas of LGE were highlighted on the SAX images, providing the absolute mass of LGE and its percentage of the total myocardial mass (*Figure 4.1*). All areas of LGE were validated by visual inspection.

Figure 4.3. Quantification of late gadolinium enhancement.

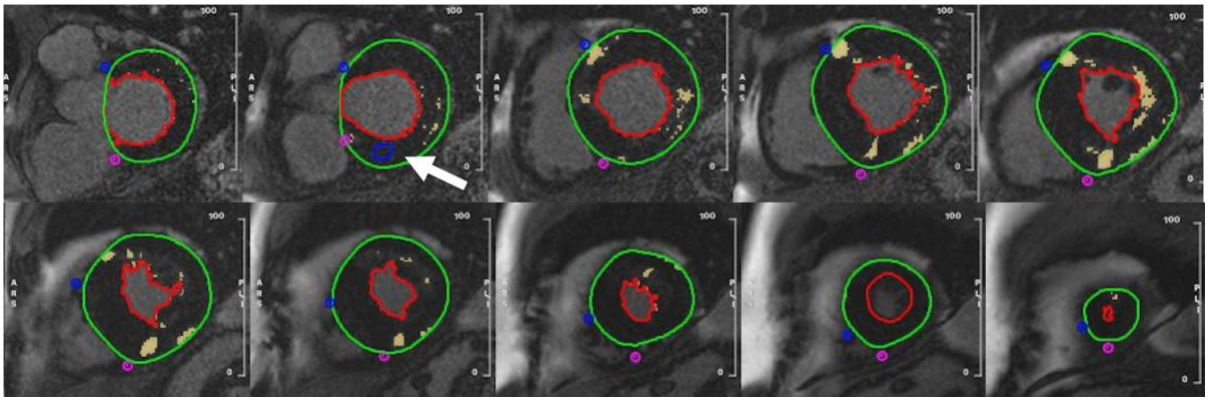

Epi- and endocardial borders were drawn on the entire LV SAX and the RV insertion point references were added. A normal myocardium reference area was drawn, as shown by the blue contour (see white arrow), and the areas of LGE are highlighted in gold. This provided the mass of LGE and its percentage of the total myocardium.

Given that T1 varies depending on magnetic field strength, image acquisition technique and gender, normal ranges were defined as mean ± two standard deviations (SD) based on healthy controls from each centre (UHB: male – 945±13, female – 966±19 and London: male – 1000±29, female – 1034±37).

4.2.3 Validity and reproducibility

Intra-observer reproducibility analysis was performed on a randomly selected subset of 10 patients. This demonstrated the following – LVM: mean absolute bias of 2.8±2.6g and an intra-class correlation (ICC) for single measures of 0.998; native T1: mean bias 5.7±4.9ms and an ICC of 0.981. Reproducibility biases were similar when evaluating inter-observer variability by a second person – LVM: mean absolute bias of 3.3±1.8g and an ICC for single measures of 0.994; native T1: mean bias 2.5±2.1ms and an ICC of 0.996. Native T1 measurements are known to differ between CMR scanners and pulse sequences, so validation of scanner stability across sites with a phantom-based quality assurance system was performed. The term phantom refers to an artificial CMR test object composed of nine agarose gel tubes with a gel/bead matrix within. The gel contains nickel chloride as the paramagnetic relaxation modifier, with a different composition providing a fixed T1 time in each tube (170). The phantom was manufactured ensuring a range of relaxation times were incorporated including those that cover, T1 and T2 times in blood/myocardium, 1.5T/3T field strengths and pre-/post-contrast administration. The phantom was scanned in all centres to ensure stability and uniformity of data (*Figure 4.2*, Birmingham: MOLLI mean coefficient of variance (CoV) for all 9 tubes 0.625%, London MOLLI mean CoV 0.805%) (170).

Figure 4.4. Internal and external structure of the phantom. Taken from Captur et al (170)

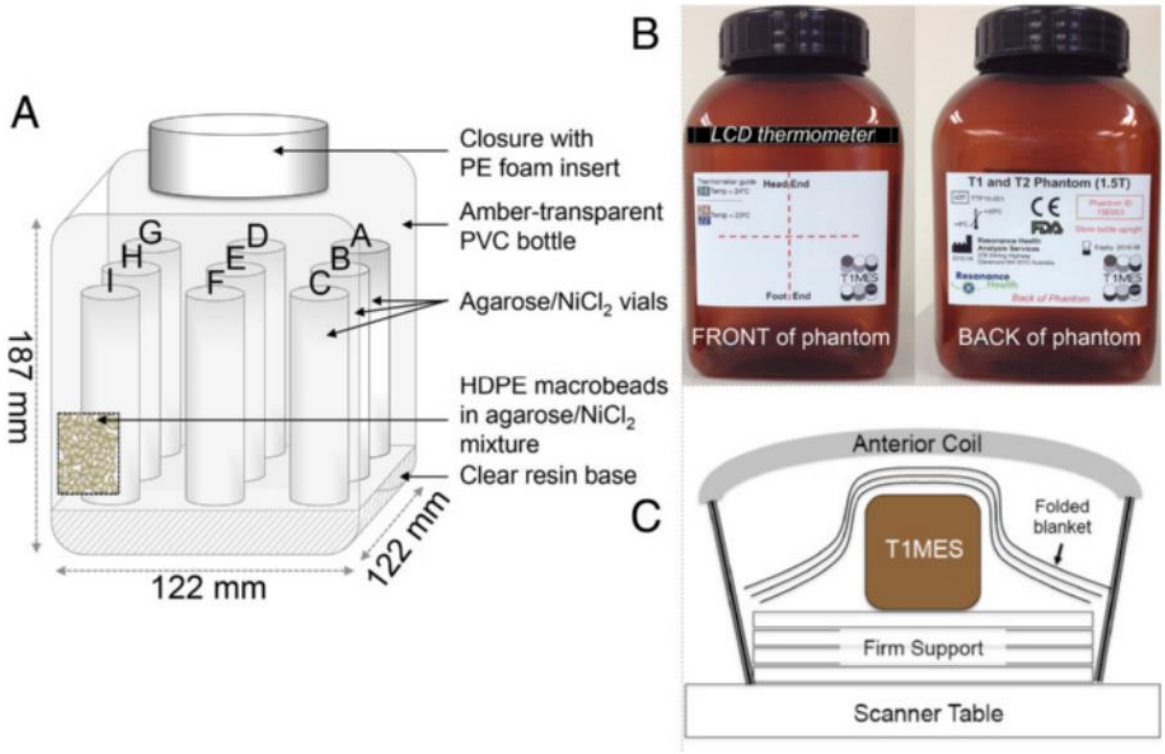

Panel A *– Phantom internal structure with nine tubes each containing a specific combination of agarose and nickel chloride.*

Panel B *– External structure of phantom (front and rear). The front of the phantom has a cross to aid positioning and to ensure scanning at isocentre.*

Panel C *– Arrangement of phantom within the CMR scanner.*

4.2.4 Statistical analysis

Statistical analyses were carried out using SPSS 23 (IBM, Armonk, NY). Initial analysis compared a range of clinical characteristics between the baseline and final visits, within subgroups defined by the patient gender. Distribution of continuous variables was assessed graphically. Those that were normally distributed were reported as mean ± standard deviation, analysed using paired t-tests, or median and interquartile range (IQR), which were

evaluated using Wilcoxon's tests. Dichotomous variables were compared between visits using McNemar's test.

The rates of change over time in each marker were subsequently assessed, with analyses performed separately for males and females, due to observed differences at baseline. General linear models were produced with the timing of the measurement relative to the baseline scan and the patient ID as fixed effects, and the marker of interest as the dependent variable. As such, each model assumed that all parameters changed with a linear trend over time, but allowed each patient to have a separate intercept, accounting for variability between patients at baseline. The residuals of the models were evaluated, to ensure the assumption of linearity was reasonable. Where poor fit was detected, the values of the marker were $\log_{10}$-transformed, and the analysis repeated. For the markers where this transformation was used, the resulting coefficients were anti-logged, and converted to percentage increases per year.
The models were extended to allow for the evaluation of the effect of ERT. A binary factor specifying ERT status was added as an additional fixed factor into each model, with an interaction term between this factor and the timing of the measurement also included. The resulting model computed separate gradients for both ERT cohorts, with the p-value for the interaction term comparing the two.

Due to extreme skew of LGE mass, on account of the large number patients without LGE, it was not possible to produce reliable models using the approach described above. Thus, this marker was analysed by initially producing separate regression models for each patient individually, with the timing of the scan as a covariate. The trend over time for the total cohort was then estimated by calculating the mean of the gradients from the resulting models, and converting this into a percentage change per year. This was subsequently compared to a

gradient of zero, using a Wilcoxon's test, to assess whether the change over time was significant. To assess the impact of ERT, the gradients were compared between groups using Mann-Whitney tests. Correlation between trends in outcome markers was assessed using similar individual patient regression methodology, with the resulting gradients being compared using Spearman's correlation coefficients. A p-value of <0.05 was deemed to be statistically significant throughout.

4.3 Results

4.3.1 Participant characteristics

In total, 100 participants were included, with a mean age at recruitment of 44±14 years and 44% men. A classical mutation was present in 59% of patients in this study and 50% were on ERT at time of the first scan (37 agalsidase-alpha; 13 agalsidase-beta). The median duration of follow-up was 37 months (IQR 20 to 60 months), during which a total of 260 follow-up visits took place (median two per patient, range 2 to 6). Demographic data from both baseline and final follow-up visits are reported in *Table 4.1*. At baseline 12% of patients had chronic kidney disease (CKD) stage 3 or above (6 male and 6 female patients), with a median eGFR of 85 ml/min/1.73m^2 (IQR 68 to >90) in men and >90 ml/min/1.73m^2 (IQR 88 to >90) in women. Additionally, 4% of patients (2 men and 2 women) had ischaemic heart disease (IHD) at baseline, which was defined as flow-limiting coronary artery disease requiring medical therapy or surgical/percutaneous revascularisation, and 10 were hypertensive requiring treatment (5 men and 5 women). There was no change in the proportion of male and female patients with CKD stage 3-5, IHD or hypertension between baseline and final study visits. The median eGFR remained stable from baseline to final study visit in male patients (85 vs. >90 ml/min/1.73m^2, p=0.590), but in female patients was significantly lower at final visit (>90 vs. 88 ml/min/1.73m^2, p<0.001).

Table 4.2 describes the CMR data of the study cohort at baseline. Cardiac chamber volume, mass and ejection fraction data on CMR and echo parameters were available at all baseline and follow-up visits. CMR tissue characterisation (T1 and T2 mapping) measurements however, became part of routine clinical imaging in 2010 for T1 mapping and 2016 for T2 mapping, thus these data were not available for all scans. Gadolinium contrast was not administered in 26 follow-up CMR scans (10 due to low eGFR and 16 due to patient choice). At baseline, men had higher LVMi and MWT compared to women (LVMi: 111.8 vs. 62.7g/m^2; MWT: 16 vs. 10mm, respectively, $p<0.001$ for both). 31 patients had LGE at baseline, with a higher proportion seen in men compared to women (49% vs. 21%, $p=0.008$). Of the total cohort, 17 patients had LGE localised to the basal inferolateral wall, 11 had extensive enhancement in more than two areas of myocardium and three patients had a small area of inferior right ventricular insertion point LGE. QRS duration was greater in men, which was in keeping with more advanced disease seen at baseline.

Table 4.1. Clinical characteristics of study population: baseline vs. final study visit.

	Male patients (n=44)			**Female patients (n=56)**		
	Baseline visit	**Final visit**	**p-value**	**Baseline visit**	**Final visit**	**p-value**
Age (years)	44 ± 13	47 ± 13	N/A	42 ± 15	46 ± 15	N/A
Classical mutation (n, %)	33 (59)	33 (59)	1.000	26 (59)	26 (59)	1.000
ERT (n, %)	32 (73)	35 (80)	0.250	18 (32)	20 (36)	0.500
BMI (kg/m^2)*	25 (20 - 27)	24 (21 - 28)	0.709	24 (21 - 27)	25 (21 - 29)	**0.030**
Heart rate (bpm)*	68 ± 12	63 ± 14	0.477	71 ± 13	72 ± 14	0.677
Systolic BP (mmHg)*	130 ± 17	129 ± 18	0.515	119 ± 13	120 ± 14	0.177
Diastolic BP (mmHg)*	75 ± 10	79 ± 13	**0.037**	72 ± 8	73 ± 9	0.859
IHD (n, %)	2 (5)	2 (5)	1.000	2 (4)	2 (4)	1.000
Hypertension (n, %)	5 (11)	7 (16)	0.500	5 (9)	6 (11)	1.000
DM (n, %)	2 (5)	3 (7)	1.000	1 (2)	1 (2)	1.000
CKD stage 3-5 (n, %)	6 (14)	6 (14)	1.000	6 (11)	6 (11)	1.000
Stroke/TIA (n, %)	4 (9)	4 (9)	1.000	1 (2)	1 (2)	1.000
eGFR ($ml/min/1.73m^2$)*	85 (68 - >90)	>90 (71 - >90)	0.590	>90 (88 - >90)	88 (79 - >90)	**<0.001**
Troponin (ng/l)*	13 (3 - 18)	18 (8 - 48)	0.125	3 (1 - 27)	5 (3 - 27)	0.180

*Data are reported as mean±SD, with p-values from paired t-tests; median (interquartile range), with p-values from Wilcoxon's tests; or as N (%), with p-values from McNemar's test, as applicable. Bold p-values are significant at p<0.05. *Analyses are based on a smaller number of cases, due to missing data.*

Table 4.2. Cardiac parameters at baseline.

	Whole Cohort (N=100)		Male (N=44)		Female (N=56)		p-value
	N	**Statistic**	**N**	**Statistic**	**N**	**Statistic**	
Cardiac MRI							
LVMi (g/m^2)	100	80 (61-120)	44	112 (85-149)	56	63 (57-83)	**<0.001**
MWT (mm)	100	12 (10-17)	44	16 (12-18)	56	10 (9-12)	**<0.001**
LV EDV indexed (ml/m^2)	100	67±13	44	70±14	56	64±11	**0.023**
LV ESV indexed (ml/m^2)	100	17±7	44	18±7	56	17±6	0.379
LVEF (%)	100	75±7	44	75±7	56	74±7	0.940
RV EDV indexed (ml/m^2)	100	66±13	44	68±12	56	64±13	0.112
RV ESV indexed (ml/m^2)	100	20±7	44	20±6	56	19±8	0.684
RVEF (%)	100	71±8	44	71±8	56	71±8	0.903
Native T1 - global mid LV (ms)	45	924±47	16	901±46	29	937±43	**0.011**
Presence of LGE (n, %)	93	31 (33)	41	20 (49)	52	11 (21)	**0.008**
*LGE Mass (g)**	31	*8 (3-18)*	20	*9 (3-20)*	11	*7 (1-15)*	0.359
*LGE Percentage (%)**	31	*3 (2-7)*	20	*4 (2-7)*	11	*2 (2-8)*	0.784
T2 – global mid LV (ms)	17	52±3	5	50±2	12	52±3	0.154
Indexed LA volume (ml/m^2)	97	40±12	42	40±13	55	39±11	0.679
RA area (cm^2)	99	19±4	43	20±4	56	18±4	0.130
2D GLS (%)	95	-17.5±3.8	41	-15.7±3.6	54	-18.8±3.5	**<0.001**
Echocardiography							
Septal e' (cm/s)	40	8 (5-11)	15	8 (4-10)	25	9 (6-12)	0.364
Septal E:e' (cm/s)	32	8 (7-12)	13	7 (7-11)	19	9 (8-16)	0.409
ECG							
PR interval (ms)	52	136 (124-156)	19	136 (127-156)	33	134 (122-156)	0.914
QRS duration (ms)	55	94 (82-106)	20	105 (98-117)	35	86 (76-96)	**<0.001**

*Data are reported as mean±SD, with p-values from independent samples t-tests; median (IQR), with p-values from Mann-Whitney tests; or as n (%), with p-values from Fisher's exact tests, as applicable. p-values are comparisons between male and female patients, and bold values are significant at p<0.05. *For the subset of patients with LGE present.*

4.3.2 Progression of cardiac parameters

Changes in cardiac markers were analysed for all study patients (n=100), with detailed data shown in *Table 4.3*. There was a significant increase in absolute LVM over time, with a gradient of 2.4% per year in men ($p<0.001$) and 1.0% per year in women ($p=0.005$). There was a similar change seen in men when using MWT as a marker of ventricular hypertrophy (1.9% increase per year, $p<0.001$). LGE mass increased by 36.6% per year in men ($p<0.001$) and by 12.0% per year in women ($p=0.011$). Native T1 decreased over time in men (3.4ms per year, $p=0.029$), but no significant change was observed in females, when evaluated as a whole cohort ($p=0.831$). There was a significant increase in PR interval and QRS duration seen in men (PR: 2.5ms per year, QRS: 2.1% per year, $p<0.001$ for both), but no change in ECG parameters was observed in women.

Table 4.3. Changes in cardiac parameters over time.

	Male				Female			
	Patients n	**Scans n**	**Gradient per year (95% CI)**	**p-value**	**Patients n**	**Scans n**	**Gradient year (95% CI)**	**p-value**
Cardiac MRI								
Absolute LVM (g)*	44	116	2.4% (1.8%, 3.1%)	**<0.001**	56	144	1.0% (0.3%, 1.7%)	**0.005**
MWT (mm)*	44	116	1.9% (1.0%, 2.7%)	**<0.001**	56	144	0.5% (-0.3%, 1.3%)	0.259
LVEF (%)	44	116	-0.3 (-0.8, 0.2)	0.200	56	144	-0.7 (-1.2, 0.2)	**0.009**
Native T1 – mid LV global (ms)	30	65	-3.4 (-6.4, -0.4)	**0.029**	44	103	-0.5 (-4.7, 3.8)	0.831
T2 – mid LV global (ms)	25	37	-0.2 (-0.7, 0.2)	0.290	41	65	-0.3 (-1.0, 0.5)	0.446
LGE mass (g)* †	40	102	36.6% (14.0%, 63.7%)	**<0.001**	48	123	12.0% (2.0%, 23.0%)	**0.011**
Indexed LA volume (ml/m^2)	44	111	0.2 (-1.0, 1.5)	0.685	56	141	0.7 (0.0, 1.4)	0.061
2D GLS (%)	43	111	0.4 (0.1, 0.6)	**0.002**	56	137	0.3 (0.1, 0.5)	**0.005**
Echocardiography								
Septal e' (cm/s)	23	58	-0.1 (-0.2, 0.1)	0.537	37	87	0.0 (-0.2, 0.2)	0.998
Septal E:e' (cm/s)*	22	53	1.5% (-2.9%, 6.1%)	0.494	37	78	-3.6% (-7.3%, 0.3%)	0.069
ECG								
PR interval (ms)	39	77	2.5 (1.3, 3.7)	**<0.001**	51	102	0.7 (-1.5,2.8)	0.538
QRS duration (ms)*	40	79	2.1% (0.9%, 3.2%)	**0.001**	54	109	0.5% (-0.2%, 1.3%)	0.180
Biomarkers								
Troponin*	35	52	18.9% (5.2%, 34.3%)	**0.008**	45	76	18.5% (3.1%, 36.3%)	**0.019**

*Results are from general linear models, as described in the methods, and represent the average increase in units per year, unless stated otherwise. Bold p-values are significant at p<0.05. *Changes over time were non-linear, hence gradients are reported as % per year increases.*

†Analysis of LGE mass was performed using an individual patient regression approach, as described in the methods.

The relationship between native T1 and LV mass has previously been shown (37) but data however, were only from a single time-point. In men, prior to the onset of LVH (LVMi <92 g/m^2), native T1 tended to reduce over time (more sphingolipid deposition, -0.77 ms per g/ m^2, p=0.182 and r=-0.340, p=0.131). Once LVH was present however, there was a reversal in the trend of native T1 (+0.37 ms per g/m^2, p=0.113 and r=0.333, p=0.027, *Figure 4.5*). No such trend was observed in women. An increase in LVMi was linked to an increase in LGE mass over time in male patients only (r=0.538, p<0.001). No other significant clinical correlations were seen. Complete correlation analysis can be seen in *Table 4.4*.

Figure 4.5. The relationship between left ventricular mass and native T1 in male patients.

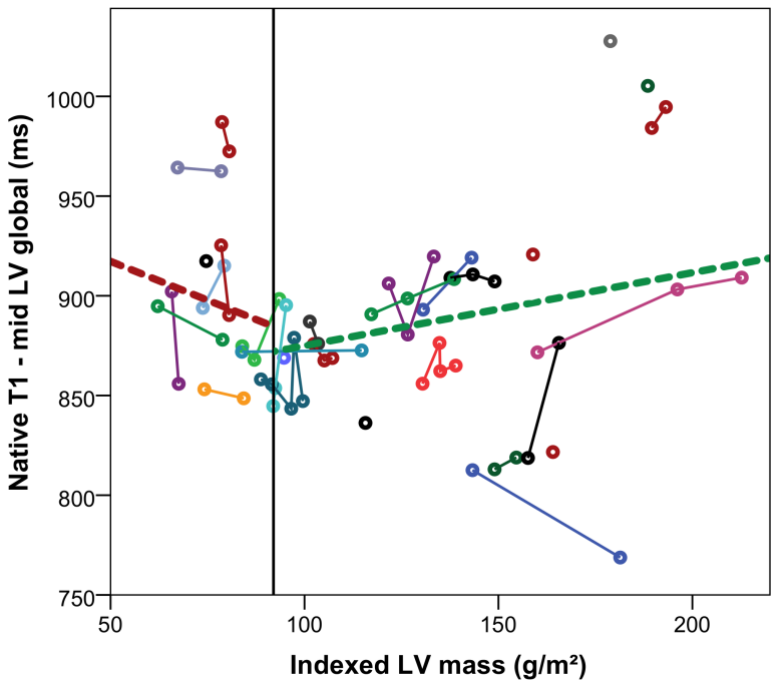

Solid lines represent individual patient trajectories. The vertical line is plotted at an LVMi of 92g/m^2. Broken lines represent the overall trends for patients without LVH (red, LVMi <92g/m^2) and those with LVH (green, LVMi >92g/m^2). They are based on general linear models, with the LVMi and patient ID as fixed factors.

No LVH (LVMi <92g/m^2): gradient of -0.77ms per g/m^2 (95% CI: -1.92, 0.37, p=0.182, r=-0.340). LVH (LVMi >92g/m^2): +0.37ms per g/m^2 (95% CI: -0.09, 0.82, p=0.113, r=0.333).

Table 4.4. Correlations between changes in cardiac markers over time.

	LVMi (g/m²)			Native T1 – mid LV global (ms)			LGE Mass (g)		
	n	***Rho***	***p-value***	***n***	***Rho***	***p-value***	***n***	***Rho***	***p-value***
Male									
LVMi (g/m²)*				-	-	-	-	-	-
*Overall**				*23*	*0.455*	***0.029***	*40*	*0.538*	***<0.001***
*LVH absent (LVMi <92g/m²)**				*10*	*0.018*	*0.960*	*15*	*0.756*	***<0.001***
*LVH present (LVMi >92g/m²)**				*13*	*0.808*	***<0.001***	*25*	*0.472*	***0.017***
MWT (mm)	44	0.494	**<0.001**	23	0.434	**0.039**	40	0.030	0.854
LVEF (%)	44	-0.214	0.163	23	0.045	0.837	40	-0.085	0.604
LGE Mass (g)	40	0.538	**<0.001**	22	0.239	0.284			
Indexed LA volume (ml/m²)	42	-0.154	0.332	22	-0.326	0.139	38	-0.184	0.269
Native T1 – mid LV global (ms)	23	0.455	**0.029**				22	0.239	0.284
T2 – mid LV global (ms)	11	-0.191	0.574	10	-0.139	0.701	11	-0.213	0.529
Septal e' (cm/s)	17	0.063	0.812	16	-0.140	0.606	16	0.375	0.153
Septal E:e' (cm/s)	16	-0.171	0.528	15	-0.146	0.603	15	-0.297	0.282
Troponin	14	0.726	**0.003**	11	-0.018	0.958	14	0.029	0.921
PR interval (ms)	22	-0.109	0.629	17	-0.373	0.141	19	0.160	0.512
QRS duration (ms)	23	0.121	0.584	18	-0.040	0.874	20	0.061	0.797
Female									
LVMi (g/m²)				38	0.169	0.309	48	0.026	0.861
MWT (mm)	56	0.346	**0.009**	38	0.415	**0.010**	48	0.089	0.546
LVEF (%)	56	-0.085	0.534	38	-0.001	0.993	48	-0.131	0.374
LGE Mass (g)	48	0.026	0.861	33	0.438	**0.011**			
Indexed LA volume (ml/m²)	55	0.093	0.499	37	-0.082	0.631	47	-0.198	0.183
Native T1 – mid LV global (ms)	38	0.169	0.309				33	0.438	**0.011**
T2 – mid LV global (ms)	22	0.420	0.052	22	0.324	0.142	20	0.153	0.519
Septal e' (cm/s)	27	0.047	0.816	25	0.138	0.509	24	0.103	0.633
Septal E:e' (cm/s)	24	0.176	0.412	23	-0.121	0.584	22	0.065	0.775
Troponin	27	-0.005	0.980	25	-0.102	0.626	23	-0.236	0.279
PR interval (ms)	36	0.110	0.525	33	-0.024	0.893	30	0.020	0.917
QRS duration (ms)	39	0.011	0.948	33	-0.090	0.618	33	0.051	0.779

4.3.3 Effect of ERT

Five patients were commenced on ERT during the period of follow-up and were excluded from analysis by ERT status. For the remaining 95% of patients, ERT usage differed significantly by gender, with 32/41 (78%) men on ERT compared to 18/54 (33%) women ($p<0.001$). Of those on ERT, three patients switched to oral chaperone therapy prior to their final CMR scan. Subgroup analysis showed that the increase in LVM over time remained in both male and female patients despite the use of ERT (*Figure 4.6*), with changes tending to be slightly higher in men. Similar gradients were observed with MWT in male patients only (*Table 4.5*).

Figure 4.6. Change in absolute left ventricular mass over time split by gender and use of enzyme replacement therapy.

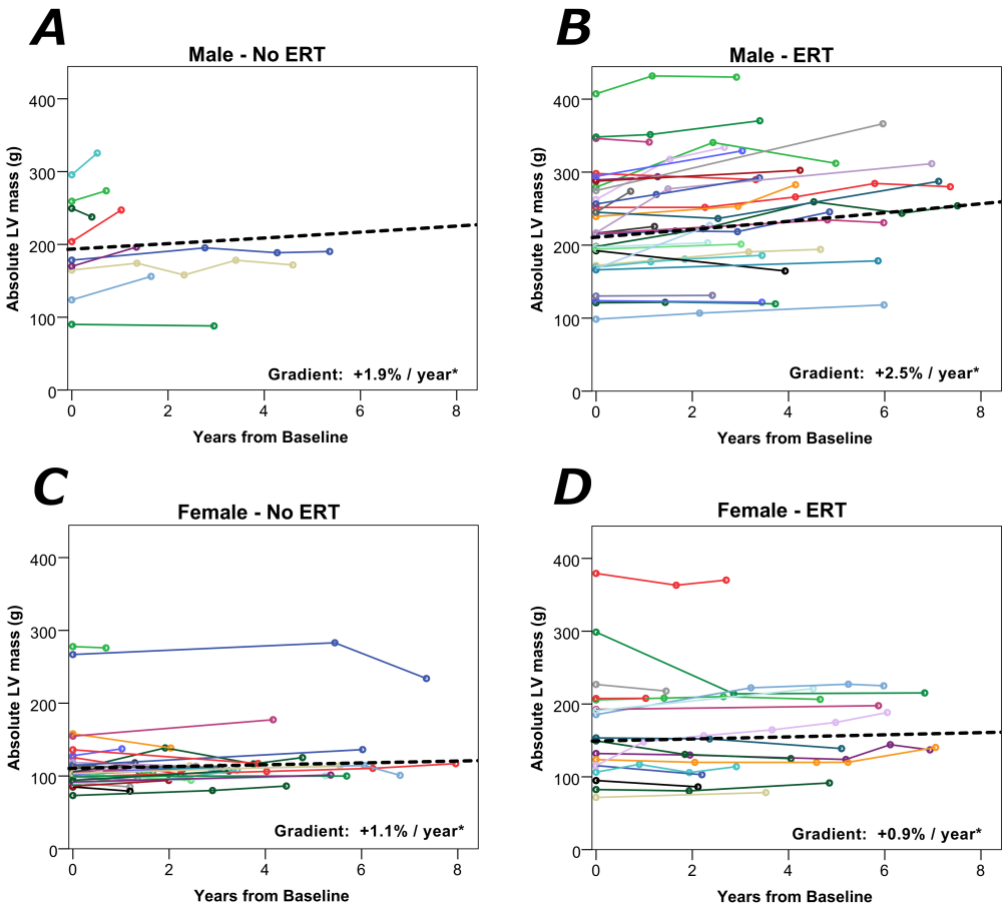

*Solid lines represent the trajectories for individual patients. The black broken lines and reported gradients are based on the general linear models from Table 4.5. *Significant at p<0.05.*

Global native T1 (measured at mid LV cavity) reduced over time in men (more sphingolipid). Although there was a tendency to a smaller reduction in male patients on ERT compared to those not on ERT, this did not reach statistical significance (gradient: -2.4ms per year vs. -7.6ms per year respectively, p=0.064; *Figure 4.7 A and B)*. In women, the rate of change in native T1 was found to differ by ERT use (p<0.001), with an average increase of 6.2ms per year (less storage, p=0.004) in the ERT group, compared to a reduction of 8.3ms per year (more storage, p<0.001) in those that not on therapy (*Figure 4.7 C and D*). The mass of LGE increased in male patients, by an average of 36.6% per year, and this gradient did not differ significantly with ERT therapy (p=0.496). This was not the case however, in the female cohort where an increase in LGE mass was observed in those on ERT (increase of 37.6% per year, p=0.004), but not in those who were not on enzyme therapy (increase of 1.2% per year, p=0.844). The PR interval increased in all male patients irrespective of ERT (no ERT: increase by 2.8ms per year , p=0.005 vs ERT: increase of 2.3ms per year, p<0.001). The QRS duration however, increased by 2.3% in those on ERT but did not change in those not on ERT, likely due to low numbers. In women, the PR interval increased by 3.4ms per year in those not on any treatment (p=0.002), but there was a reduction in the PR interval by 2.2ms per year (normalisation) in those on ERT (p=0.019), with a significant difference seen between the two groups (p<0.001). The effect of ERT on all CMR outcome variables can be seen in *Table 4.5*.

Figure 4.7. Change in native T1 over time split by gender and use of enzyme replacement therapy.

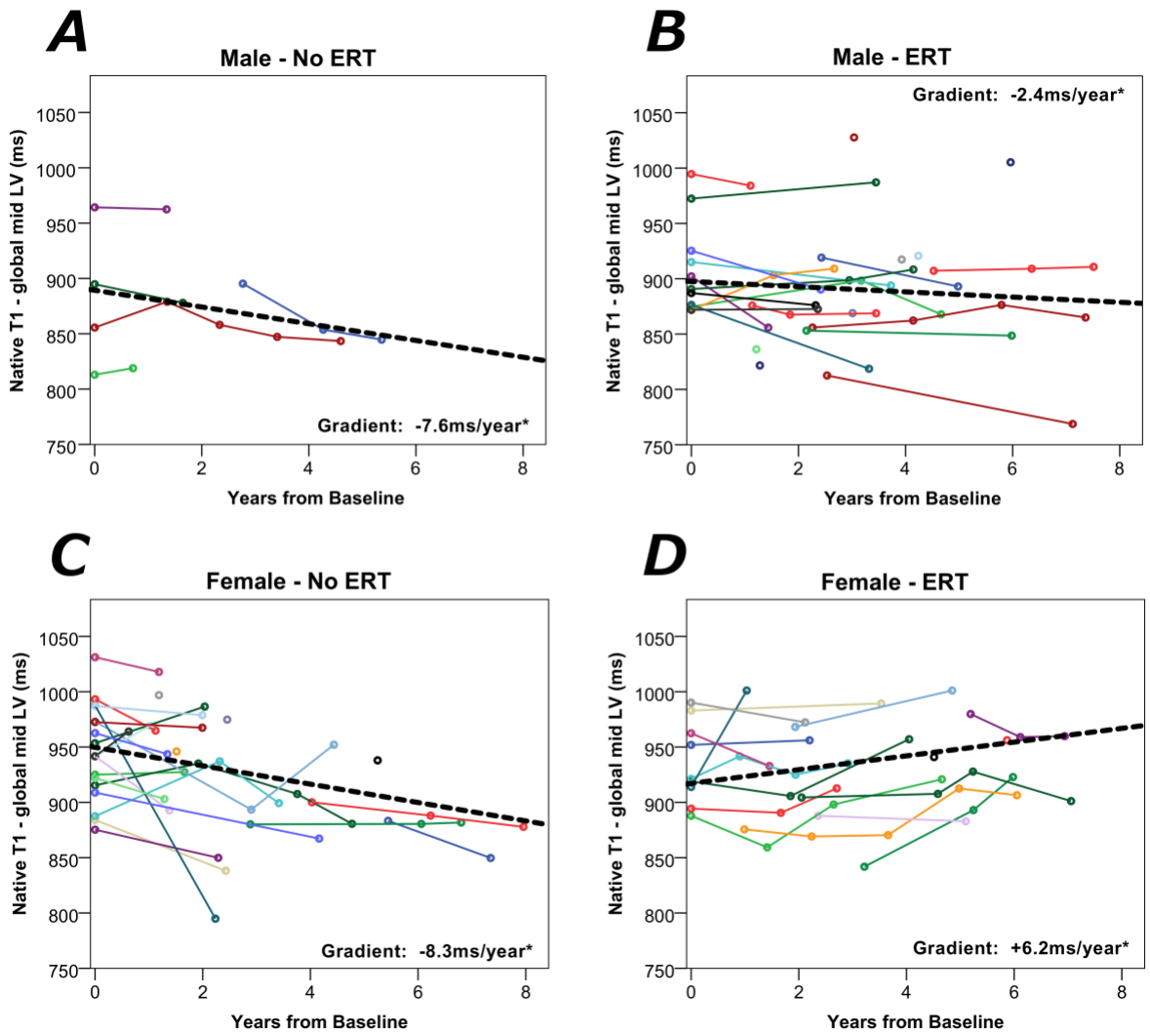

*Solid lines represent the trajectories for individual patients. The black broken lines and observed gradients are based on the general linear models from Table 4.5. *Significant at p<0.05.*

Table 4.5. Effect of ERT on changes in cardiac parameters over time.

	No ERT		ERT		No ERT vs. ERT
	Gradient per year (95% CI)	***p-value***	***Gradient per year (95% CI)***	***p-value***	***p-value***
Male *(total cohort: n=41; No ERT: n=9,ERT: n=32)*					
Absolute LVM (g)*	1.9% (0.3%, 3.6%)	**0.020**	2.5% (1.9%, 3.0%)	**<0.001**	0.508
MWT (mm)*	2.9% (0.7%, 5.1%)	**0.008**	1.7% (1.0%, 2.4%)	**<0.001**	0.317
LGE Mass (g)* †	55.7% (5.7%, 129.5%)	0.063	34.8% (7.6%, 69.0%)	**0.002**	0.496
Native T1 – mid LV global (ms)	-7.6 (-12.6, -2.5)	**0.003**	-2.4 (-4.6, -0.1)	**0.039**	0.064
T2 – mid LV global (ms)	-0.8 (-1.2, -0.3)	**<0.001**	-0.1 (-0.3, 0.2)	0.581	**0.007**
Septal e' (cm/s)	-0.1 (-0.4, 0.2)	0.605	-0.1 (-0.2, 0.1)	0.481	0.847
Septal E:e' (cm/s)*	3.9% (-3.8%, 12.2%)	0.326	1.2% (-2.3%, 4.8%)	0.510	0.536
PR interval (ms)	2.8 (0.9, 4.8)	**0.005**	2.3 (1.5, 3.2)	**<0.001**	0.669
QRS duration (ms)	0.5% (-1.6%, 2.7%)	0.638	2.3% (1.5%, 3.2%)	**<0.001**	0.128
Female *(total cohort: n=54; No ERT: n=36, ERT: n=18)*					
Absolute LVM (g)*	1.1% (0.3%, 1.9%)	**0.005**	0.9% (0.1%, 1.8%)	**0.025**	0.780
MWT (mm)*	0.1% (0.7%, 1.0%)	0.795	0.7% (-0.2%, 1.6%)	0.146	0.377
LGE Mass (g)* †	1.2% (-7.6%, 11.0%)	0.844	37.6% (13.7%, 66.5%)	**0.004**	**<0.001**
Native T1 – mid LV global (ms)	-8.3 (-12.7, -3.9)	**<0.001**	6.2 (2.0%, 10.4%)	**0.004**	**<0.001**
T2 – mid LV global (ms)	-0.7 (-1.3, -0.2)	**0.004**	0.2 (-0.4, 0.8)	0.556	**0.023**
Septal e' (cm/s)	-0.1 (-0.4, 0.2)	0.537	0.0 (-0.1, 0.2)	0.665	0.452
Septal E:e' (cm/s)*	-3.2% (8.1%, 2.0%)	0.226	-3.9% (-7.4%, -0.3%)	**0.035**	0.818
PR interval (ms)	3.4 (1.3, 5.6)	**0.002**	-2.2 (-4.0, -0.4)	**0.019**	**<0.001**
QRS duration (ms)	0.7% (-0.2%, 1.6%)	0.123	0.2% (-0.5%, 0.8%)	0.638	0.358

Results are from general linear models, as described in the methods, and represent the average increase in units per year, unless stated otherwise. p-values comparing no ERT vs. ERT are from interaction terms, thus represent comparisons between the two gradients. Bold p-

*values are significant at $p<0.05$. *Changes over time were non-linear, hence gradients are reported as % per year increases. †Analysis of LGE mass was performed using an individual patient regression approach, as described in the methods.*

4.4 Discussion

This is the first multi-centre CMR study evaluating longitudinal change in cardiac structure and function and supports a gender-specific myocardial response in FD. It is the largest non-registry study of patients with longitudinal data over a 10 year follow-up period. In groups of similar age, male patients had more advanced cardiac involvement reflected in a higher LVM and greater wall thickness and demonstrated progression of cardiac involvement at a faster rate than females. Existing data has demonstrated a possible model of disease development, suggesting that there may be distinct phases within the natural progression of FD (37). These include: (i) an accumulation phase, with subclinical sphingolipid storage within the myocardium; (ii) an inflammatory and myocyte hypertrophy phase, with progressive increase in myocardial mass and extent of LGE; and (iii) late fibrosis and impairment phase, with fibrosis, thinning and LV dysfunction (37). This model, however, was based on cross-sectional data and there has been no study evaluating changes in CMR parameters at multiple time points. The changes in men were consistent with the paradigm of disease progression in Fabry involving sphingolipid storage within the myocardium reflected by a falling T1, a myocyte hypertrophy phase, and progressive increase in myocardial mass and extent of LGE. This deterioration and progression occurred despite the use of disease modifying therapy. The pattern in women was less clear and may have been confounded by the differential impact of ERT, amongst other factors such as hypertension, CKD, IHD. In female patients on ERT, although there was a progressive increase in LVM, native T1 time significantly improved, suggesting a potential improvement in cardiovascular involvement.

The natural progression of Fabry cardiomyopathy has been a topic of great interest over the last decade with a number of studies highlighting an increase in ventricular mass in untreated patients (76,134). A study by Kampmann et al using echocardiography demonstrated an

annual increment in LV mass of 4g/m^2 in men and 2g/m^2 in women not on any disease modifying therapy (131). The data presented in this chapter are consistent with these changes but with the addition that progressive hypertrophy in males is associated with fall in native T1, reflecting progressive sphingolipid deposition, and with progressive accumulation of LGE, reflecting fibrosis. Literature describing the effect of ERT on cardiac mass however, has been more variable with some studies demonstrating a marked reduction in mass over time (132-134), but others showing stability or an increase in LVM (135). The majority of studies have used echocardiography to measure LV mass, although limits of agreement of both M-mode and 2D quantification are known to be much wider between echo studies compared to CMR. This study has shown that in men despite the use of ERT, there continues to be progression of sphingolipid deposition, cardiac hypertrophy and fibrosis. In women however, the progression in LV mass does appear to be slower and those on therapy demonstrate a potential reduction in myocardial sphingolipid storage. This gender difference is in keeping with previous literature demonstrating a more favourable disease course in women (131,160).

4.4.1 Gender dimorphism of cardiovascular disease

Gender differences in the cardiac phenotype have previously been described with male patients developing LVH first, subsequent myocardial replacement fibrosis and ultimately end-stage heart failure (113,171,172). Female patients however, often develop LGE prior to the onset of a hypertrophic response (173) and it has been suggested that this may represent a chronic inflammatory state rather than myocardial fibrosis (36). This study has demonstrated this gender disparity with an increase in myocardial hypertrophy by 2.4% per year occurring in male patients, and females tending to show more limited changes in LVM. Functional differences between men and women have also been described with male patients having

earlier impairment in myocardial strain prior to the onset of LVH (174). This study has shown that at baseline male patients have greater impairment in global longitudinal strain compared to females, despite a preserved ejection fraction. Both groups however, continued to show progressive deterioration in myocardial strain over the course of this study, suggesting that myocyte hypertrophy and increase in LV mass may be a less important intermediary step in the development of fibrosis (demonstrated by LGE) and left ventricular failure (demonstrated by impaired LV strain).

4.4.2 Variability in CMR measurement and the future of CMR assessment

Measurement of LV mass and MWT on CMR is central to diagnosis, surveillance and risk stratification in FD. As previously discussed, echocardiography has limitations and can often under or overestimate the true LVM, thus minimising its usefulness in the clinical setting. Although CMR provides greater accuracy, the variability of human measurement is currently of significant interest. Earlier studies by Moody et al (175) assessing variability in LV mass measures using 48 healthy volunteers, found that no significant changes occurred at 12 months. The smallest detectable change that could be identified with 95% confidence on serial study assessment was 5.9g, thus suggesting that any change in mass greater than this may be attributed to disease related factors. Other studies have suggested that although intra-observer error is low, the main sources of inter-observer error occurs in basal slice selection and contour definition, and emphasises the importance of consistent analysis techniques for CMR reproducibility (176).

More recently, Augusto et al (177) described significant inter-observer variability in MWT measurement even when performed by expert cardiac imaging clinicians. They evaluated 60 patients with hypertrophic cardiomyopathy and found measured MWT varied from 14.9±4.2

to 19.0±4.7mm ($p<0.001$) between observers. Review of contouring techniques also demonstrated significant variability with MWT measurements often taken at varying myocardial segments and on occasion from different short axis cine images. Automated machine learning methods have shown potential to eradicate a significant proportion of this variability. The same study compared expert observer analysis with that of machine learning, where the automated algorithm had been trained to segment endo- and epi-cardial contours from a separate, multicentre, multi-disease cohort of 1923 patients. The mean MWT evaluated from machine learning was 16.8±4.1mm and was also found to be significantly superior to human measurement, with a test-retest difference of 0.7±0.6mm with machine learning and 1.1±0.9 to 3.7±2.0mm in human expert observers ($p<0.001$) (177). Furthermore, three experts measured significantly different MWT on repeat measures, leading to a reclassification of the patients LVH status, consequently altering their risk stratification score for implantation of a primary prevention ICD. Machine learning however, was found to be consistent with no change in recommendations for device therapy in any patients. This demonstrates the future potential of machine learning to provide much better accuracy in the assessment of cardiac geometry and thus potentially enhancing our ability to track disease progression and predict adverse patient outcomes.

4.4.3 Limitations

The limitations of this study include the small size of the cohort, particularly compared to previous registry studies where echocardiography has been used to evaluate the cardiovascular effects of ERT (178). However, consistency and uniformity of the cardiac MRI protocol was maintained for all subjects. The age range of our patient cohort was limited and thus we were unable to evaluate specific changes in cardiac parameters that occur within varying age profiles. Additionally, the study cohort may be subject to selection bias.

Patients on ERT tend to have more advanced disease with more frequent CMR follow-up and thus may inherently be at risk of greater progression irrespective of therapy. Furthermore, it was beyond the scope of this observational study to assess symptom scores and changes in exercise capacity. Further randomised controlled trials described later in this thesis would be beneficial in evaluating whether the changes in LV mass, fibrosis and sphingolipid deposition observed have a functional effect on patients.

4.4.4 Conclusion

In males over time LV mass increases, T1 falls and LGE increases, despite therapy; suggesting that myocyte hypertrophy, storage and progressive fibrosis occur whether on or off enzyme replacement therapy. Over the time frame of this study, these changes in sphingolipid deposition, hypertrophy and fibrosis were less clear in women with Fabry disease, and the impact of ERT more pronounced. Although female patients receiving ERT showed an increase in LV mass, there was an improvement in T1 time, demonstrating a possible sex-dependent response to therapy.

5. Results: Early markers of Fabry heart disease: The interaction between myocardial mechanics and sphingolipid deposition

The work in this chapter is based on the published first author original article, where this data was first presented:

Vijapurapu R, Nordin S, Baig S et al. Global longitudinal strain, myocardial storage and hypertrophy in Fabry disease. *Heart*. 2019 Jan; 105: 470-46. DOI: 10.1136/heartjnl-2018-313699.

Extent of personal contribution

This study was a multi-centre study with patients recruited from the Fabry400 study. I performed the CMR studies, 12-lead ECGs and TTE for the patients recruited within UHB. Following completion of recruitment to this study, I analysed of CMR images blinded to demographic and disease information. I performed the statistical analysis and wrote the first draft of the manuscript. I was responsible for all editing and subsequent revisions.

5.1 Introduction

Cardiac involvement is a major contributor to morbidity and mortality in FD and although the definitive effect of ERT remains unclear, it has been suggested that best outcomes may occur with early initiation of therapy (113). Low native T1 as a marker of early cardiac disease has been described in detail in chapter 4, but it does have limitations and is not always readily available. Thus identification of other early phenotypic markers and utilising them in combination with each other will aid identification of early disease and may provide a potential therapeutic window before the onset of advanced hypertrophic disease. Assessment

of myocardial deformation has been demonstrated as an early marker of cardiovascular disease in general cardiology and may offer potential in FD. Contractile reserve is typically assessed by changes in left ventricular volumes, which provide the volume of blood ejected from the heart during a single cardiac cycle, but this lacks reproducibility and is extremely sensitive to haemodynamic changes within the heart. Myocardial deformation is a technique that provides more detailed objective and reproducible measures of overall cardiac function (179). The mechanics of the myocardium have been well described. During systole the ventricular myocardium shortens in longitudinal and circumferential planes and thickens in the radial plane, with reciprocal changes in diastole (179). Myocardial deformation imaging enables detailed assessment of the shortening and lengthening of muscle fibres throughout the cardiac cycle. Myocardial strain refers to the percentage change in length of a muscle fibre relative to the resting length and the strain rate is the rate at which the muscle fibre deformation occurs (179). Since there is longitudinal and circumferential shortening of muscle fibres during systole, these strain values are negative. Radial strain however is positive as the muscle fibres thicken and increase in length.

Speckle-tracking echocardiography (STE) is commonly used to assess myocardial deformation. It evaluates the motion of the ultrasound backscatter speckle pattern within the myocardium (*Figure 5.1a*). The motion of each individual speckle is assessed and combined to represent shortening and lengthening of a specific myocardial region (*Figure 5.1b*). This produces a graph showing the change in speckle motion or 'myocardial deformation' against time (*Figure 5.1c*) (179,180). STE is known to be more robust and reproducible than older Doppler based methods of assessing myocardial deformation, as it is performed on 2D echo images thus removing any error attributed to the location of the ultrasound beam (181).

Furthermore, STE does not need to be recorded real-time and can be performed post-hoc on any 2D echo images.

Figure 5.1. Speckle tracking echocardiography. Taken from Shah et al (179).

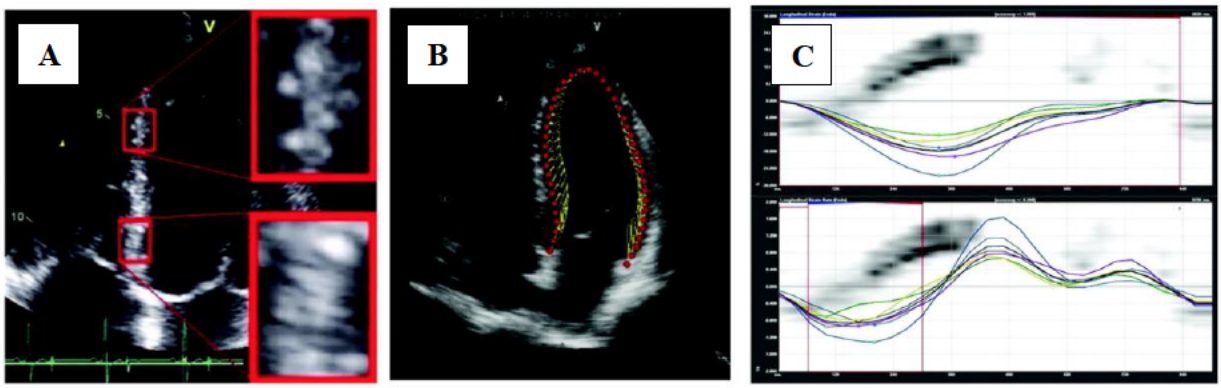

Panel A *– Ultrasound backscatter speckles used from 2D echocardiography images.*

Panel B *– Each individual speckle is allocated a specific marker and motion is tracked during the cardiac cycle.*

Panel C *– Graphical output of percentage change from resting state of individual speckles against time.*

Evaluation of myocardial deformation has provided a greater understanding of functional changes that occur prior to the impairment of LVEF. Particular interest has been in identifying the transition from subclinical disease to overt phenotypic disease. Subclinical changes in longitudinal and circumferential strain are well documented in many conditions that predispose patients to overt heart failure, such as hypertension, chronic kidney disease and AF (182-184). Its use in FD in patients with and without LVH has also been described. A study by Shanks et al in 2013 (185) compared 16 FD patients with 24 healthy volunteers (HV) and found that longitudinal systolic strain and diastolic isovolumic strain rate were more impaired (less negative) in FD compared to HV, following correction for LVH status (longitudinal strain: FD -16±3.8 vs HV -19.5±1.8, $p<0.001$; diastolic strain rate: FD

0.15±0.08 vs HV 0.35±0.11, p<0.001). A more recent study comparing a group of 19 FD patients without LVH to 19 age, gender, BMI and cardiovascular risk factor matched HV has supported these findings. When compared to HV the FD patients had lower mean systolic myocardial velocity (7.33±1.28 vs 10.8±1.63cm/s, p<0.0001) and a more impaired (less negative) systolic strain (-18.07±1.72 vs -21.15±2.22%, p<0.0001) (186). Despite these changes still being within the normal range, they are strongly associated with a worse functional status and deterioration in NYHA classification (187).

Historically myocardial deformation was assessed on CMR using myocardial grid tagging, which requires specific image sequences, dedicated post processing software and can be extremely time-consuming for the operator (188). More recently CMR feature-tracking (CMR-FT) has been shown to effectively quantify myocardial strain, using tissue voxel motion tracking on SSFP cine images to accurately identify myocardial deformation parameters (188). Studies comparing STE and CMR-FT have shown a high degree of correlation between the two modalities (r=0.71, p<0.001), but reproducibility was found to be greater with parameters evaluated by CMR-FT (188,189).

Abnormalities in CMR-FT have been described in Fabry patients with progressive cardiomyopathy. A study by Zhao et al (190) of 20 FD patients found that global longitudinal and circumferential strain deteriorated in patients with progression through the stages of Fabry cardiomyopathy (GLS: LVH negative -14.1±2.4 vs LVH positive -11.4±27 vs LVH positive with extensive LGE -7.7±1.4%). No study to date however has utilised native T1 mapping to identify FD patients with subclinical cardiac disease and compare changes in myocardial deformation to those with advanced disease.

5.1.1 Hypothesis

Mechanical dysfunction on CMR is associated with early sphingolipid storage and ECG abnormalities prior to the onset of structural change.

5.1.2 Aims

The aims of this study were to determine whether early storage (low native T1 measured using T1 mapping) would alter myocardial contractility (measured using CMR-FT) before the development of LV hypertrophy.

5.2 Brief methodology

5.2.1 Study population and design

This was a multi-centre trial with patients recruited from four Fabry clinics as part of the Fabry400 study (NCT03199001) – three UK sites and one international site in Australia. Patients were eligible for recruitment into the Fabry400 trial if they were gene-positive for FD and ≥18 years of age. Patients were excluded from this study if they had any contraindications to CMR. CMR and blood sampling was done during the same study visit. Hs-troponin T was measured in the UK and hs-troponin I in Australia (hs-TnT and hsTnI) , with normal ranges of 0-14 and 0-15ng/l respectively. Additionally, a cohort of HV were provided by our collaborative research group for comparison within this study. They were prospectively recruited as part of a study of myocardial native T1 and extracellular volume with healthy ageing and gender (191). These participants were recruited from the Bart's Heart Centre, London and had no history or symptoms of cardiovascular disease or diabetes mellitus. All HV had a normal health questionnaire and were not on any cardioactive medication unless for primary prevention.

5.2.2 Ethical and clinical governance approval

This study was approved by the relevant Research Ethics Committees and local Clinical Governance departments, as described in section 4.2.2. Written informed consent was obtained from all patients, as part of recruitment to Fabry400.

5.2.3 Additional CMR analysis: 2D global longitudinal strain

All CMR scans were analysed as described in Chapter 3, blinded to patient ID and clinical details (CVI42 ®, version 5.3.4, Circle Cardiovascular Imaging, Calgary). In addition to the standard CMR analysis methods described previously, 2D global longitudinal strain (GLS) was also evaluated. Smooth epicardial and endocardial borders were manually drawn on the end-diastolic frame of all long axis images (4-chamber, 2-chamber and 3-chamber views), and then strain (peak GLS, the most negative value during systole) was obtained from the applied automatic feature-tracking (FT) algorithm (example, *Figure 5.2*). FT evaluates myocardial strain by utilising a deformable 2D model and translating this onto all 2D cine slices selected over the entirety of the cardiac cycle. The extent of deformation is determined by motion of an imaginary line placed between endo- and epicardial boundaries, which are tracked throughout the cardiac cycle by a pre-determined algorithm as previously described (192,193). The accuracy of FT was confirmed manually for each case and to ensure reproducibility a maximum of five operator corrections were performed during analysis.

Figure 5.2. Evaluation of myocardial deformation using CMR feature tracking.

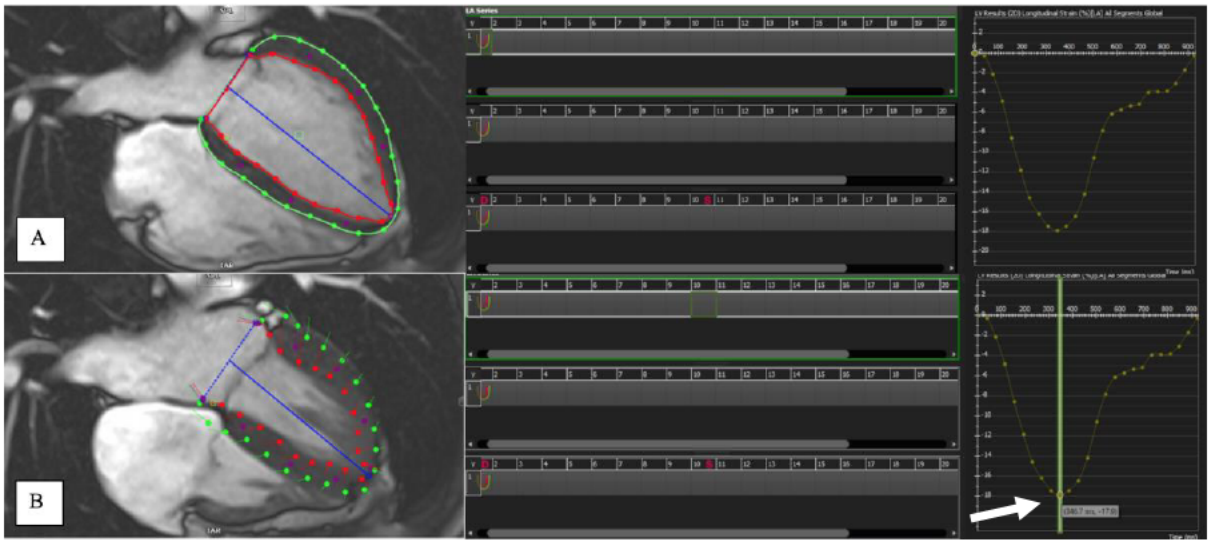

2D feature tracking performed using VLA, HLA and 3 chamber LV cines. Epi- and endocardial borders and LV reference axes are manually drawn on the end-diastolic phase (panel A). The feature tracking module on Circle Cvi42 formulates markers that track the myocardium throughout the cardiac cycle. This demonstrates motion of individual components of the myocardium providing a graph of percentage deformation over time. From the end-systolic phase (panel B), the peak global longitudinal strain can be identified (see arrow).

5.2.4 Validity and reproducibility

Intra-observer reproducibility analysis performed following repeat evaluation of 30 CMR scans demonstrated a mean absolute bias of 0.7±0.6 with an ICC for single measures of 0.98 (95% CI: 0.96-0.99). Reproducibility biases were similar when assessing inter-observer reproducibility following analysis of a subset of 20 CMR scans by an alternative observer – mean absolute bias 0.6±0.5 and ICC for single measures of 0.99 (95%CI: 0.97-1.0).

5.2.5 Statistical analysis

Statistical analyses were carried out using SPSS 22 (IBM, Armonk, NY). Continuous variables are expressed as mean ± SD, categorical as frequencies or percentages. Normality was checked by visual inspection of histogram data and using the Shapiro-Wilk test. Groups were compared using the independent-samples t-test for normally distributed data or Mann-Whitney U testing for non-normally distributed data. Chi-squared testing was used to compare proportions between two groups. Troponin values were analysed after log transformation using parametric testing. Linear regression analysis (stepwise backward method) was performed to evaluate the relationship between multiple continuous variables and the study outcome. A p-value of <0.05 was considered statistically significant.

5.3 Results

5.3.1 Participant characteristics

In total 298 patients were included in this study (221 FD and 77 HV). Baseline demographics can be seen in *Table 5.1*. The mean age for the FD cohort was 45±15 years with 85 males (39%) and 136 females (62%). The HV population was age-matched (± 2 years) with a mean age of 49±14 years (52% men). LV function (as defined by LVEF) was normal in 73±8% of the FD cohort. LVMi and MWT were higher in FD compared to HV (LVMi: FD – 89±39 vs. HV – 56±10g/m^2, MWT: FD – 12±5 vs. HV – 9±2mm, p<0.01). There was significant correlation between LVMi and MWT in both groups (FD: r=0.9 and HV: r=0.7, p<0.001). A classical mutation was present in 71% of patients. Of the FD cohort, 102 (46%) were LVH positive.

Table 5.1. Participant demographics and basic CMR findings.

	Healthy volunteers	Fabry Total	Fabry Males	Fabry Females	p-value*
Sample size (n, %)	77 (100)	221 (100)	85 (38.5)	136 (61.5)	-
Age (years)	49±14	45±15	45±15	44±15	NS
LVEF (%)	70±6	73±8	71±9	74±7	<0.05
LVEDV (ml)	132±28	131±32	146±37	121±23	<0.05
LVESV (ml)	40±12	36±17	43±21	32±13	<0.05
GLS	-19.3±2.0	-18.5±3.6	-16.3±3.3	-19.9±3.0	<0.05
Native T1 (ms)	955±30	879±64	839±52	905±58	<0.05
LGE (n,%)	0 (0)	77 (100)	36 (46.8)	41 (53.2)	<0.05
LVH-positive (n,%)	0 (0)	102 (100)	63 (61.8)	39 (38.2)	<0.05
LVMi (g/m^2)	56±10	89±39	116±43	71±25	<0.05
MWT (mm)	9±2	12±5	15±5	10±4	<0.05
Troponin (µg/L) †	N/A	6 (1-31)	18 (4-50)	4 (1-17)	<0.05

**p-value is for Fabry male-to-female comparisons.* † Non-parametric data presented as median (IQR).

5.3.2 Global Myocardial Strain

Ventricular function measured by LVEF did not correlate with LVMi (r=0.004, p=0.9). GLS, however, became increasingly impaired (values becoming less negative) as there was an increase in LVMi (r=0.728, p<0.001, *Figure 5.3 A and B*). The LVH positive FD group demonstrated greater impairment in GLS compared to FD patients who were LVH negative and HV (*Table 5.2,* p<0.05). This was similar when split by gender, however a greater difference was seen in men (*Table 5.2*). Similar relationships were observed when correlating LVEF and GLS with MWT as a marker of myocardial hypertrophy (*Table 5.3*).

Figure 5.3. Correlation between functional markers and LV mass.

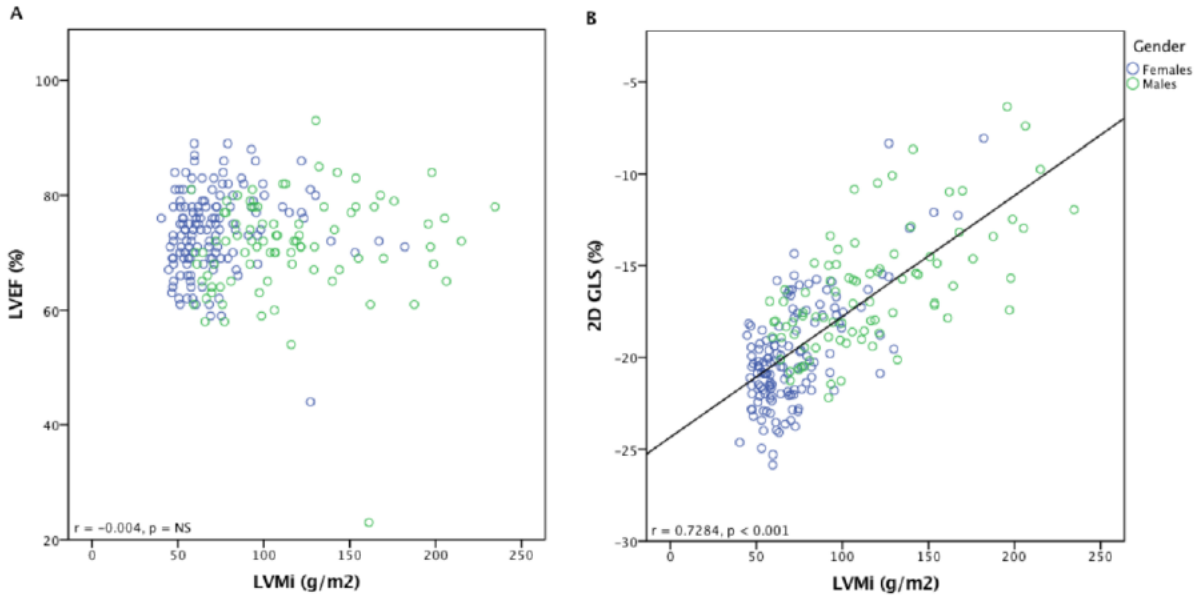

Graph A *– LV ejection fraction compared to LVMi demonstrated no correlation.*

Graph B *– There was a positive correlation between 2D GLS and LVMi.*

Table 5.2. Mean global longitudinal strain in various groups of the total study population.

	Healthy volunteers		Fabry disease		p-value*
	N	Mean ± SD	N	Mean ± SD	
Study population					
Total	77	-19.3 ± 2.0	221	-18.5 ± 3.6	0.02
Male	40	-18.5 ± 1.8	85	-16.4 ± 3.3	0.001
Female	37	-20.2 ± 1.9	136	-19.9 ± 3.0	0.46
LVH positive					
Total			102	-16.4 ± 3.6	0.001
Male			63	-15.5 ± 3.4	0.001
Female			39	-17.8 ± 3.5	0.001
LVH negative					
Total			119	-20.3 ± 2.6	0.001
Male			22	-18.3 ± 1.6	0.62
Female			97	-20.9 ± 2.5	0.19

**p-values are comparing Fabry to healthy volunteers in all groups.*

Table 5.3. Correlation between different variables in the total population and the LVH negative cohort.

Variables	Correlation coefficient (R^2)	p-value
Total cohort (n=221)		
LVMi + MWT	0.9	<0.001
MWT + LVEF	0.1	<0.05
MWT + GLS	0.7	<0.01
LVH negative (n=131)*		
T1 + GLS	-0.3	0.03

**LVH negative classified as MWT ≤12mm*

5.3.3 Myocardial Native T1 and Strain

In the total FD cohort, 72% (n=159/221) had a low native T1 – 91% of those were LVH positive (93/102) and 56% LVH negative (66/119). There was a negative correlation between GLS and native T1 in the total FD cohort (r=-0.515, p<0.05; *Figure 5.4a)*.

Figure 5.4. Relationship between native T1 and 2D global longitudinal strain.

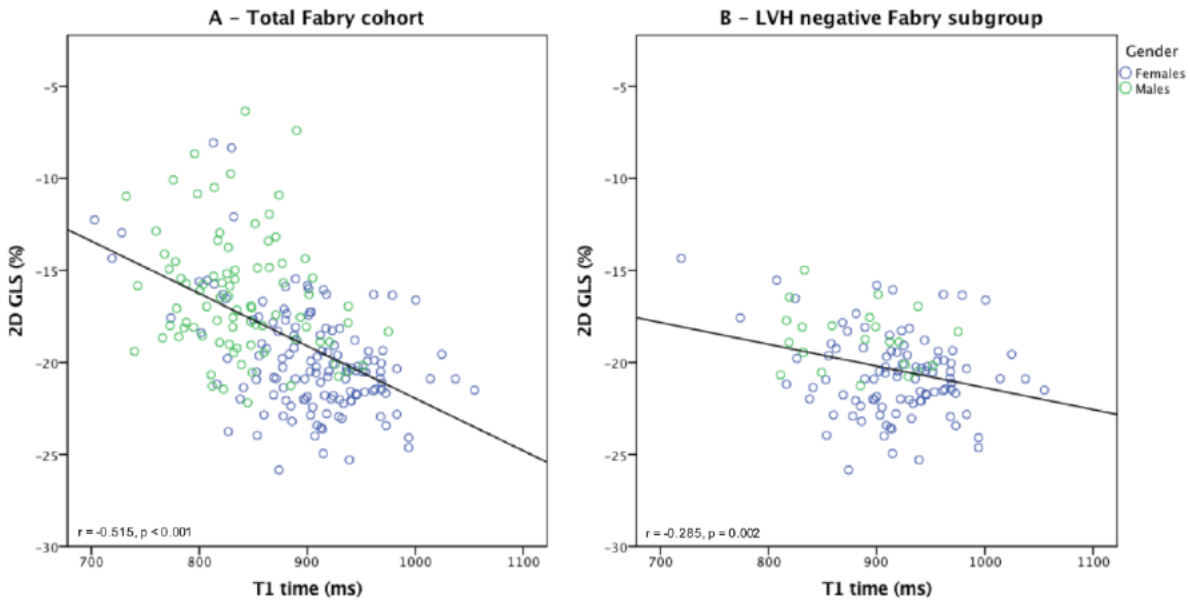

Graph A *– Total Fabry cohort*

Graph B *– LVH negative Fabry subgroup: weaker but significant correlation.*

5.3.4 LVH Negative FD Population

Of the total FD population 119 (54%) were LVH negative (defined using LVMi ranges). The mean age of this group was 37±13 years, which was lower than the LVH positive group (53±12 years, p<0.05). 82% were female and a classical mutation was present in 69%. LVMi was higher compared to HV (FD: 62±10 vs. HV: 56±10g/m2, p<0.05), but no difference in MWT was observed (FD: 9±2 vs. HV: 9±2mm, p=0.5). GLS in LVH negative FD was lower (less impaired) when compared to HV (-20.3±2.9 and -19.3±2.0, p<0.05). When split by gender no differences were observed (*Table 5.2*).

In LVH negative FD patients, as native T1 reduced an impairment in GLS was seen (r=-0.285, p<0.05; *Figure 5.4b)*. When split by gender only males demonstrated impairment in GLS as T1 reduced (*Figure 5.5*, *Table 5.4*). When classifying LVH by MWT similar significant trends were observed.

Figure 5.5. Mean global longitudinal strain in Fabry patients and healthy volunteers.

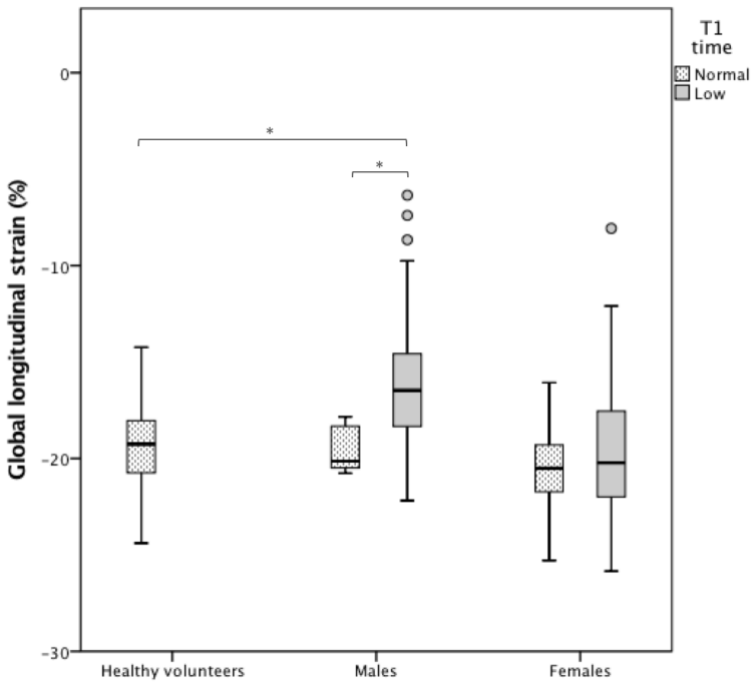

denotes p-value <0.005

Table 5.4. Global longitudinal strain in the LVH negative Fabry population classified according to native T1 compared to healthy volunteers.

	Healthy volunteers		Fabry disease			
			Normal T1		Low T1	
	N	Mean ± SD	N	Mean ± SD	N	Mean ± SD
Total	77	-19.3 ± 2.0	53	-20.5 ± 1.9	66	-20.2 ± 2.6
Male	40	-18.5 ± 1.8	5	-20.0 ± 1.0	17	-18.3 ± 1.6
Female	37	-20.2 ± 1.9	48	-20.6 ± 2.0	49	-20.9 ± 2.5

Regression analysis identified firstly that LVMi and ECG abnormalities were independent predictors of an impairment in GLS, and secondly, that LVMi and GLS were predictors of low T1. These associations were observed in both the total population and the LVH negative cohort (*Table 5.5*).

Table 5.5. The relationship of GLS and native T1 with baseline clinical characteristics (linear regression analysis).

Dependent variable	Independent variables	Uni-variable analysis				Multivariable model			
		Coefficient	95% CI	p	R^2	Coefficient	95% CI	p	R^2
Total population (n=221)									
GLS (%)	Age (years)	0.35	0.05-0.11	<0.01	0.12				
	LVMi (g/m^2)	0.68	0.05-0.07	<0.01	0.46	0.60	0.04 to 0.07	<0.01	0.49
	LGE	0.36	1.62-3.11	<0.01	0.13	-0.15	-2.04 to 0.08	0.069	
	Male gender	0.35	1.04-1.98	<0.01	0.12				
	Troponin	0.52	1.80-3.11	<0.01	0.27				
	T1 time (ms)	-0.47	-0.03-0.18	<0.01	0.22	0.27	-0.02 to 0.006	<0.01	
T1 time (ms)	LVMi (g/m^2)	-0.58	-1.20 to -0.86	<0.01	0.34	-0.22	-0.70 to -0.07	0.016	0.35
	GLS (%)	-0.47	-11.59 to -7.44	<0.01	0.22	-0.27	-8.50 to -1.94	0.002	
	Age (years)	-0.35	-2.02 to -9.6	<0.01	0.12	-0.17	-1.29 to -0.17	0.011	
	LGE	-0.53	-91.15 to -61.38	<0.01	0.28				
	ERT	-0.46	-76.10 to -48.49	<0.01	0.21	-0.13	-32.92 to -0.27	0.046	
LVH negative (n=119)									
GLS (%)	Age (years)	-0.15	-0.06 to 0.005	0.096	0.024				
	LVMi (g/m^2)	0.386	0.05 to 0.12	<0.01	0.15	0.35	0.03 to 0.12	0.001	0.22
	Male gender	0.34	1.00 to 3.03	<0.01	0.12				
	T1 time (ms)	-0.29	-0.02 to -0.01	0.002	0.081	-0.20	-0.17 to 0.00	0.058	
	Troponin	0.17	-0.23 to 2.03	0.118	0.03				
T1 time (ms)	LVMi (g/m^2)	-0.40	-2.99 to -1.20	<0.01	0.16	-0.28	-2.48 to -0.52	0.003	0.29
	GLS (%)	-0.29	-11.10 to -2.64	0.002	0.08	-0.18	-9.14 to -0.52	0.047	
	Age (years)	-0.10	-1.18 to 0.33	0.267	0.01	-0.30	-74.53 to -20.76	0.001	
	LGE	-0.29	-75.21 to -16.38	0.03	0.09				
	ERT	-0.22	-45.58 to-4.33	0.18	0.05	-0.19	-41.0 to -1.89	0.032	

5.3.5 ECG abnormalities

ECG abnormalities were identified in 45% of the total FD population, with a greater proportion seen in LVH positive patients compared to those without evidence of LVH (LVH positive: 75% vs. LVH negative: 25%). In the total cohort, GLS was more impaired in patients who were found to have ECG abnormalities (ECG abnormal: -16.7±3.5 vs. ECG normal: -20.2±2.4, p<0.001). When evaluating according to LVM, the same trends were seen in the LVH positive group, but only females showed a difference in GLS with ECG abnormalities in the LVH negative group (*Table 5.6*).

Table 5.6. Global longitudinal strain in LVH positive and LVH negative Fabry patients classified according to ECG abnormalities.

		ECG normal		ECG abnormal		p-value
	N	N	Mean ± SD	N	Mean ± SD	
Total cohort						
Fabry total	204	112	-20.2±2.4	92	-16.7±3.5	<0.001
Male	77	29	-18.4±2,0	48	-15.6±3.1	<0.001
Female	127	83	-20.8±2.2	44	-18.0±3.6	<0.001
LVH positive						
Fabry Total	93	23	-18.7±2.6	70	-15.9±3.4	<0.001
Male	56	13	-17.8±2.2	43	-15.2±3.1	0.006
Female	37	10	-19.9±2.7	27	-17.0±3.7	0.03
LVH negative						
Fabry Total	111	89	-20.6 ± 2.2	22	-19.3 ± 2.6	0.02
Male	21	16	-18.8 ± 1.8	5	-18.7 ± 0.5	0.80
Female	90	73	-21.0 ± 2.1	17	-19.5 ± 3.0	0.02

p-values are comparing ECG normal vs. ECG abnormal in all groups.

5.3.6 ERT

ERT usage occurred in 54%, with a difference in peak GLS in those on ERT (on ERT: -17.6±3.8 vs. no ERT: -19.7±2.9, p<0.01). Evaluation by gender demonstrated this difference in females only (female: on ERT -19.2±3.5 vs. no ERT -20.4±2.5, p<0.05; male: on ERT -

16.2±3.5 vs. no ERT -16.9±2.5, p=NS). Within the LVH negative group 36% were on ERT, but no differences in GLS were seen.

5.3.7 Late Gadolinium Enhancement

Of those patients who had Gadolinium contrast imaging 77 (35%) had LGE. GLS was more impaired in FD patients with LGE (LGE: -17.1±3.7 vs. no LGE: -19.7±2.5, $p<0.05$). FD patients with LGE also had a more impaired GLS when compared to HV (FD LGE: -17.1±3.7 vs. HV: 19.3±2.0, $p<0.05$). Of the patients without LVH, 14 had LGE (17%, all females) and no change in GLS was seen (LGE: -20.4±2.2 vs. no LGE: -20.1±2.2 vs. HV: 19.3±2.0, p=0.6).

5.3.8 Biomarkers

156 (71%) had hs-TnT or hs-TnI measured and 28% had an elevated level above reference ranges. Median troponin in the total study population was 6.0µg/L (IQR: 1-31µg/L). An increasing troponin level was associated with impairment in GLS in the total FD population ($r=0.516$, $p<0.05$). In the LVH negative group only five had an elevated troponin level with all other patients having a value <5ug/L. No significant relationship was demonstrated between GLS and troponin in this group ($r=0.169$, $p=0.118$).

5.4 Discussion

This study has shown that impaired GLS occurs despite a normal LVEF. The impairment in GLS occurs in proportion with an increase in LVM and storage in the overall FD cohort, and correlates with progressive myocardial damage (demonstrated by LGE and increased serum troponin). In pre-phenotypic FD (LVH-negative), an impairment in GLS is associated with low native T1 in males, but not in females, suggesting that Fabry males may have mechanical

dysfunction prior to the onset of LVH when there is evidence of sphingolipid deposition (low T1). Females, however, only display mechanical dysfunction once phenotypic disease (LVH) is present.

As described throughout this thesis cardiovascular disease is the commonest cause of morbidity and mortality in FD. Thus, prompt identification of cardiovascular involvement and earlier initiation of treatment is essential to improve disease outcomes. Subclinical sphingolipid deposition can be identified through T1 mapping on CMR, and T1 is known to be low in 40-50% of LVH negative patients, suggesting that sphingolipid deposition occurs earlier in the process before the onset of hypertrophy (121,123). The presence of LGE without myocardial thinning and aneurysm formation has been associated with an elevated T2 signal on CMR and increased troponin, suggesting that this LGE may represent an area of chronic inflammation and not scar (36). Consequently the precise pattern and development of the Fabry cardiac phenotype is gradually being pieced together, with a specific model of disease progression described in recent literature. This study has described a new biomarker of myocardial mechanical dysfunction that appears to be more sensitive than the ejection fraction to early changes in myocardial performance. This study supports the existing echocardiographic literature describing impairment in GLS when overt cardiac involvement is present (LVH positive disease), but provides a clearer insight into patients with earlier subclinical disease. Existing data has demonstrated impairment in GLS by STE in a small sample (n=25) of LVH-negative FD with low T1 compared to LVH-negative with normal T1. This study expands on these findings by using a much larger cohort and is the first study to assess myocardial strain by CMR in conjunction with T1 mapping to demonstrate a gender difference.

5.4.1 Gender dimorphism in Fabry cardiomyopathy

The possibility of gender differences in the myocardial response to sphingolipid deposition is being increasingly discussed within Fabry disease (87). As LVH progresses, male patients tend to demonstrate a pseudonormalisation of T1, which may occur as a result of an increasing myocardial mass diluting the proportion of sphingolipid within the cardiac tissue. Furthermore, differences in LGE have also been described, with female patients often exhibiting LGE within the basal inferolateral wall prior to the onset of LVH, but male patients without LVH rarely demonstrating any LGE (111,173). This study has demonstrated that mechanical dysfunction also appears to have gender dimorphism with female patients who are LVH negative tolerating sphingolipid deposition better than males. The data within this chapter has shown that GLS remained unchanged in females irrespective of T1, whereas men had an impaired GLS with T1 lowering. This may suggest that sphingolipid deposition is poorly tolerated in men, thus leading to earlier functional impairment.

5.4.2 Limitations

The limitations of this study include that it is only a single time point study with no follow-up data, but it is multicentre with a relatively large number of participants for a rare disease. Furthermore, this study is only evaluating 2D GLS and not 3D strain. Earlier data analyses included assessment of 3D longitudinal, circumferential and radial strain, all of which demonstrated similar patterns to 2D GLS. When using LV short axis images to assess 3D strain parameters in FD patients with LVH and cavity obliteration, there was significant impairment in myocardial border tracking, thus excluding a large proportion of the study cohort. As a result of this only 2D GLS was evaluated as part of this study. Further studies are also required to establish whether earlier initiation of ERT based on a low T1 or impaired GLS in the absence of LVH will affect the progression of cardiac involvement.

5.4.3 Conclusion

In FD patients with LVH, myocardial strain (measured by GLS) reduces with hypertrophy, storage (measured by a low T1) and scar (measured by LGE). In pre-phenotypic disease (LVH negative), GLS is impaired in men, but preserved in females when T1 is low, suggesting a possible gender difference in the myocardial functional response to storage.

6. The use of digital advanced electrocardiogram analysis in detection of cardiovascular disease in Fabry

The work in this chapter is based on the first author original article, which is currently under review in JACC: Cardiovascular Imaging, where this data was first presented:

Vijapurapu R, Maanja M, Schlegel T et al. Advanced electrocardiography predicts early cardiac involvement and incident arrhythmia in Fabry disease. Under review in JACC CVI. 2022.

Extent of personal contribution

This study was a multi-centre study with patients recruited from the Fabry400 study and from UHB clinical service. I performed the CMR studies, 12-lead ECGs and TTE for the patients recruited within UHB.

Following completion of recruitment to this study, I analysed of all CMR images and 12 lead ECGs blinded to demographic and disease information. I visited the International SpaceEKG Headquarters in Switzerland, to learn and perform the advanced ECG analysis using specialised software. I performed the statistical analysis and wrote the first draft of the manuscript. I was responsible for all editing and subsequent revisions.

6.1 Introduction

6.1.1 The conduction system of the heart

Cardiac cells all have an intrinsic capability to generate and propagate an action potential, leading to synchronous myocardial contraction. The process by which this occurs involves coordinated movement of sodium, potassium and calcium ions across voltage-gated ion

channels within the lipid bilayer of cardiac myocytes (194,195). At rest a transmembrane potential of approximately -90mV exists largely due to a differing concentration of sodium and potassium ions, within the intra- and extra-cellular volumes. Systematic opening and closing of ion channels, generates 4 distinct phases of the cardiac action potential (*Figure 6.1*). Once a threshold potential is passed, activation of sodium channels leads to a rapid influx of positively charged sodium ions within the intracellular space, leading to the initial upstroke of the action potential and a short period where the transmembrane potential is positively charged (phase 0, +15mV) (195). Subsequent opening of potassium channels leads to a slight efflux of potassium ions during phase 1 and a reduction in the membrane potential. Phase 2 is known as the plateau phase, where the myocyte is refractory to any further electrical impulse. This involves a complex interaction between inward calcium and sodium channels and outward rapid and slow potassium channels, leading to a net membrane potential of approximately 0mV (195). Subsequent myocyte repolarisation occurs as the outward current transfer exceeds any inward current, leading to regeneration of the resting transmembrane potential (phase 3). Once this occurs phase 4 is a diastolic period during which the myocyte is fully excitable and can respond to other electrical stimuli.

Figure 6.1. Temporal relationship between the myocardial action potential and the surface 12-lead ECG. Adapted from George AL (196).

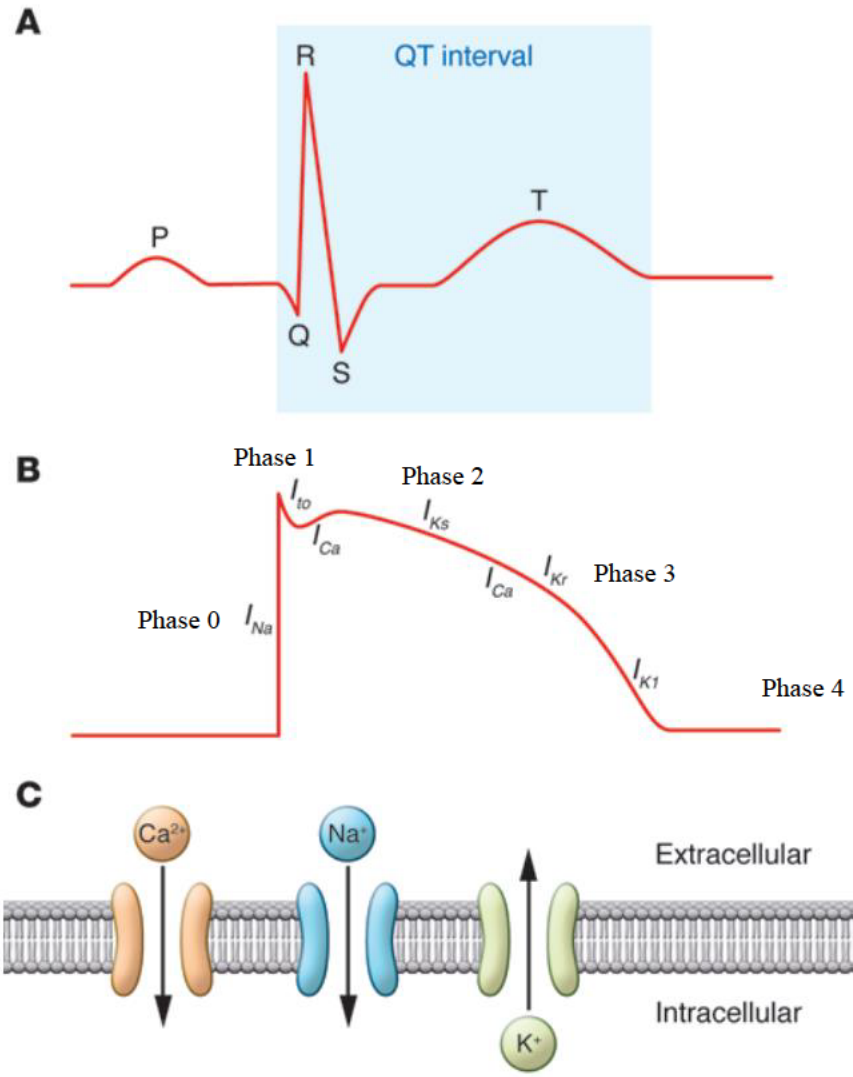

Panel A *– the surface 12-lead ECG: the p-wave indicated atrial depolarisation, the QRS wave ventricular depolarisation and the T-wave ventricular repolarisation.*

Panel B *– the myocardial action potential with four phases of depolarisation, plateau and repolarisation.*

Panel C *– the corresponding inward motion of calcium and sodium ions and outward movement of potassium ions.*

Although all myocardial cells have the potential to generate an action potential, specialised groups of pacemaker cells have an intrinsic capability to generate regular action potentials and form the starting point of the hearts conduction system. These are located within the sinoatrial node, which is present within the roof of the right atrium (*Figure 6.2*). The initial action potential is propagated across the atrial myocytes via specialised gap junctions, which are non-selective channels allowing passage of any ions thus leading to atrial contraction (197). The impulse subsequently reaches a second group of specialised pacemaker cells known as the AV node, occurring within the floor of the right atrium (197). This acts to delay conduction and continues the electrical impulse through the His-Purkinje system facilitating ventricular depolarisation and contraction.

Figure 6.2. Conduction system of the heart. Taken from Ganesan et al (198).

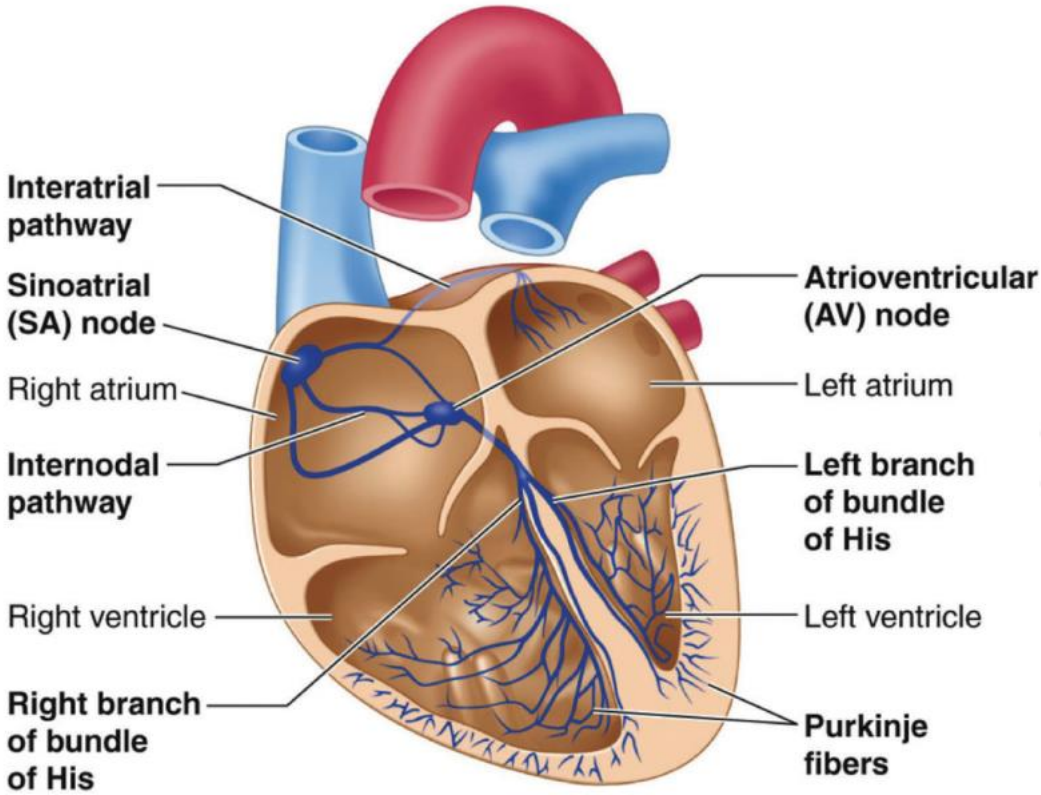

Propagation of this electrical activity can vary within cardiovascular disease and can be visualised on the 12-lead surface ECG.

6.1.2 Electrocardiography

6.1.2.1 Standard 12-lead electrocardiogram

The use of the surface ECG in humans was first proposed by Augustus Waller in 1887, but the technique was further refined and utilised in a clinical setting by Willem Einthoven in 1901 (199). The 12-lead surface ECG uses ten electrodes placed at certain locations on the body to capture the underlying electrical depolarisation and repolarisation. They include six precordial electrodes (V1-V6), three limb electrodes (I, II and III placed on the right arm, left arm and left leg) and a ground electrode (placed on the right leg). The three limb leads (I, II, and III) are bipolar electrodes that were the primary components of Einthoven's original surface ECG. They measure differences in electrical voltage between two extremities (*Table 6.1*), which provides information on the overall direction of electrical flow within the myocardium.

Table 6.1. Electrical voltages measured by the limb lead electrodes (200).

	Electrical voltage measured	Summary
Lead I	Difference between left arm (LA) and right arm (RA)	LA - RA
Lead II	Difference between left leg (LL) and right arm (RA)	LL - RA
Lead III	Difference between left leg (LL) and left arm (LA)	LL - LA

The differences measured between the limb electrodes have been represented schematically by Einthoven's Triangle (*Figure 6.3a*), which shows that lead I is horizontal with predominant direction of electrical flow towards the left arm and leads II and III are directed diagonally downwards, with predominant electrical flow occurring inferiorly. Three unipolar

augmented limb leads (aVR, aVL and aVF) and the six precordial leads were incorporated in the 1930s to form the standard 12-lead ECG used today (*Figure 6.3b*). These latter unipolar leads provide information on electrical flow at any single location relative to an electrode with close to zero potential, instead of the voltage recorded in another limb extremity. Thus information on direction of electrical flow from all areas of the myocardium is demonstrated on the 12 leads of the surface ECG, with differing features being described in various cardiovascular disorders.

Figure 6.3. The component leads of the 12-lead surface ECG. Adapted from Abi-Saleh et al and Koelsch et al (201,202).

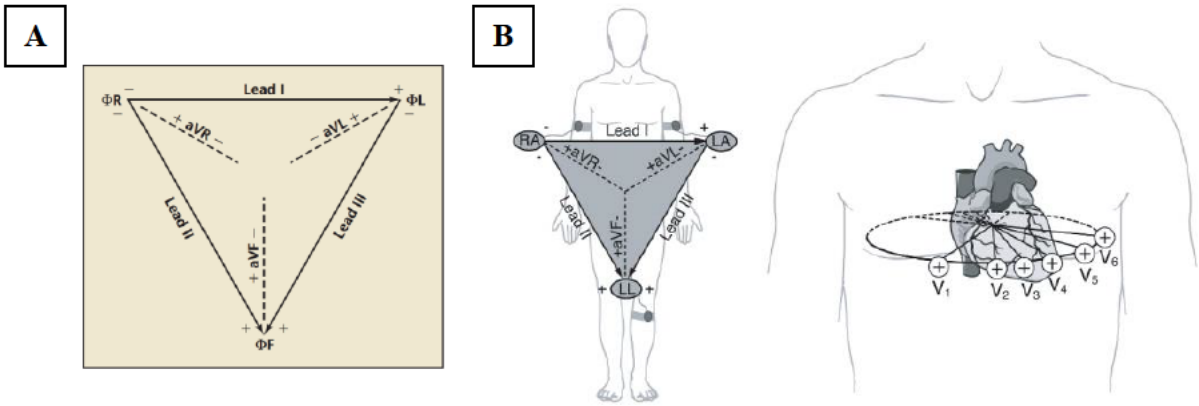

Panel A *– Einthoven's triangle demonstrating the orientation of the three bipolar limb leads and the predominant direction of electrical flow – lead I, II and III.*

Panel B *– Illustration demonstrating the orientation of all six limb leads and precordial leads. The spatial relationship of the three bipolar limb leads (I, II and III) and the three augmented limb leads (aVF, aVR, aVL) is demonstrated by the grey triangle, which records electrical voltages in the frontal plane of the body. The oval shape encompassing the precordial leads demonstrates the spatial relationship of these leads, which records any electrical voltage transmitted in the horizontal plane.*

6.1.2.2 Advanced electrocardiogram

The advanced electrocardiogram (A-ECG) uses multiple ECG techniques to identify various electrical characteristics of the myocardium from a digital ECG recording, taken over either 10 seconds or five minutes (203). In combination with standard 12-lead ECG measurements, vectorcardiography, QRS complex and T wave complexity analysis, high frequency QRS wave assessment, P wave analysis and individual RR- and QT-variability evaluation, all constitute A-ECG analysis. The software used in this analysis was initially developed for screening of CV disease in astronauts by the National Aeronautics and Space Administration (NASA), Johnson Space Centre, Texas, USA and as such is often termed Space-EKG. Two of the most fundamental techniques that have been shown to be predictive of cardiovascular disease are vectorcardiography and QRS/T wave complexity analysis (204,205).

6.1.2.2.1 Vectorcardiography

Mathematical modelling used to describe the cardiac cycle is based on a moving dipole, which results in a vector of electrical forces within individual myocytes during each cardiac cycle. This vector constitutes electrical force in three orthogonal axes and time (206). The standard 12-lead ECG combines the electrical activity captured across a single of these planes, but vectorcardiography derives data from all component planes, creating an electrical loop in three-dimensional space (207). The vectorcardiogram (VCG) was first demonstrated by Frank et al in 1956 (208), using three leads placed on the frontal plane in a modified Einthoven's triangle. Electrode placement was further refined providing definitive placement of seven leads, which provided information projected in three mutually perpendicular planes – sagittal, transverse and frontal (*Figure 6.4a*). The VCG was of particular use as it provides a visual representation of the electrical activity and its spatial variation during each heart beat (206,209). The modern day VCG however, can be derived from the standard 12-lead ECG

using a mathematical transformation matrix either with the Kors regression transformation method (210) or the inverse Dower matrix (211). The direction of electrical activity within each plane forms three loops, representing individual components of the cardiac cycle, considering the contours, rotational effect and direction of the cardiac axis (212). The first and smallest electrical loop represents P wave activity. The second loop is commonly the largest of the three and demonstrates QRS complex activity and the third loop represents T wave activity. These can be represented two-dimensionally (*Figure 6.4b*) or three-dimensionally after each corresponding loop from all three planes is combined (*Figure 6.4c*).

Figure 6.4. Vectorcardiography. Taken from Jaros et al (212)

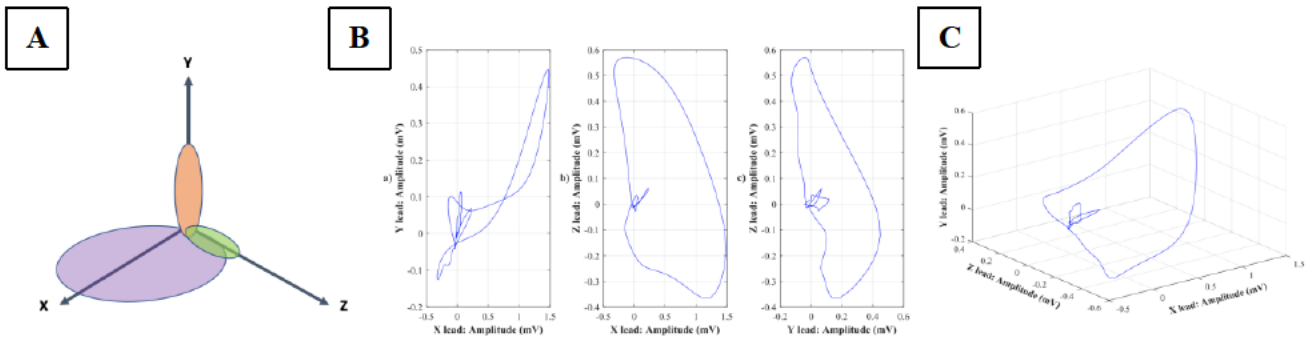

Panel A *– Schematic representation of three vectorcardiogram planes.*

Panel B *– 2D image demonstrating three vectorcardiogram planes. A) Frontal plane, X lead to Y lead, B) Transverse plane, X lead to Z lead and C) Sagittal plane, Y lead to Z lead.*

Panel C *– 3D image combining electrical loops from all three planes.*

The QRS and T wave loops are most frequently described in the literature, as abnormalities in these parameters are associated with cardiovascular pathology. In particular the QRS-T angle, which is measured as the angle between the peak magnitude of the QRS complex and T wave loop vectors (213). This angle is typically narrow in a normal heart and increases as a result of cardiac disease (213). A widened QRS-T angle has been associated with arrhythmia

and has also been described as an independent predictor of mortality in cardiovascular disease (214,215).

6.1.2.2.2 QRS and T wave complexity

Singular value decomposition (SVD) is a mathematical processing technique commonly used to extract certain components of the ECG. The overall ECG signal is deconstructed into a set of basic component patterns (216), and the depolarising QRS complex and repolarising T wave can be characterised into specific eigenvectors. Eigenvectors are measured in microvolts and are 3-dimensional loops representing this electrical depolarisation and repolarisation across specific areas of the myocardium (217-219), *Figure 6.5*. As described earlier the 12-lead ECG is composed of ten individual electrodes, with eight specific channels representing eight dimensions of electrical activity. These form eight different eigenvectors for each component of the ECG (P wave, QRS complex and T wave). The first eigenvector is typically the largest, with a reducing size of electrical activity thereafter. In a normal heart, there tends to be a smaller amount of electrical activity from eigenvector 4 onwards. The presence of cardiac disease however, leads to a shift in the eigenvector energy profile with larger electrical loops occurring in later eigenvectors (220).

Figure 6.5. Schematic representation of the initial three eigenvectors in three-dimensional space. Adapted from Maanja et al (221).

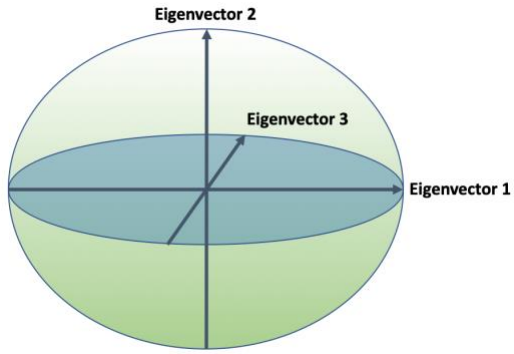

6.1.2.2.2 Heart age

The concept of heart age was first developed in 2014 (222) and is a means of evaluating a patient's cardiovascular age based on their cardiovascular risk profile. The 12-lead ECG is known to alter both as patient's age and also in the presence of cardiac disease, with certain parameters predictive of adverse clinical outcomes. Integration of electrocardiographic data into heart age calculation using artificial intelligence (AI) technology has been shown to have a greater sensitivity and specificity for assessment of cardiovascular risk when compared to more traditional cardiovascular risk estimation models (223). These methods however, can be time consuming, require extensive technology support and thus make integration into clinical medicine less practical. A study by Lindow et al however, concluded that ECG heart age could accurately be determined from standard ECG measures taken from a 10 second digital ECG without the use of AI techniques (224), thus making this methodology potentially more clinically applicable. They also identified that the difference between A-ECG heart age and chronological age (termed heart age gap) increases with progressive cardiovascular disease and can be predictive of adverse outcomes (224).

6.1.2.2.3 Global wall thickness

Global wall thickness (GWT) is a novel means of assessing global patterns of myocardial hypertrophy. Traditionally RWT has been used as a surrogate marker to describe patterns of hypertrophy and remodelling, but this is based on single measures of the septal and posterior wall thickness. GWT, however, is derived from the total LVM and LVEDV without any specialised software and thus provides structural information from the whole myocardium. A recent study by Lundin et al (225) evaluating multiple methods of myocardial hypertrophy assessment, described the significant benefits of GWT. Abnormalities in GWT occurred prior to the onset of LVH in patients with known cardiac disease, thus suggesting that an elevated GWT may be an early disease marker. LVMi is well known to be predictive of adverse cardiac outcomes. This study found that GWT was also a strong predictor of future scar burden, heart failure hospitalisation and mortality (HR 1.14, 95%CI 1.09-1.19) and thus its use in combination with LVMi could accurately characterise myocardial hypertrophy and predict future adverse events.

6.1.3 The Advanced ECG and cardiac arrhythmia in Fabry

These digital advanced ECG markers have been shown to have both a higher sensitivity and specificity than the conventional ECG in prediction of arrhythmic risk and in the assessment of conditions such as LVH, HCM and ischaemic heart disease (203,210,226). One study of 534 patients with known cardiovascular disease identified that a wide QRS-T angle (>110degrees) was a strong predictor of VT in patients with left ventricular systolic dysfunction, with a 3-fold increase in malignant ventricular arrhythmia compared to patients with a normal QRS-T angle (205). Additionally, when used in the general population, a QRS-T angle >100 degrees has shown a greater sensitivity for SCD and arrhythmia than standard ECG parameters (227). *Figure 6.6* shows a schematic comparison of a normal and wide

QRS-T angle. Detailed T-wave analysis has also shown promise as a marker for arrhythmia in patients with LVH. It is known that myocardial hypertrophy can lead to alterations in ventricular repolarisation gradients that contribute to T-wave morphology. Consequently, subtle alterations within the T-wave can reveal arrhythmic vulnerability in patients with LVH (204). LVH is an extremely common finding in FD and its severity is considered a significant marker of prognosis. Despite evidence that the QRS-T angle, T-wave and QT variability index analyses are strong independent predictors of cardiovascular mortality and SCD in LVH, this relationship has not been investigated in FD.

Figure 6.6. Schematic representation of varying QRS-T angle.

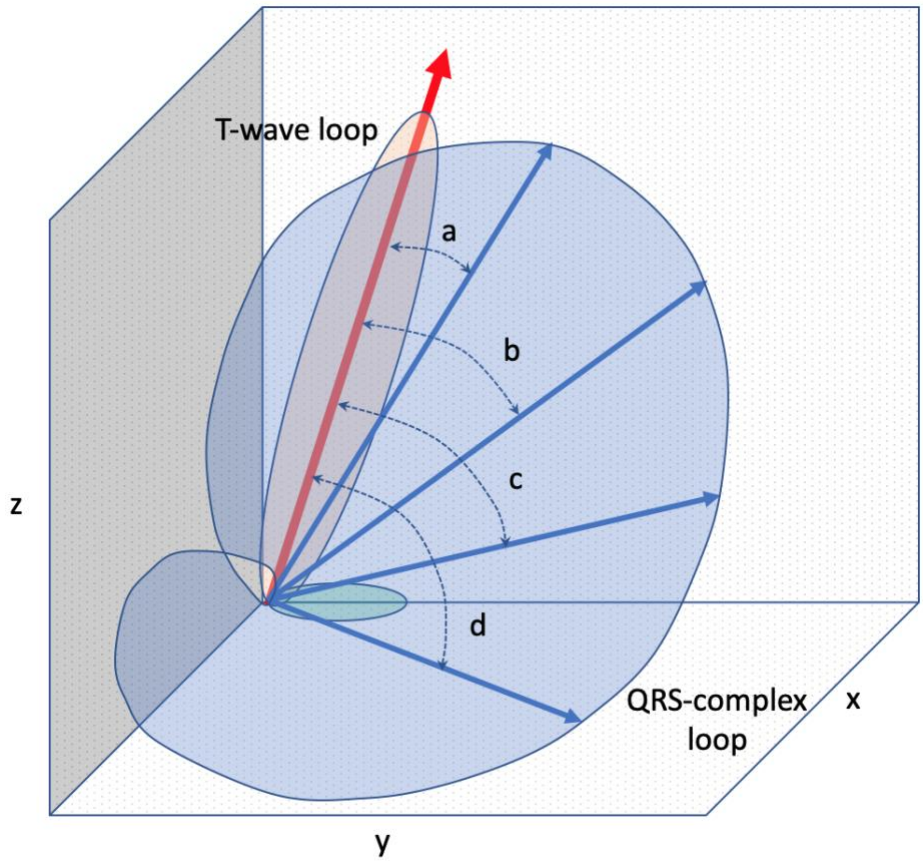

Three dimensional representation of ECG vectors. Red ellipsoid denotes T-wave loop and blue shape represents the QRS complex loop varying with different pathological processes. The solid red and blue arrows demonstrate the predominant direction of electrical flow

within the respective loops. The angle between the T-wave loop (red arrow) and the QRS-complex loop (blue arrow) is the QRS-T angle. A normal QRS-T angle is demonstrated by angle A and a progressively widening angle by angles B-D.

6.2 Brief methodology

6.2.1 Study population and design

This was a multi-centre study with patients recruited from two groups. The larger group were patients recruited to the prospective, observational international Fabry400 study (NCT03199001) from UHB, Royal Free Hospital London and the National Hospital for Neurology and Neurosurgery London. Patients were eligible for the Fabry400 study if they were ≥ 18 years of age and had a genetically confirmed diagnosis of FD. Patients were excluded if they had an absolute or a relative contra-indication to CMR. A smaller proportion of study patients were taken from consecutive adults with genetically proven FD attending the UHB Rare Diseases Centre. Patients were recruited from August 2016 to November 2019. Demographic data were collected as described in Chapter 3.

6.2.2 Ethical and clinical governance approval

HRA and ethical approval was obtained for the prospective Fabry400 study by the chief investigator (14/LO/1948), with local UHB R&D registration (RRK5361). In accordance with HRA guidance, ethical approval was not required for use of data historically collected as part of clinical service, where its inclusion in research is secondary. This study conformed to the principles of the Helsinki Declaration.

6.2.4 Advanced ECG analysis

12-lead ECGs were captured using local GE ECG machines in all participants and subsequently stored as digital files (MUSE® Cardiology Information System, Version 8.0 SP2, GE Healthcare, Chicago, IL, USA), with individual 10-second recordings taken at a sample rate of 250Hz. Data were retrieved as .xml formatted files. Anonymised files were subsequently converted to a basic binary format and these data were transformed into vectorcardiographic data using the Frank-lead reconstruction technique (206). These data were signal averaged and analysed using specialised digital semi-automatic A-ECG software (Cardiosoft®, NASA, Johnson Space Centre, Houston, Texas, USA) (203,210,228). All cases were manually reviewed for artefact during the transformation process and excluded from analysis if significant artefact was present. The A-ECG parameters were collected as previously described (203,221,229).

A-ECG heart age was calculated by inputting the following parameters into a predefined mathematical formula, as described by Lindow et al (229).

1. Conventional ECG parameters: heart rate, R-R interval, P wave, PR interval, QRS duration, QT/QTc, Tq interval (RR interval minus the QT interval of the previous beat), cardiac axis and electrical amplitudes on ECG.
2. Vectorcardiographic data: spatial QRST angle (mean and peak), spatial ventricular gradient and QRS/T wave components, spatial QRS and T wave axes, waveform amplitudes/areas, spatial QRS and T wave velocities.
3. QRS and T wave complexity based on SVD.

6.2.5 Additional CMR analysis: global wall thickness

Global wall thickness was calculated using the total LV mass and the LVEDV. These parameters were determined using standard CMR analysis techniques as described in Chapter 3 and entered in the formula below to calculate the GWT in millimetres (221). This was then divided by the BSA calculated using the Mosteller method providing an indexed GWT (GTI).

$$GWT\ (mm) = 0.05 + 1.60\ (LVM^{0.84} \times LVEDV^{-0.49})$$

6.2.6 Statistical analysis

Statistical analyses were carried out using SPSS 22 (IBM, Armonk, NY) and R version 3.4.3 (R Foundation for Statistical Computing, Vienna, Austria). Normality was checked using the Shapiro-Wilk test and by visual review of histogram data for all variables. Normally distributed data were expressed as mean ± standard deviation and compared using the independent-samples t-test or one-way ANOVA with post-hoc Tukey correction. Non-normally distributed data were described using median and IQR with comparisons between groups using Mann-Whitney U or Kruskall-Wallis test, as appropriate. Categorical data were described as frequencies or percentages and chi-squared testing utilised when comparing proportions of a variable between two groups.

Diagnostic and prognostic scores for outcome markers were determined using continuous A-ECG data and stepwise forward logistic regression. A maximum of one parameter for ten events was used. To confirm accuracy of the scores derived from regression modelling the area under the ROC curve (AUC) was calculated and bootstrapped 2000 times to obtain 95% confidence intervals (95% CI) and the score with the higher AUC was used. A Youden index was utilised to identify the cut off scores that optimised sensitivity and specificity. A p-value of <0.05 was considered statistically significant.

6.3 Results

6.3.1 Participant characteristics

There were 155 Fabry patients included in this study, with a mean age of 46±14 years. There were 62 men (40%) and 93 women (60%). A non-classical cardiac mutation was present in 30% of patients and 61 patients (39%) were on ERT at time of recruitment. CKD stage 3 or above was present in 8% of the total cohort with a lower eGFR in men (87 [59-90] vs. 90 [79-90] ml/min/1.73m^2, p=0.040). Ten percent of patients had a confirmed diagnosis of hypertension on treatment, but none had evidence of IHD at recruitment. Demographic data can be seen in *Table 6.2*.

Table 6.2. Demographic data for the study cohort.

	Total	**Male**	**Female**	***p-value****
Sample size (n, %)	155 (100)	62 (40)	93 (60)	*N/A*
Age (yrs)	46±14	46±14	45±13	*0.728*
A-ECG heart age (yrs)	57±20	60±22	55±19	*0.112*
A-ECG heart age gap (yrs)	11±10	14±11	9±10	***0.008***
On ERT (n, %)	61 (39)	37 (60)	24 (26)	***<0.001***
Cardiac mutation (n, %)	45 (30)	20 (32)	25 (27)	*0.578*
BMI (kg/m^2)	25.2±4.8	24.9±4.2	25.4±5.2	*0.523*
HR (bpm)	56±16	57±15	56±16	*0.577*
SBP (mmHg)	118±16	124±15	115±16	***0.003***
DBP (mmHg)	73±9	75±10	72±9	*0.065*
Comorbidities				
IHD (n, %)	0 (0)	0 (0)	0 (0)	*N/A*
CKD stage 3-5 (n, %)	13 (8)	10 (16)	3 (3)	***0.008***
HTN (n, %)	15 (10)	8 (13)	7 (8)	*0.269*
DM (n, %)	1 (1)	0 (0)	1 (1)	*1.000*
Stroke/TIA (n, %)	2 (2)	1 (2)	1 (1)	*1.000*

Table 6.3 demonstrates the CMR and blood biomarker data of the study cohort. Men tended to have a higher LVMi and MWT compared to women (LVMi: 106.0 vs. 58.8 g/m^2, MWT: 14.0 vs. 9.0 mm, p<0.001 for both). Of the total cohort 92 patients (80%) had low native T1

according to local reference ranges (men: 40/62, 65% vs. women: 52/93, 56%, p=0.004). Of the total cohort 51% had LGE (defined as visual LGE in more than two AHA segments of the LV). This was significantly higher in men than women (37/54, 69% vs. 33/82, 40%, p=0.004). Hs-troponin and NT-pro BNP were within the normal range, but levels were greater in men.

Table 6.3. Cardiac investigation and biomarker data.

	Total	**Male**	**Female**	***p-value****
CMR				
LVMi (g/m^2)*	70 (57-100)	106 (78-138)	59 (53-74)	***<0.001***
MWT (mm)	10 (8-14)	14 (12-18)	9 (8-11)	***<0.001***
GTI (mm/m^2)	5 (4-7)	6 (5-8)	4 (4-5)	***<0.001***
LVEDVi (ml/m^2)	73±13	78±15	70±10	***0.001***
LVESVi (ml/m^2)	20.0±7.2	21.9±7.6	18.8±6.7	***0.010***
LVSVi (ml/m^2)	56±40	56±12	57	*0.874*
Global native T1 – mid LV cavity (ms)*	944 (908 – 984)	933 (891-950)	968 (911-991)	*0.055*
Low T1 (n, %)	92 (80)	40 (65)	52 (56)	*0.245*
LGE (n, %)	70/136 (51)	37/54 (69)	33/82 (40)	***0.004***
RVEDVi (ml/m^2)	76±16	78±18	74±14	*0.304*
RVESVi (ml/m^2)	31±12	35±17	29±9	*0.241*
RVSVi (ml/m^2)	47±10	46±12	47±9	*0.882*
Biomarkers				
High sensitive troponin T (ng/L)*	12 (1-33)	21 (4-58)	4 (1-23)	***<0.001***
NT-pro BNP (ng/l)*	13 (4-48)	18 (3-120)	11 (4-38)	*0.283*
eGFR ($ml/min/1.73m^2$)*	90 (75-90)	87 (59-90)	90 (79-90)	***0.040***

** non-parametric data so presented as median (IQR)*

6.3.1 Other characteristics

The average A-ECG derived heart age across the total cohort was 57±20 years (men: 60±22 vs. women: 55±19, p=0.112). Patients with Fabry disease tended to have a higher A-ECG heart age compared to chronological age. The A-ECG heart age gap was greater in men

compared to women (see *Table 6.2*). There was a positive correlation between the use of LVMi and GTI to evaluate the presence or absence of LVH (r=464, p<0.001).

6.3.1 AECG predictors of outcome variables

6.3.1.1 Low native T1

Of the total cohort 92 patients (80%) were found to have low T1, with 40 men and 52 women. 50 patients (53%) with a normal LV mass had low native T1, suggestive of subclinical sphingolipid deposition (mean native T1: 904±39 ms; men: 12 (13%), 897±27 ms; women 38 (40%), 906±42 ms, p=0.700). When using GTI as a marker of myocardial hypertrophy 18 patients (45%) with a normal GTI had low native T1 (mean native T1: 931±12 ms; men: 4 (10%), 933 ms; women 14 (35%), 931±15 ms, p=0.913). *Table 6.4* demonstrates the individual A-ECG parameters that in combination were found to be predictive of low native T1. This diagnostic score was found to have an AUC of 0.84 (95% CI 0.77-0.90), a sensitivity of 83% (95% CI 61-97) and a specificity of 76% (95% CI 56-94), *Figure 6.7a*.

Table 6.4. A-ECG parameters predictive of low native T1.

A-ECG parameter	**Beta coefficient**	**Standard error**	**p-value**	**AUC (95% CI)**
Spatial ventricular activation time	3.093	0.0258	<0.001	0.84 (0.77-0.90)
Elevation angle in 3D QRS loop (8/8)	-2.347	0.0048	<0.05	
Elevation angle of the polar vector	-3.296	0.0054	<0.001	
Elevation angle in 3D QRS loop (6/8)	-3.540	0.0053	<0.001	
Absolute QRS voltage	-3.462	0.0057	<0.001	
T wave area in lead Z	2.406	0.0052	<0.05	
Magnitude of 3D QRS loop (3/8)	2.475	0.0053	<0.05	

Eigenvector 7	-2.182	0.0054	<0.05	
Eigenvector 4	2.135	0.0058	<0.05	

6.3.1.2. Arrhythmia

Of the total cohort 34 patients (22%) had an arrhythmic event documented over a mean follow-up period of 3.2±0.6 years. This comprised of 13 patients with AF needing anticoagulation (6 women and 7 men), 12 with atrioventricular nodal re-entry tachycardia (AVNRT) requiring medical therapy (6 women and 6 men) and 13 with NSVT (6 women and 7 men). No patients had sustained VT. A combined predictive score for the occurrence of any arrhythmia had an AUC of 0.89 (95% CI 0.82-0.95), sensitivity of 82% (95% CI 68-94) and specificity of 88% (95% CI 70-96). When evaluating predictive markers for AF requiring anticoagulation the predictive score had an AUC of 0.89 (95% CI 0.80-0.96), sensitivity of 92% (95% CI 77-100) and a specificity of 83% (95% CI 76-92). No significant A-ECG predictors were found for the occurrence of NSVT or sustained VT. *Table 6.5* and *Figures 6.7b and 6.7c* describe the individual components of the A-ECG predictive score for any arrhythmia and AF.

Table 6.5. A-ECG parameters predictive for the occurrence of any arrhythmia and AF.

A-ECG parameter	**Beta coefficient**	**Standard error**	**p-value**	**AUC (95% CI)**
1) Any arrhythmia requiring therapy				
QRS axis	-3.515	0.004	<0.001	0.89 (0.82-0.95)
Magnitude of the QRS loop 7/8	3.139	0.008	<0.010	
Maximum voltage of the Z-lead in the QRS complex	4.108	0.011	<0.001	
Amplitude of second singular value of the T wave	2.873	0.006	<0.010	
Maximum spatial velocity of the magnitude of the spatial T wave	-2.556	0.008	<0.050	

Total QRS loop in frontal plane	-2.527	0.011	<0.050	
2) AF requiring anticoagulation				
Maximum voltage of the Z-lead in the QRS complex	3.55	0.013	<0.001	0.89 (0.80-0.96)
Absolute area subtended by the T wave in the Z-lead	-2.50	0.008	<0.050	

6.3.1.3 Scar burden on CMR

Of those who underwent LGE imaging 70 patients had evidence of LGE (women: 33/82, 40% and men: 37/54, 69%; p=0.004). Those with RV insertion point LGE were not included in data analysis. The components of the score predictive of LGE are shown in *Table 6.6.*

Table 6.6. A-ECG parameters predictive of LGE.

A-ECG parameter	**Beta coefficient**	**Standard error**	**p-value**	**AUC (95% CI)**
T wave morphology	4.197	0.258	<0.001	0.94 (0.89-0.97)*
Elevation angle of the spatial ventricular gradient (left sagittal plane)	-3.289	0.007	<0.01	
Magnitude of 3D QRS loop (7/8)	-3.117	0.008	<0.01	
Elevation angle in 3D QRS loop (1/8)	-3.407	0.007	<0.001	
T wave eigenvector 8	-3.062	0.009	<0.01	
Absolute area of the T wave in lead Y	2.848	0.007	<0.01	
Amplitude of the second singular T wave value (from SVD)	2.343	0.007	<0.05	

* Sensitivity 86% (95% CI 71-96) and specificity 91% (95% CI 79-100).

6.3.1.4 Heart failure hospitalisation and sudden death

Six patients (3 women and 3 men) required hospitalisation for treatment of decompensated heart failure (HF) and no deaths were recorded during the follow-up period. No significant A-ECG predictors were found for either of these outcome variables.

Figure 6.7. Receiver operating characteristic curves demonstrating the sensitivity and specificity of the A-ECG Fabry score.

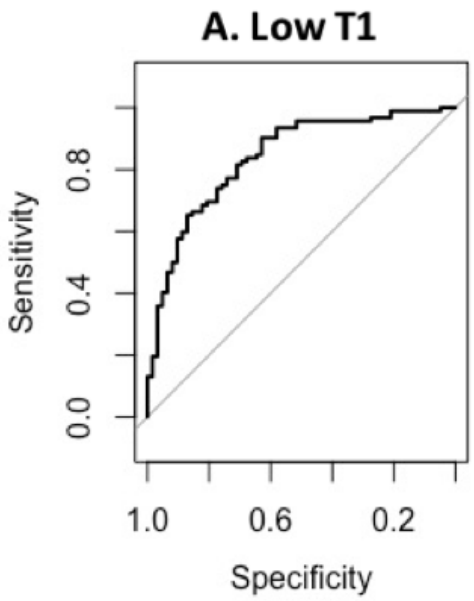

AUC	0.84	95%CI 0.77-0.90
Sensitivity	83%	95%CI 61-97
Specificity	76%	95%CI 56-94

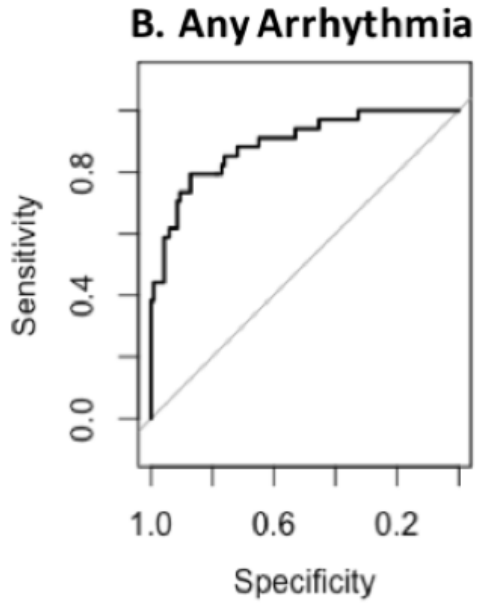

AUC	0.89	95%CI 0.82-0.95
Sensitivity	82%	95%CI 68-94
Specificity	88%	95%CI 70-96

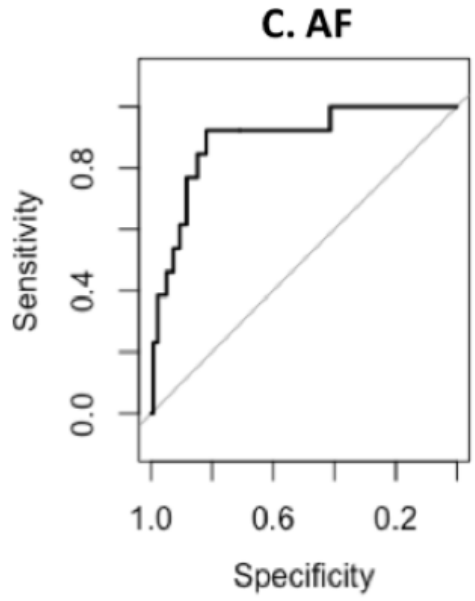

AUC	0.89	95%CI 0.80-0.96
Sensitivity	92%	95%CI 77-100
Specificity	83%	95%CI 76-92

6.4 Discussion

This is the first study evaluating the ability of A-ECG to detect sphingolipid deposition measured by low T1 on CMR. Detection of early cardiovascular disease with CMR T1 mapping is well recognised and has revolutionised the diagnostic pathway of Fabry cardiomyopathy. This study has demonstrated that A-ECG analysis of the standard 12-lead ECG can be strongly predictive of low T1 and therefore subclinical cardiac disease. From a total of 234 A-ECG variables, a global predictive model incorporating seven of these A-ECG parameters, primarily derived from the QRS and ST vectors, were found in combination to be highly predictive of low T1, with an AUC of 0.84. In addition to its diagnostic power this study has demonstrated the value of A-ECG in predicting adverse arrhythmic outcomes. In particular two A-ECG parameters were demonstrated to be strongly predictive of AF requiring anticoagulation, over a relatively short follow-up time.

Abnormalities in the resting 12-lead ECG have historically been described in Fabry cardiomyopathy with more significant electrical changes observed with advancing cardiac disease (33). More recent literature has evaluated the ECG in greater detail and described evidence of electrical abnormality much earlier in the disease phenotype. Nordin et al (87) demonstrated that ECG abnormalities tended to co-segregate with low T1 even in the LVH negative population, suggesting that a combined assessment of ECG and CMR may be beneficial. This was further evaluated by Augusto et al (230), who identified that certain ECG abnormalities within the T wave occurred in a very early pre-phenotypic stage of Fabry cardiomyopathy (LVH negative, normal T1) compared to healthy controls, suggesting that more advanced ECG abnormalities occur much early than previously thought. The results described in this chapter highlight that using more sophisticated A-ECG analysis techniques, a global predictive score of seven A-ECG parameters predominantly from the QRS and T

wave vectors is highly predictive of early cardiac disease. Consequently, this technology could offer a cheaper, more widely accessible ECG method for monitoring early cardiovascular disease that could potentially replace the need for frequent CMR surveillance.

6.4.1 Adverse outcome prediction

The use of AI derived advanced ECG analysis as a predictor of arrhythmia has been widely described over the past few years. A study by Christopoulos et al (231) of 1936 healthy volunteers aged between 70-89 years utilised an AI enabled convolutional neural network ECG algorithm to determine the probability of developing AF. They found that by using AI-ECG analysis software a predictive model output greater than 0.5 led to a 2-year cumulative risk of AF of 21.5% and a 10-year risk 52.2%, highlighting the benefit of ECG based predictive scoring (231,232). This methodology however, was slightly more time-consuming requiring specialist computer technology to perform analysis. More recently Sanz-Garcia et al (233) demonstrated the potential use of automated ECG analysis techniques as a low-cost screening strategy for AF in healthy volunteers. They identified 32 specific ECG variables that demonstrated predictive value of AF, with an AUC of 0.776. The A-ECG techniques described in this chapter were similar in simplicity to achieve but yielded a greater number of vectorcardiographic parameters. Despite shorter follow-up and consequently lower number of outcome events, two specific parameters predictive of AF in Fabry were identified with an AUC 0.89, thus highlighting this methodology as potentially valuable predictor of adverse arrhythmic outcomes.

The importance of the QRS-T angle in predicting adverse clinical outcomes has also been described in the literature. A study of 1915 patients presenting to a tertiary centre with symptoms of breathlessness demonstrated that a wide QRS-T angle was a strong

discriminator between a diagnosis of acutely decompensated HF and non-cardiac causes of breathlessness (234). Sub study analysis also identified the QRS-T angle as a strong predictor of 2-year mortality in HF. Due to the shorter follow-up time of our study, fewer HF hospitalisation episodes were identified and consequently no statistically significant variables were identified.

6.4.2 Limitations

The limitations of this study include the small size of the study cohort, which made detailed sub-analysis impossible due to very low numbers in individual groups. Furthermore, the follow-up time of this cohort was relatively short, resulting in a low detection rate of outcome markers such as individual arrhythmia, HF hospitalisation and mortality. The addition of a healthy volunteer control group and a Fabry validation cohort would have been of significant value, however, this was out of the scope of this initial study and further follow-on work described in Chapter 8 will provide this data.

6.4.3 Conclusion

A-ECG analysis of the resting 12-lead ECG has good diagnostic performance for predicting early myocardial involvement and the occurrence of arrhythmias in Fabry disease. This supports the use of A-ECG both as a screening tool to diagnose early cardiac disease, and for identifying those at risk of adverse arrhythmic outcomes.

7. Cardiac device implantation in advanced Fabry cardiomyopathy

The work in this chapter is based on the following published first author original articles, where this data was first presented:

Vijapurapu R, Geberhiwot T, Jovanovic A et al. Study of indications for cardiac device implantation and utilisation in Fabry Cardiomyopathy. *Heart.* 2019; 105: 1825-1831. DOI: 10.1136/heartjnl-2019-315586.

Vijapurapu R, Bradlow W, Leyva F et al. Cardiac device implantation and device usage in Fabry and Hypertrophic cardiomyopathy. Orphanet Journal of Rare Diseases. 2022; 17(6): 1-6. DOI: 10.1186/s13023-021-02133-4.

Vijapurapu R, Kotecha D, Demetriades P et al. Fabry disease and the risk of atrial fibrillation and pacemaker implantation: A systematic review. Under review in JACC EP, 2022.

Extent of personal contribution

This was a multi-centre study with patients recruited from clinical service and the Fabry 400 study. I recruited all patients from the clinical service and a proportion of the patients were taken from the Fabry400 study, of which UHB was the second largest contributor and whose patients I recruited. I performed the CMR studies, 12-lead ECGs and TTEs for the patients recruited through the Fabry400 study.

Following completion of recruitment, I analysed all of the data in this study. The first drafts of the above manuscripts were written by myself and I was responsible for all editing and subsequent revisions.

7.1 Introduction

Cardiovascular involvement includes progressive LVH, myocardial inflammation, fibrosis, arrhythmia, congestive cardiac failure and sudden death (52). Disordered sphingolipid metabolism results in Gb3 and lysoGb3 accumulating in all cardiac cells including the conduction system (86). In addition to the mechanical effects caused by sphingolipid deposition, secondary processes are believed to trigger a cascade of cellular reactions leading to a pro-inflammatory microenvironment with local tissue injury and apoptosis (88). Two primary mechanisms of arrhythmogenesis have been described. Birket et al (35) have shown on a molecular level that sphingolipids can alter ion channel expression and function leading to a significant change in molecular trafficking within the cell membrane. The ensuing damage to conductive tissue cell structure contributes to electrical instability and subsequent development of arrhythmia. Inflammation is also thought to be central in the development of malignant arrhythmia. Gb3 and lyso-Gb3 themselves, may act as antigenic particles triggering an autoimmune response with natural killer T cells generating a chronic inflammatory state, which can act as a focus of arrhythmia generation (38,138,235).

Although symptoms such as palpitations and dizziness are common in FD, occurring in up to 27% of the population, little is known regarding the true frequency of arrhythmia (89). Registry data and small single centre studies suggest that the rate of atrial arrhythmia (commonly AF) could be as high as 13% (90), whilst the reported incidence of ventricular arrhythmia varies widely from 5 to 30% (42,90,91), with a progressive increase with advancing age (92). Symptoms such as syncope are less common and have been reported in 4% of the Fabry population (89). The incidence of chronotropic incompetence with or without sinus node dysfunction or high grade AV block is variably reported between seven and 30% (71). Consequently, data regarding indications and implantation of cardiac devices

are limited. A small study by O'Mahoney et al (95) has suggested that rates of PPM implantation for symptomatic bradyarrhythmia are more than 25 times that seen in the general population, with a high burden of atrial and ventricular pacing in those with devices.

MVA and sudden death are believed to be more common with higher rates identified in a systematic review of 13 studies and 4185 patients over a follow-up period of 1.2-10 years (73). Of the 8.2% of deaths described within the cohorts, 75% were secondary to cardiovascular disease and 62% directly resulted from sudden cardiac death. Despite this, guidance for use of ICDs in Fabry is unclear. Limited data have identified the following potential risk factors for MVA and sudden death: LVH, the presence of LGE on CMR, left atrial dilatation, a QRS duration (QRSd) greater than 120 ms, previously documented NSVT, and an elevated MSSI (73). Additionally, abnormalities on a 12-lead ECG, including prolonged PR interval and QRSd, have been identified as independent predictors of pacemaker implantation in FD (95). No definitive criteria exist however, to guide implantation of cardiac devices for primary prevention and FD is specifically excluded from the SCD risk prediction tool used for HCM (96), despite similarities in risk factors between FD and sarcomeric HCM (97). Consequently in current practice, implantation of devices is predominantly based on secondary prevention indications following a clinically significant bradyarrhythmia, symptomatic ventricular arrhythmia or aborted SCD but data are lacking (236).

The aims of this study are to: evaluate the indications currently applied in clinical practice for device implantation in FD; quantify arrhythmia burden/device usage; and investigate any association between usage and potential arrhythmic risk factors. A second sub study was also

set-up to compare the risk of arrhythmia in FD with sarcomeric HCM, which is described within section 7.5.

7.2 Brief methodology

7.2.1 Study population and design

This was a multi-centre, observational, retrospective cohort study with patients recruited as demonstrated in Figure 3.1. The study included those with genetically confirmed FD who had a therapeutic cardiac device (CD), which included a PPM, an ICD or a cardiac resynchronisation therapy (CRT) device implanted between 1st December 2000 and 1st February 2018 (FD-CD group). Those with diagnostic CDs (ILRs) were also evaluated as a separate group within this study. All patients were followed up at national specialist centres within the UK: Queen Elizabeth Hospital, Birmingham; Salford Royal Hospital, Salford; Royal Free Hospital, London; Addenbrookes Hospital, Cambridge. To define the study cohort the clinical notes of all Fabry patients, both currently and historically under follow-up, were reviewed to identify if a cardiac device had been implanted. A comparator group included FD patients who have not undergone CD implantation and are under routine follow-up (FD-NonCD group). The FD-NonCD patients were taken from the Fabry400 study (NCT03199001).

7.2.2 Baseline assessment and follow-up

All demographic and clinical data were collected from patient notes and electronic records. Baseline FD specific information included genetic mutation, other FD-target organ involvement and MSSI were used to assess overall severity of FD. Disease stability was assessed by patient reported symptoms described in clinical review correspondence. Cardiovascular and renal co-morbidities were also recorded. The presence of IHD was

defined as evidence of a flow-limiting lesion on coronary angiography requiring treatment (surgical, percutaneous or medical). Information on device implantation was obtained from clinical records and local cardiac physiology departments. In the FD-CD group, cardiac investigations (12 lead ECGs/TTE/CMR) were recorded if these had been performed before or within 3 months following device implantation. In the FD-NonCD cohort however, the most recent investigations were captured. Classification of an ECG as abnormal included the presence of any irregularities (prolonged or shortened PR interval, QRS duration >120ms, minor conduction abnormalities, the presence of LVH by Sokolow-Lyon criteria, T wave inversion in at least two contiguous leads and the presence of multifocal ventricular ectopy).

7.2.3 Cardiac device electrocardiogram analysis

CD follow-up reports were obtained from local departments. Review of follow-up reports included summary dot plot analysis and subsequent atrial and ventricular electrogram (EGM) review to confirm for the presence of arrhythmia (*Figure 7.1*). ATP and defibrillation therapy delivered from ICDs was also evaluated for appropriateness. Details of corresponding changes in treatment were obtained from clinical notes.

Figure 7.1. Example electrocardiogram from a dual chamber ICD demonstrating sustained ventricular tachycardia requiring defibrillation. Adapted from Fields et al and Saini et al (237,238).

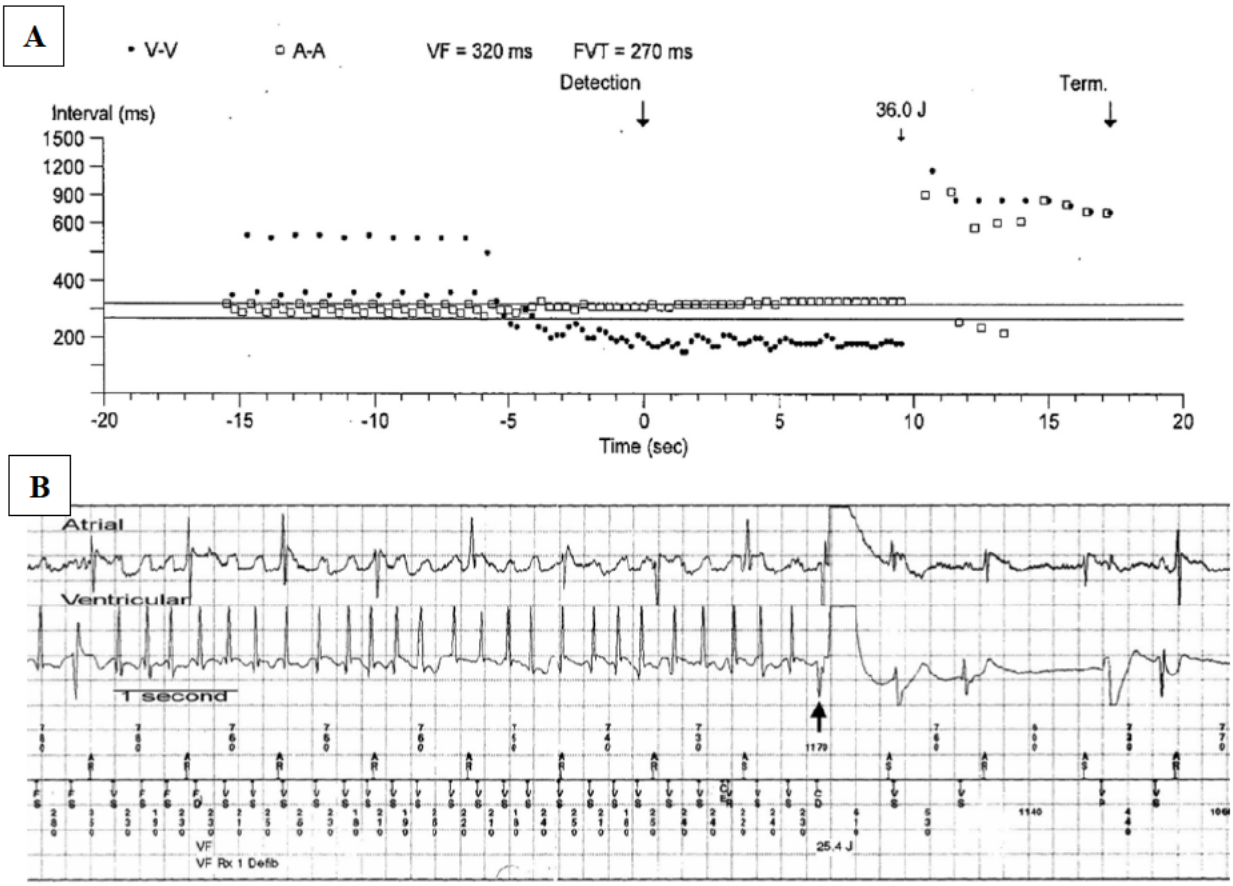

Panel A *– Dot plot demonstrating a regular and rapid ventricular rate with short V-V intervals, suggesting sustained ventricular tachycardia. This falls within the programmed fast VT zone and is treated with a 36.0J shock.*

Panel B *– Atrial and ventricular EGM. Regular atrial conduction can be seen, but there is an abrupt decrease in ventricular cycle length with AV dissociation at a rate of 267bpm suggestive of VT. This was successfully terminated with a 25.4J shock.*

7.2.4 Ethical and clinical governance approval

HRA and ethical approval was obtained for the prospective Fabry400 study by the chief investigator (14/LO/1948), with local UHB R&D registration (RRK5361). In accordance with HRA guidance, ethical approval was not required for use of data historically collected as part of clinical service, where its inclusion in research is secondary. This study was registered with UHB R&D (RRK6621) and conformed to the principles of the Helsinki Declaration.

7.2.5 Statistical analysis

Statistical analyses were carried out using SPSS 23 (IBM, Armonk, NY). All continuous variables are expressed as mean ± standard deviation and all non-continuous data are expressed as frequencies or percentages. Normality was evaluated using the Shapiro-Wilk test. Groups were compared with independent t-testing for parametric data and Mann-Whitney U testing for non-parametric data. Chi-squared or Fishers-exact testing was used to compare proportions within two independent groups. Comparisons between multiple groups were performed using ANOVA testing with post-hoc Tukey correction. Time-to-event (survival) analysis was performed to evaluate the presence of arrhythmic events. The follow-up period was calculated from date of device implantation to the study end date (1st February 2018). Kaplan-Meier curves were utilised to estimate the cumulative probability of arrhythmic events, with Breslow-Wilcoxon methods used to compare analysis between groups. Cox proportional hazards regression was used to assess the relationship between predefined covariates and outcome events. A p-value of <0.05 was considered statistically significant.

7.3 Results

7.3.1 FD-CD vs. FD-NonCD

7.3.1.1 Participant characteristics & baseline data

Of the study population of 880 Fabry patients, 90 (10%) had undergone implantation of a therapeutic cardiac device (FD-CD group) and 19 (2.2%) had a diagnostic ILR implanted. Baseline demographic data are described in *Table 7.1*.

Table 7.1. Demographic information for the study population (FD-CD vs. FD-NonCD).

	FD-NonCD	**FD-CD**		***p-value****
		Therapeutic	**Diagnostic**	
Sample size (n, %)	771	90	19	-
Age (yrs)	45±17	56±13	52±11	***<0.001***
Male gender (n, %)	283 (36.7)	69 (76.7)	10 (52.6)	***<0.001***
Classical mutation (n, %)	468 (60.7)	39 (43.3)	15 (78.9)	***0.002***
BMI (kg/m^2)	26±12.3	27±5.9	26±7.6	*0.518*
HR (bpm)	69±14	71±18	70±12	*0.544*
SBP (mmHg)	124±17	125±18	124±21	*0.614*
DBP (mmHg)	75±10	74±11	74±12	*0.654*
On ERT (n, %)	389 (50.5)	62 (68.9)	16 (84.2)	***0.001***

**p-values are comparing FD-NonCD vs. therapeutic FD-CD.*

The mean age for the FD-CD cohort was 56±13 years, with a male to female ratio of 2.6:1. A classical mutation was identified in 39 patients (43%), with the remaining 51 patients (57%) having a non-classical mutation (predominantly with an N215S protein sequence change). Of the 771 Fabry patients without a device, detailed cardiac information was fully available for 276 and these patients were used as a comparator group (FD-NonCD). The clinical, ECG and TTE characteristics are shown in *Table 7.2*. 19 FD-CD patients (21%) had undergone either invasive or computed tomography coronary angiography and of these only six (7%) had flow-limiting coronary artery disease and required percutaneous or surgical revascularisation. 18 patients (20%) had CKD stage 3 or above, with 2 of these patients previously having

undergone renal transplantation. 62 patients (69%) were on ERT at time of device implantation. The FD-CD group had a mean MSSI of 15.1±9.7 (M: 15.6±9.8, F: 13.4±9.4, p=0.36). The mean age of the FD-NonCD cohort was 46±16 years, with 100 males (36%). 163 patients (59%) had a classical mutation and the mean MSSI was 7.3±7.7, both of which were significantly lower than the FD-CD group (15.1±9.7 and 39 patients (43%), p<0.05).

Table 7.2. Patient demographics and baseline investigation data: comparator groups (FD-CD vs. FD-NonCD).

	FD-CD	**FD-NonCD**	***p-value****
Sample size (n, %)	90	276	-
Age (yrs)	56±13	46±16	***<0.001***
Male gender (n, %)	69 (76.7)	100 (36.2)	***<0.001***
On ERT (n, %)	62 (68.9)	131 (47.5)	***0.001***
Classical mutation (n, %)	39 (43)	163 (59)	***0.010***
MSSI	15.1±9.7	7.3±7.7	***<0.001***
Comorbidities			
IHD (n, %)	6 (6.7)	7 (2.5)	*0.095*
CKD (n, %)	18 (20)	26 (9.4)	***0.014***
HTN (n, %)	18 (20)	35 (12.7)	*0.119*
DM (n, %)	8 (8.9)	8 (2.9)	***0.032***
Stroke/TIA (n, %)	22 (24.4)	11 (4.0)	***<0.001***
ECG	n=76	n=239	
Abnormal (n, %)	74 (97.4)	115 (48.1)	***<0.001***
PR interval (ms)	174±40	147±29	***<0.001***
QRS duration (ms)	136±32	99±20	***<0.001***
Holter monitoring	n=52	n=85	
Abnormal	37 (71.2)	12 (14.1)	***<0.001***
Echocardiography	n=82	n=91	
LVEF (%)	57±13	62±7	***0.002***
LVH (n, %)	78 (95.1)	36 (39.6)	***<0.001***
LA dilatation (n, %)	56 (68.3)	13 (14.3)	***<0.001***
CMR	n=46	n=210	
LVMi (g/m^2)	150±37.3	83±36	***<0.001***
MWT (mm)	20±4.9	12±4.6	***<0.001***
LVEDVi (ml/m^2)	82±32	70±14	*0.143*
LVESVi (ml/m^2)	31±31	19±7	*0.150*
LGE (n, %)	29 (63.0)	85 (40.5)	***<0.05***

**p-values are comparing FD-CD vs. FD-NonCD.*

The incidence of LVH was greater in the FD-CD cohort (78/82 (95%) vs. 36/91 (40%) and mean LVMi was higher (150±37.3g/m^2 vs. 83±36g/m^2, p<0.001). ECG abnormalities were also more frequent in the FD-CD cohort, with a longer PR interval and QRS duration (PR interval: FD-CD – 174±40ms vs. FD-NonCD – 147±29ms, QRS duration: FD-CD – 136±32ms vs. FD-NonCD – 99±20ms; p<0.001). 46/90 (51%) FD-CD and 210/276 (76%) FD-NonCD patients underwent CMR imaging. LGE was more frequent in the FD-CD group (29/46 (63%) vs. 85/210 (41%), p<0.05).

7.3.1.2 FD-CD device implantation

In total, 90 patients were identified with a therapeutic CD. The following devices were implanted: PPMs for bradycardia 38/90 (42%), ICDs for ventricular tachyarrhythmia 43/90 (48%), and CRT for heart failure 9/90 (10%). Of those with PPMs 79% had a class 1 indication for device implantation and 13% a class 2a indication, according to European Society of Cardiology (ESC) guidance (98). Detailed indications for CD implantation are given in *Table 7.3*.

Table 7.3. Indications for CD insertion in FD cohort.

FD-CD indication	**Frequency**	**Percentage (%)**
PPM (n=38)		
Tachy-brady with co-existing AF	5	13.2
Sinus node dysfunction	9	23.7
Bi- & tri-fascicular block	3	7.9
2nd degree AV block	10	26.2
3rd degree AV block	9	23.7
No indication	2	5.3
ICD (n=43)		
Presumed dual pathology with HCM	7 (3 confirmed mutation)	16.3 (7.0)
Symptomatic VT	9	20.9

Multiple risk factors	14	32.6
PPM indication with asymptomatic NSVT	4	9.3
Asymptomatic NSVT	8	18.6
Other (LQTS with syncope)	1	2.3
CRT (n=9)		
Symptomatic LVSD (NYHA class 3) with LBBB	7	77.8
Unknown	2	22.2

7.3.1.3 Follow-up and arrhythmic risk factors

7.3.1.3.1 Arrhythmia follow-up

Mean follow-up for the FD-CD cohort was 5.3±3.8 years. A total of 58/90 (64%) had at least one documented arrhythmic event. As shown in *Figure 7.2*, 40 of these patients (44%) required initiation of or a change in therapy: 17/58 (29%) were diagnosed with new AF requiring anticoagulation and rate control medication, 4/58 (6.9%) had supraventricular tachycardia (SVT) requiring beta-blocker therapy, and 15/58 (26%) had NSVT requiring medical therapy.

Figure 7.2. Incidence of arrhythmic events in the FD-CD cohort.

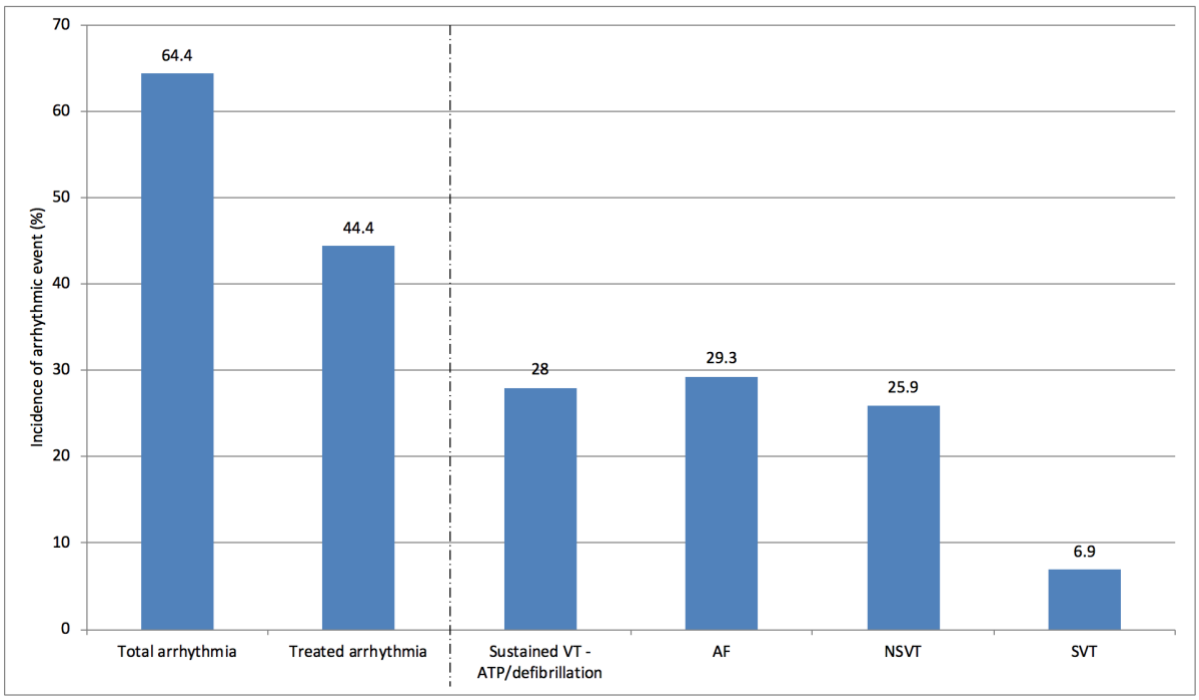

The incidence of arrhythmic events in the FD-CD cohort (n=90): (i) total documented arrhythmia and treated arrhythmia (including initiation of or a change in medication) and (ii) individual arrhythmia (sustained VT requiring ATP and/or defibrillation therapy, AF, NSVT and SVT).

Decision to commence medical therapy for NSVT and subsequent dose titration was variable depending on follow-up centre, frequency of NSVT and the presence of other arrhythmic risk factors. Not all patients commenced on treatment for NSVT were symptomatic. 25/90 (28%) of the FD-CD cohort had short episodes of asymptomatic NSVT (3-5 beats) during follow-up that were not treated. Survival free from atrial and ventricular arrhythmic events in the FD-CD group are shown in *Figure 7.3*. Of the 17 patients who had AF diagnosed on CD follow-up, 3 strokes were recorded prior to anticoagulation and no further episodes documented after treatment. *Table 7.4* highlights the number of total arrhythmic events per 100 patient years in the FD-CD group.

Figure 7.3. Kaplan-Meier curves illustrating cumulative freedom from atrial and ventricular arrhythmic events in the FD-CD cohort.

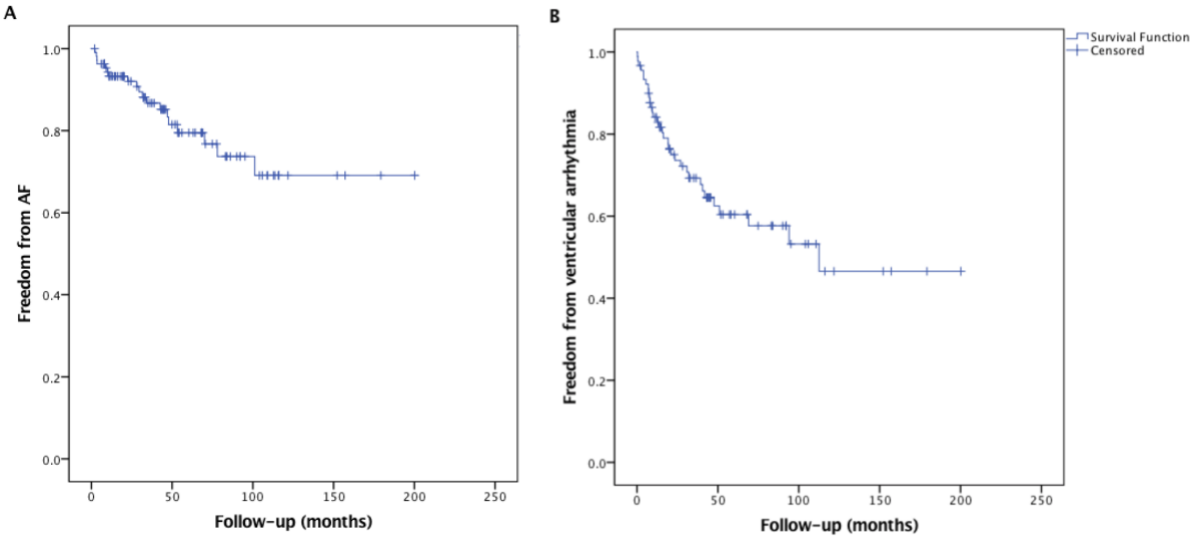

The event rates in the FD-CD patients (n=90). Panel A: time to first new diagnosis of AF. Panel B: time to first episode of ventricular arrhythmia.

Table 7.4. Number of arrhythmic events per 100 patient years in the FD-CD cohort.

	Events per 100 patient years
	FD-CD
All documented arrhythmia	12.6
Arrhythmia needing treatment	8.6
AF needing anticoagulation	3.8
NSVT	2.9
VT needing ATP and/or defibrillation	6.5
VT needing defibrillation	3.7

In the FD-CD group, baseline Holter monitoring was performed in 52/90 patients (58%) and 37 of these (71%) were abnormal leading to initiation of medical therapy or device

implantation (NSVT: 22/52, 42%; SVT: 6/52, 12%; AV conduction abnormality: 9/52, 17%). Of the FD-NonCD cohort, 85/276 underwent Holter monitoring (31%), with 12 of these identifying abnormalities. An alteration in therapy was required in 10/85 patients (12%) – NSVT: 4 requiring medication and one currently under consideration for ICD implantation; SVT: 4 requiring anticoagulation/beta blockade for AF and one medical treatment for AVNRT. Of the 6 FD-CD patients with flow-limiting IHD, 2 were found to have an arrhythmia requiring medical treatment – one with NSVT and another with a short burst of AF (both less than 30 seconds in duration).

7.3.1.3.2 Risk factors for arrhythmia

The incidence of risk factors and documented arrhythmia (AF, NSVT or VT/VF) can be seen in *Table 7.5*.

Table 7.5. Incidence of arrhythmic risk factors during the follow up period.

	FD-CD				**FD-NonCD**			
	No arrhythmia (n=32)	**AF (n=17)**	**VT/VF (n=15)**	***p-value***	**No arrhythmia (n=266)**	**AF (n= 11)**	**NSVT (n= 6)**	***p-value***
LVH (n, %)	28 (88)	17 (100)	14 (93)	*0.456*	89 (33)	7 (63.6)	4 (36.4)	***0.004*** †
LGE* (n, %)	9/14 (64)	10/12 (83)	5/5(100)	*0.138*	81/223 (36)	2/6 (33.3)	2/2 (100)	*0.149*
LA dilatation* (n, %)	19/32 (59)	13/17 (76)	11/15 (73)	*0.363*	8/82 (10)	4/7 (57.1)	1/4 (25)	*0.070*
PR interval (ms)	182±47	182±46	170±35	*0.232*	148±29	173±47	157±34	*0.473*
QRS duration (ms)	136±31	139±30	123±12	*0.652*	99±20	120±23	116±30	***<0.001*** †
MSSI	13.4±8.8	13.6±5.9	14.5±10.4	*0.877*	6.7±7.7	17.6±10.5	14.8±7.4	***<0.001*** ǂ

**not all underwent CMR or TTE imaging*

P-values are comparing incidence of risk factors in those with no arrhythmia, AF and ventricular arrhythmia, using an ANOVA model with post-hoc Tukey correction for continuous and Fishers-exact testing for categorical variables. † Significance was only seen between no arrhythmia and AF. ǂ Significance seen between no arrhythmia and both AF/NSVT. Arrhythmia data was collected from CD follow-up in the FD-CD group and from Holter monitor testing in the FD-NonCD group.

In those with arrhythmia requiring therapy there was no significant difference in prevalence of risk factors. In patients without arrhythmia there was a higher prevalence of risk factors in the FD-CD cohort (LVH, LA dilatation, prolonged PR interval and QRS duration, elevated MSSI, $p<0.001$). Analysis using Cox regression however, showed no significant predictors for the presence of any arrhythmic event (*Table 7.6*).

Table 7.6. The relationship of baseline clinical characteristics and occurrence of any arrhythmia during follow-up (Cox regression analysis).

Predictor variable	**Univariable analysis**		
	HR	**95% CI**	**p-value**
Age (years)*	1.01	0.99-1.03	0.294
Male gender	0.88	0.48-1.63	0.685
QRSd (ms)*	1.00	0.99-1.01	0.514
MWT	1.00	0.93-1.08	0.939
LA dilatation	0.87	0.48-1.60	0.659
LGE	1.70	0.93-3.13	0.088

**HR for age is defined using 10-year intervals and for QRSd using 10ms intervals.*

In addition to the 8 patients who had haemodynamically significant VT requiring defibrillation, one additional patient with a PPM died from sustained VT degenerating into VF, which was identified from post-mortem device interrogation. Of these 9 patients with

symptomatic VT, 7 had at least four arrhythmic risk factors (male >40yrs, severe LVH, extensive LGE, abnormal ECG with a QRS duration >120ms). The remaining patients included a female with co-existing familial long QT syndrome and a history of recurrent sustained VT, but no other FD specific risk factors; and a 52 year old male who had an ICD implanted following a short episode of NSVT, but no other arrhythmic risk factors. There were 9 deaths during follow-up. Three of these were cardiac deaths related to FD (two with sustained ventricular arrhythmia and one with end-stage heart failure).

7.3.1.3.3 ERT vs. no ERT

Of the FD-CD cohort, 62 patients (69%) were commenced on ERT prior to device implantation. Exact duration of ERT is not known as historical data was not available; however, all of these patients were on treatment for at least 1 year. In the ERT group there was a higher rate of arrhythmia compared to those patients not on ERT (ERT vs. no ERT: 46/62, 74% vs. 12/28, 43%; p=0.008). The incidence of arrhythmia requiring therapy however, was similar in the two groups (ERT vs. no ERT: 32/62, 51.6% vs. 8/28, 28.6%, p=0.066). This was also the case when evaluating the rates of newly diagnosed AF requiring anticoagulation, and sustained VT requiring ATP/defibrillation (*Figure 7.4*).

Figure 7.4. Incidence of arrhythmic events in those on ERT vs. no therapy (FD-CD cohort).

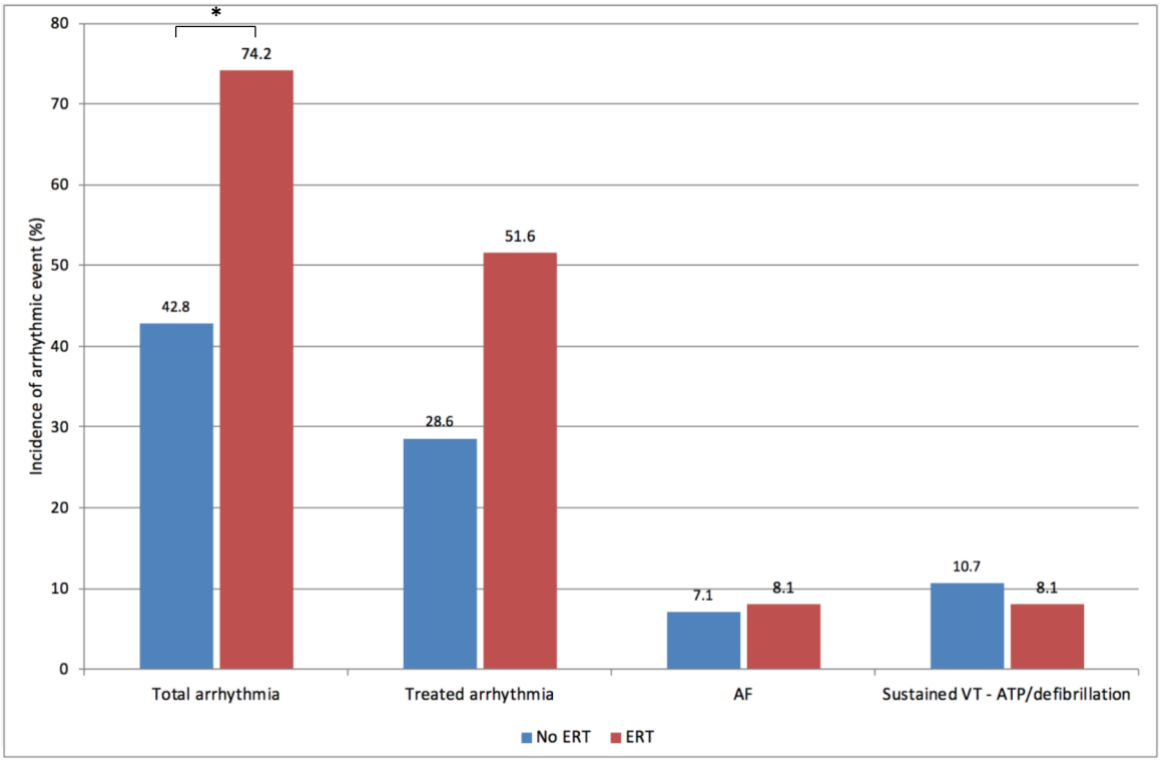

*The incidence of arrhythmic events in the FD-CD group on ERT vs. no therapy. It includes the following: (i) total documented arrhythmia, (ii) treated arrhythmia (including initiation of or a change in medication) and (iii) individual arrhythmia (AF and sustained VT requiring therapy). * denotes p=0.008. All other comparisons were non-significant.*

7.3.2 Diagnostic cardiac devices

ILRs were implanted in 19 patients. There was a male to female ratio of 1:1.1 and mean follow-up period of 2.7±2.2 years. Indications included: 1) Investigation of symptoms – palpitations and dizziness, 8 patients, 42%, 2) Investigation of possible AF with previous stroke – 3 patients, 16%, 3) Suspected ventricular arrhythmia – 5 patients, 26%, and 4) Abnormal but inconclusive Holter monitoring – 3 patients, 16%. Arrhythmia was identified in 7 patients (37%) – AF requiring anticoagulation in 3 patients, frequent ventricular ectopy requiring initiation of beta-blocker therapy in one, and bradycardia/pauses in 3 patients that did not fulfil criteria for pacemaker insertion.

7.4 Discussion

This study has demonstrated a clear lack of guidance for primary prevention device implantation in FD (66,239). ICD delivered therapy (ATP and defibrillation) occurred in over a quarter of the FD-CD population, highlighting the increased incidence of life-threatening ventricular arrhythmia in these patients. Additionally, the occurrence of arrhythmia in FD patients after device implantation was high and modification of therapy was also frequent. Diagnosis of asymptomatic atrial high rate episodes suggestive of AF from a device was also common and it is possible that this may contribute to the increased risk of ischemic stroke, which is the second highest cause of mortality in FD patients. Although the indication for ICD implantation in FD was variable, this study has demonstrated that an increasing number are inserted for primary prevention without guidance. Multiple parameters known to confer risk of MVA were common in the FD population, including ECG abnormalities, LVH and LGE.

7.4.1 Ventricular arrhythmia and sudden death

CV involvement is a common cause of morbidity and mortality in FD, with arrhythmia a significant and ongoing cause of death. There is no conclusive evidence to guide treatment in FD patients and the frequency of MVA reported in the literature varies widely (42,66,90,91). Previous studies have reported very low levels of clinically significant arrhythmia identified on device follow-up with a MVA incidence of 5.2% over 4 years (90) and AV conduction disease of 3.8% over 2.8 years (240). In this population however, the burden of ventricular arrhythmia appears to be much higher than previously thought with 44% of the study population affected and 26% requiring therapy over a 5-year follow-up period. Although the precise mechanisms of arrhythmia are not fully understood, certain structural changes have been suggested to predispose to ventricular arrhythmia and SCD, including LVH, ventricular dysfunction and extensive fibrosis with myocardial scarring (241) that suggest early therapeutic intervention may be beneficial (145). Risk models utilised with other hypertrophic disease processes however, cannot be mutually applicable due to differing pathophysiological processes. Although the actual number of patients who underwent a CMR was limited in this study, the evidence of an underlying inflammatory component leading to scar may be a potential explanation for any increase in arrhythmic risk in FD patients with LGE on CMR (36). Further research is needed; as such a finding may have significant implications on future monitoring and treatment in FD patients with cardiac involvement.

The incidence and predictive factors for ventricular arrhythmia requiring treatment and sudden death are not well defined in FD; with only limited data from small single-centre studies (73). These potential risk factors are common in FD patients who have a cardiac device and there is a tendency towards an increased frequency in those who develop arrhythmia. Furthermore, these risk factors are common in a large proportion of FD patients

without a cardiac device, raising a question as to whether device therapy is underused in this disease (73). Male patients tend to have progressive disease with extensive cardiac involvement, and in combination with advancing age, these factors are thought to increase the risk of ventricular arrhythmia (73). This study has also shown that those who underwent insertion of therapeutic cardiac devices were older and more frequently male (77%) compared to the remainder of the Fabry cohort, thus supporting the impact of age and gender on arrhythmic risk. The incidence of renal impairment was higher in patients with a cardiac device and informally observed differences within our centre have suggested that patients with certain co-morbid conditions, such as advanced CKD, may demonstrate more severe phenotypic patterns and consequently have greater risk of arrhythmia.

7.4.2 Atrial fibrillation and bradyarrhythmia

Although palpitations and syncope are common in FD, occurring in up to 30% of patients, data are mixed on incidence and risk factors of AF and bradyarrhythmia. As part of this study, a systematic review (PROSPERO CRD42019132045) was performed to define these factors within existing literature. Of the 1138 studies identified from database searches (Embase, Medline, PubMed, Web of Science, CINAHL, Cochrane), 11 were included. All were observational, with one designed as a non-randomised interventional trial. Nine studies were longitudinal (6 retrospective and 3 prospective), one was a registry data review and one a single time point cross-sectional study. Pooled median follow-up was 4.5 years and the weighted mean age was 39 years with an average male: female ratio of 1.5. The risk of bias was high in 10 studies, most notable in the confounding variables, incomplete dataset and blinding of outcome assessment domains. Eight studies provided data on incidence of AF (n=710) and PPM implantation (n=651). One registry study provided incidence of composite cardiovascular events, of which AF and PPM implantation were included. The weighted

estimate of event rates was 10.0% (95% CI 6.6-14.8) for AF needing anticoagulation and 12.2% (7.2-19.7) for PPM implantation.

Data on risk factors for AF were limited. Age was significantly but weakly associated with incident AF in 3 studies (328 participants), with odds ratios ranging from 1.05 to 1.20 per 1 year increase in age (66,242,243). Increasing LV mass also had limited value, with two studies (285 patients) demonstrating a link with incidental AF (66,242). A significant but very weak association was seen in one study using echocardiographic LVMi (HR 1.02, 95% CI 1.01-1.03) (242) and similarly in another study where AF was part of a composite endpoint with stroke (HR 1.02, p=0.016) (243). In a retrospective case-control study (n=50), Pichette et al (243) identified multiple parameters on echocardiography predictive of AF and stroke occurring in 9 patients over 4 years as a composite endpoint. These included an impaired (less negative) early diastolic strain (HR 0.777, p=0.006), a reduced (less negative) early diastolic strain rate (HR 7.64, p=0.028) and an impaired (less negative) LV global longitudinal strain (HR 1.63, p=0.006). Advanced severity of cardiac disease (elevated MSSI and extensive fibrosis on CMR, defined by LGE on more than 2 AHA segments of the LV myocardium) were both associated with the development of AF – elevated MSSI: HR 1.07, p=0.004, and LGE on CMR: no AF 19/29 vs. AF 10/11, p=0.033 (66).

Data on risk factors for PPM implantation were similarly limited. Increasing age was a common risk factor for PPM implantation, with three studies identifying an increased incidence with in older patients (OR 1.03 [1.01-1.04] per 1 year increase in age) (66,95,244). Female gender was also noted to be protective of the need for pacemaker – HR 0.27 (95% CI 0.07-0.99) (66) and HR 0.26 (0.06- 0.79) (95). Elevated LV mass was described in five studies as a strong predictor of PPM implantation. Three of these found a HR of 1.01 (95%

CI 1.00-1.01) (66,95,245) and one retrospective study of 49 patients (8 year follow-up) found that LVH was more common in those requiring a PPM (PPM: 8/9 vs. no PPM 14/40, $p<0.001$) (90). Prolonged PR interval and QRS duration were noted as clinical predictors of PPM implantation in three studies (PR interval: HR 1.02-1.03, QRS duration: HR 1.01-1.05; $p<0.05$) (66,95,245). Increasing MSSI was associated with PPM implantation in two studies (HR 1.05-1.07, $p<0.05$) (66,95).

This systematic review found that there is a major burden of both AF and brady-arrhythmia requiring PPM implantation in FD at a much younger age than would be expected in the general population. Although a number of traditional clinical predictors for AF (age, LVH and LA strain parameters) and PPM implantation (age, LVH, prolonged PR/QRS and beta blocker therapy) were identified, the strength of association was again much lower than would be expected in the general population, with HRs between one and 1.2 for most.

When comparing this to the initial study described in this chapter, the incidence of AF was found to be much higher in the FD-CD cohort, with 29.3% having a new diagnosis of AF requiring anticoagulation, compared to only 10% described within the systematic review of existing literature. Thus it is possible that the high burden of AF in FD may contribute to the increased risk of ischemic stroke, which is the second highest cause of mortality in FD patients.

7.4.2.1 Atrial fibrillation and ischaemic stroke

Ischaemic stroke is a common and serious clinical finding in early and advanced FD. The prevalence in men aged 25-44 years has been found to be 12 times higher in FD compared with the general population (246). Although the precise pathophysiology is not known, a number of pathophysiological processes have been hypothesised to play a predominant role

in its aetiology. These include endothelial dysfunction from vascular endothelial sphingolipid accumulation, cerebral hypoperfusion, a pro-thrombotic state in FD and vascular endothelial damage from the greater proportion of reactive oxygen species in FD (61,246). This study has shown that the rate of asymptomatic paroxysmal AF in those with advanced Fabry cardiomyopathy is high, suggesting that thromboembolic disease may have a more significant role in the aetiology of ischaemic stroke than previously suspected. Arrhythmic risk factors, such as left atrial dilatation, LVH and LGE were common in these patients, indicating the importance of detailed investigation in those at risk. There is currently no FD specific guidance for choice of anticoagulant therapy and the use of the CHA_2DS_2-VASc scoring system is not recommended in FD to guide its initiation (145,247). Given the high incidence and risk of stroke in FD, current literature suggests lifelong anticoagulation in those with AF (145).

7.4.3 Limitations

The limitations of this study include the possibility that the burden of arrhythmia could be underestimated. Specific arrhythmias, such as slow VT that are not within the device detection range may have been overlooked. Additionally, there may have been inappropriate identification of arrhythmia by the device, such as AF or noise mistaken for VT, and consequent mislabelling of a rhythm disturbance. To minimise this, in cases where the diagnosis of arrhythmia was unclear from the device interrogation report all EGM traces were reviewed in detail. Further prospective studies with real-time correlation between imaging and electrical biomarkers are needed to definitively characterise arrhythmic risk and guide treatment based on their risk stratification.

7.4.4 Conclusion

Cardiac pacemaker implantation in FD is always carried out following a clinically significant bradyarrhythmia. Indications for ICD insertion however, are variable with many devices now inserted based on presumed increased arrhythmic risk. Arrhythmias are common in Fabry patients following CD implantation, with high levels of asymptomatic AF and ventricular arrhythmia requiring ICD device use. Risk factors thought to be predictive of arrhythmia (age, male gender, LVH, LGE and a QRS duration >120ms) were more common in FD patients with a CD, supporting the need for Fabry specific guidance in this population.

7.5 Sub study: FD-CD vs. HCM

7.5.1 Background

Sarcomeric HCM is a genetic condition with an incidence of 1 in 500 individuals (248). Progressive myocardial hypertrophy occurs with ensuing fibrosis, diastolic dysfunction and eventual end-stage heart failure. Complications such as MVA and SCD have an annual risk of up to 1% (249) with risk factors such as myocardial fibrosis, LV aneurysm formation and coronary microvascular dysfunction commonly described (248). Consequently, arrhythmic risk stratification in HCM is widely understood and strict guidance exists for the use of primary prevention ICDs in these patients. Despite similarities in the disease phenotype and risk factor profile between sarcomeric HCM and FD, pathologically they are very distinct disease processes with different triggers of hypertrophy and thus risk stratification tools cannot be interchangeably used. The results presented in this chapter thus far have demonstrated the significant arrhythmic burden in FD. This sub study, however, was undertaken to increase awareness of Fabry cardiomyopathy amongst clinicians and further highlight the potential for arrhythmogenicity, by comparing the frequency of ICD device usage in patients with Fabry cardiomyopathy and sarcomeric HCM.

7.5.2 Brief methodology, study population and design

As part of this sub study, an additional comparator group included patients with genetically confirmed HCM who had undergone insertion of an ICD, recruited through clinical service. These patients were all followed up in specialist HCM services at the Queen Elizabeth Hospital, Birmingham and were identified through a regional HCM registry search. All HCM patients were age-matched (± 2 years) with the FD-CD cohort.

All demographic and clinical data were collected as per the main study methodology. CD electrocardiograms were manually reviewed to confirm presence of an arrhythmic event.

7.5.3 Participant characteristics and baseline data

The indications for ICD implantation in FD were more variable with only 30% having a class 1 indication for device insertion (99). 28% of patients underwent ICD implantation for secondary prevention following symptomatic ventricular arrhythmia. The remaining 72% were implanted for primary prevention outside of national guidance, but based on suspected arrhythmic risk (severe LVH, extensive LGE, abnormal resting ECG, previous NSVT on ECG monitoring, or a family history of sudden cardiac death). In all cases, the decision to implant a device followed discussion within an electrophysiology multi-disciplinary team meeting. In 24% device implantation preceded a diagnosis of FD. All HCM patients were risk stratified and underwent device implantation for primary prevention based on an estimated ESC 5-year risk of SCD greater than 4% and as such all comparisons between FD and HCM were of patients who underwent device implantation for primary prevention only.

The HCM comparator group had a mean age of 53±19 years, with 43 males (67%) and 21 females (33%). Only 3 HCM patients (5%) were found to have IHD that required any treatment at time of device implantation and none had CKD. Fabry patients who underwent secondary prevention ICD implantation, tended to have clinical parameters suggestive of more advanced disease. Baseline LVMi on CMR was higher in those who had devices implanted for secondary prevention (FD primary prevention: 144±38 vs. FD secondary prevention: 164±45, p=0.379), but the extent of LGE was greater in those who underwent device implantation for primary prevention purposes (FD primary prevention: 14, 52% vs. FD secondary prevention: 5, 19%, p=0.072), although neither reached statistical significance due to low numbers. While recognising that the pathogenesis of cardiac involvement in FD and HCM cohorts is different and therefore that disease phenotypes may be different, comparison of established risk factors for SCD risk stratification revealed higher LVMi on

CMR in FD compared to HCM (FD: 144±38g/m^2 vs. HCM: 102±36g/m^2, p=0.009) (96,250). MWT thickness, however, was similar in both groups (FD: 22±6 vs. HCM: 22±5, p=0.972). The proportion of patients with asymptomatic NSVT on Holter monitoring prior to device implantation was greater in FD (FD: 17/50, 34% vs. HCM: 11/53, 21%, p=0.049). There was a tendency to a reduced LV function in Fabry patients (LVEF <50% on echocardiography - FD: 12/38, 32% vs. HCM: 7/57, 12%, p=0.079). The degree of LGE on CMR was similar in both cohorts (FD: 14/27, 52% vs. HCM: 25/28, 89%, p=0.982). Although no change in PR interval was observed, QRS duration was greater in FD (FD: 135±32ms vs. HCM: 116±30ms, p=0.006). FD patients had greater hs-troponin (FD: 121 vs HCM: 19ng/l, p<0.001) but a non-significant trend toward higher NT-pro-BNP (FD: 1708 vs HCM: 888ng/l, p=0.086). Detailed demographic and investigation data can be seen in *Table 7.7*.

Table 7.7. Clinical demographics and investigation data: Fabry vs. HCM.

	Fabry			**HCM: Primary prevention**	***p-value ‡***
	Primary prevention	**Secondary prevention**	***p-value †***		
Sample size (n, %)	36 (72)	14 (28)	*N/A*	64	*N/A*
Follow-up duration (yrs)	3.8±2.6	5.8±3.9	*0.036*	6.4±2.9	*<0.001*
Age (yrs)	58±12	57±12	*0.922*	56±19	*0.516*
Male gender (n, %)	8 (16)	2 (4)	*0.704*	21 (33)	*0.359*
On ERT (n, %)	23 (46)	11 (22)	*0.501*	-	*N/A*
Classical mutation (n, %)	16 (32)	4 (8)	*0.353*	-	*N/A*
BMI (kg/m^2)	27±6	32±7	*0.087*	28±6	*0.411*
HR (bpm)	64±16	55±8	*0.265*	66±12	*0.633*
SBP (mmHg)	122±22	124±19	*0.824*	128±22	*0.436*
DBP (mmHg)	71±16	73±7	*0.785*	76±12	*0.292*
MSSI	16.7±9.4	11.9±7.1	*0.104*	-	*N/A*
Comorbidities					
IHD (n, %)	2 (4)	0 (0)	*1.000*	3 (5)	*1.000*
CKD stage 3-5 (n, %)	8 (16)	0 (0)	*0.087*	0 (0)	***<0.005***
HTN (n, %)	8 (16)	2 (4)	*0.704*	16 (25)	*0.812*
DM (n, %)	3 (6)	2 (4)	*0.611*	4 (6)	*0.700*
Stroke/TIA (n, %)	7 (14)	0 (0)	*0.169*	2 (3)	***0.010***

ECG	n=48			n=53	
Abnormal (n, %)	33 (69)	13 (27)	*1.000*	43 (81)	*0.114*
AF/PAF (n, %)	3 (6)	0 (0)	*0.550*	3 (6)	*0.664*
PR interval (ms)	172±36	145±30	*0.051*	178±39	*0.557*
QRS duration (ms)	135±32	134±32	*0.939*	116±31	***0.006***
Echocardiography	n=48			n=62	
LVH (n, %)	32 (67)	12 (25)	*1.000*	55 (89)	*0.485*
LA dilated (n, %)	24 (50)	10 (21)	*1.000*	60 (37-91)	*0.052*
CMR	n=27			n=28	
LVEDV (ml)	158±75	143±18	*0.791*	145±53	*0.564*
LVESV (ml)	73±80	26	*0.594*	54±44	*0.386*
LVEF (%)*	58 (53-65)	55 (43-65)	*0.747*	57 (55-64)	*0.904*
LVMi (g/m^2)	144±38	164±45	*0.379*	102±36	***0.009***
MWT (mm)	22±5	21±4	*0.867*	22±6	*0.965*
LGE (n, %)	14 (52)	5 (19)	*0.072*	25 (89)	*0.982*
Extensive (>3 AHA segments)	*11 (41)*	3 (11)	*0.115*	*14 (50)*	*0.344*
Mild (1-2 AHA segment e.g.BIFL)	*3 (11)*	2 (7)	*1.000*	*9 (32)*	*0.487*
RV insertion point	*0 (0)*	0 (0)	*N/A*	*2 (7)*	*0.526*
Biomarkers					
High sensitive troponin T (ng/L)*	121 (51-154)	90 (44-272)	*0.927*	19 (13-38)	***<0.001***
NT-pro BNP (ng/l)*	1708 (626-4068)	1319 (719-1894)	*0.667*	888 (353-2070)	*0.081*

**non-parametric data so presented as median (IQR), † p-value comparing primary and secondary prevention device implantation in FD, ‡ p-value comparing primary prevention device implantation in FD and HCM.*

7.5.4 Follow-up and arrhythmic risk factors

The occurrence of any arrhythmia requiring treatment as a combined endpoint or AF alone as a single endpoint tended to be higher in Fabry patients who had a device implanted for secondary prevention, although this did not reach statistical significance due to low numbers (any arrhythmia: FD primary - 17/36, 47% vs. FD secondary - 10/14, 71%, p=0.206 and AF: FD primary - 7/36, 19% vs. FD secondary - 4/14, 29%, p=0.476). VT requiring immediate shock therapy however, occurred more frequently in those with a secondary prevention device HR 2.7, 95% CI 1.2-5.7, p<0.001). Of the 14 Fabry patients with ventricular

arrhythmia requiring ICD therapy (ATP +/- defibrillation), 10 had devices for primary prevention and 4 for secondary prevention. Within the primary prevention cohort, 6 patients were treated with ATP alone and 4 patients with ATP and subsequent defibrillation. All patients within the secondary prevention cohort required defibrillation. All therapies were for sustained monomorphic VT.

The HCM comparator group had a significantly longer mean follow-up of 6.3±2.9 years ($p<0.05$). When evaluating FD and HCM primary prevention devices, arrhythmia occurred more frequently in FD over shorter follow-up (HR 4.2, 95% CI 2.0-8.6, $p<0.001$). VT requiring ATP ± defibrillation therapy was more common in the Fabry cohort (HR 4.5, 95% CI 1.7-11.7, p=0.002, see *Figure 7.5 panel C*). Defibrillation therapy for sustained VT was also more common in FD (HR 2.5, 95% CI 1.6-3.9, $p<0.001$). There was a greater burden of AF needing anticoagulation and NSVT in FD compared with HCM (AF: HR 6.2, 95% CI 1.8-21.6, p=0.004, NSVT: HR 3.1, 95% CI 1.7-5.6, $p<0.001$). FD was also found to be an independent predictor of all arrhythmia types in multivariate Cox regression with age and gender (*Table 7.8*). FD patients who had arrhythmia were often older, had greater LV mass, more scar tissue, a larger left atrium and a broader QRS duration. This did not however, reach statistical significance possibly due to low numbers.

Table 7.8. Predictors of any arrhythmia requiring treatment using multivariate Cox regression

Predictor	**HR**	**p-value**
Fabry disease	4.6	***<0.001***
Age	1.1	0.070
Male gender	0.9	0.624

Figure 7.5. Survival free of any arrhythmic event, atrial fibrillation and ventricular arrhythmia requiring ATP/defibrillation therapy, in Fabry and hypertrophic cardiomyopathy.

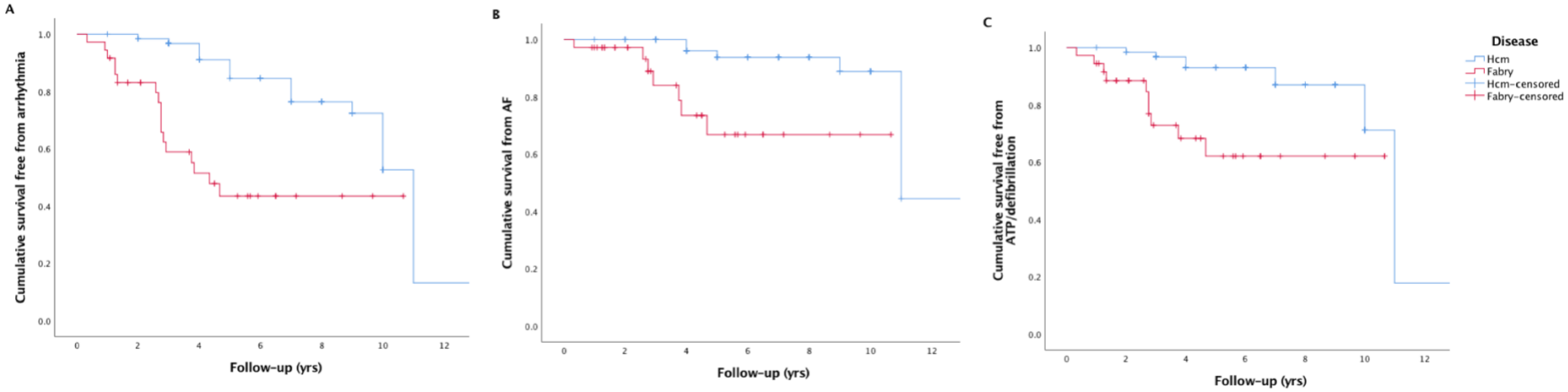

Event rates in Fabry and HCM. Panel A: time to first arrhythmic event (p<0.001). Panel B: time to first episode of AF requiring anticoagulation (p=0.001). Panel C: time to first appropriate ATP/defibrillation therapy (p<0.001).

7.5.5 Discussion and conclusion

This sub study has demonstrated a greater frequency of VT requiring ATP or defibrillation in FD compared with age and gender-matched sarcomeric HCM patients. Despite indications for ICD implantation in FD being more variable, device therapy occurred more frequently compared to HCM, where strict guidance exists for use of primary prevention ICDs. Furthermore, the common arrhythmic risk factors used to guide device implantation in HCM occurred more frequently in the FD population and their presence may be strongly associated with MVA (251).

Despite complexities in the understanding of the underlying arrhythmic mechanisms, there are similarities between FD and HCM in the structural changes known to be associated with MVA and SCD (LVH, ventricular dysfunction and advanced myocardial fibrosis), all of which would support the concept of early intervention with cardiac devices in FD (145). The incidence of sustained MVA requiring device therapy was higher however, in the FD cohort compared to both the HCM cohort and previous studies of subjects with non-ischaemic cardiomyopathy (252), thus suggesting that device implantation in FD is delayed until the disease is more advanced or complex compared to other disease processes (251). This sub study raises the hypothesis that Fabry cardiomyopathy may be more arrhythmogenic than HCM and as such existing risk stratification tools certainly cannot be mutually applicable. Further research is needed, which will be described in Chapter 8, as this will have significant implications on monitoring and treatment in Fabry cardiomyopathy.

One of the main limitations of this sub study is that direct phenotypic comparisons between FD and HCM were not possible as matching patients for age, gender and disease severity (LVMi) was not possible due to rarity of FD.

8. Discussion

Cardiovascular manifestations of Fabry disease are common and include progressive LVH, chronic myocardial inflammation (36), fibrosis, congestive cardiac failure, arrhythmia and sudden death (52). Despite Fabry specific and symptomatic cardiac therapies being widely available, cardiac involvement has a significant prognostic impact and is still the leading cause of morbidity and mortality in FD (69), with the effectiveness of disease modifying therapy known to be more limited in advanced disease. Thus early identification of cardiovascular involvement is key to enable initiation of therapy at the earliest opportunity and prevent progressive cardiomyopathy. Existing literature has demonstrated the value of CMR in diagnosing subclinical cardiac involvement, with further value in on going disease surveillance. The use of this multiparametric imaging modality in combination with other novel diagnostic tools described in this thesis demonstrate a potential platform to facilitate an earlier diagnosis of Fabry cardiomyopathy and thus improve our understanding of the complex pathophysiological processes involved.

The main findings of this thesis include:

- Male Fabry patients demonstrate progressive myocyte hypertrophy, storage and fibrosis (defined by increased LVMi, T1 lowering and increased LGE) irrespective of Fabry specific therapy. The biological response in women however is less clear, with a reduction in storage (improvement in T1 time) in those on treatment, suggesting a more significant impact of ERT in women.
- Myocardial strain (measured by GLS on CMR) is impaired in patients with existing cardiac disease, demonstrated by its association with LVMi, low T1 and progressive LGE. In patients with subclinical disease (LVH negative, low T1) however, GLS is

impaired in men but normal in women, demonstrating a gender difference in the myocardial functional response to storage.

- Novel A-ECG analysis techniques have the ability of predicting early myocardial involvement and adverse arrhythmic outcomes in FD. Thus, A-ECG not only has potential as a screening tool to diagnose early cardiac disease, but also in identifying those potentially at risk of adverse arrhythmic outcomes.
- Indications for cardiac device implantation in advanced Fabry cardiomyopathy are variable. A large proportion of ICDs are implanted for primary prevention outside of current guidance (99,236), but based on suspected arrhythmic risk. Device follow-up in these patients has demonstrated a high burden of AF and ventricular arrhythmia requiring either ATP or defibrillation therapy, with certain clinical parameters (age, male gender, LVH, LGE and a QRS duration >120ms) occurring more frequently and thus potentially predicative of these arrhythmia.

8.1 The gender dimorphism in the biological response to storage

Gender differences in the cardiovascular phenotype are well known with male patients exhibiting a clear pattern of myocardial disease, developing LVH earlier, subsequent myocardial fibrosis and ultimately adverse clinical outcomes including end-stage heart failure, arrhythmia and SCD (113,171,172). Female patients however, have a much more indolent disease process with LGE typically occurring within the basal inferolateral wall prior to the onset of LVH or any adverse clinical outcome (173). Nordin et al (36) showed that this area, which previously was assumed to be scar, also demonstrated an elevated T2 signal suggesting that this may in fact represent an area of chronic inflammation. Furthermore, the pattern of sphingolipid deposition within the myocardium differs between the genders as cardiovascular disease progresses. Women show progressive T1 lowering over

time but there appears to be pseudonormalisation of T1 in men as hypertrophy progresses (87). Thus two distinct pathways for men and women have been described in the Fabry cardiomyopathy disease model (37). The longitudinal data presented in Chapter 4 has supported this concept of a gender disparity both globally in the progression of LVH, but also on a microscopic level when evaluating how myocardial sphingolipid deposition changes over the course of the disease. An increase in myocardial hypertrophy of 2.4% per year was seen in male patients, but females tended to show more limited changes in LVM overall. When assessing the response to therapy men demonstrated progression of hypertrophy and storage irrespective of treatment, following trends previously described. Women however, showed a slower rise in LVM and interestingly a normalisation of T1 (6.2% increase), suggesting a possible hypothesis that females may be exhibiting removal of existing sphingolipid in response to treatment, with consequent slowing of the hypertrophic response. The existing literature describing changes in the cardiac phenotype over time is variable and largely uses TTE, which is known to have limitations. The data from this thesis, however, has used CMR with advanced tissue characterisation to provide a new insight into the myocardial response to storage and potential effect of therapy.

Functional differences between men and women have also been described in Chapter 5, with male patients having earlier impairment in myocardial strain prior to the onset of LVH (174). This study demonstrated that at baseline male patients have greater impairment in global longitudinal strain compared to females, despite a preserved ejection fraction. Both groups however, continued to show progressive deterioration in myocardial strain over the course of this study, suggesting that myocyte hypertrophy and increase in LV mass may be a less important intermediary step in the development of fibrosis and early left ventricular failure as shown by impaired GLS. In early disease (LVH negative and low T1), women appear to

tolerate sphingolipid deposition better than men, with a normal GLS observed in the females, but a significantly impaired GLS in males. This may be indicative of a higher degree of sphingolipid storage within the myocardium of males, which is poorly tolerated; consequently leading to earlier functional impairment.

8.2 Predictors of early cardiomyopathy

Technological advancements in cardiac imaging over the past 15 years have provided greater clarity on the biology of Fabry cardiomyopathy. Consequently the importance of early detection of cardiac disease has been brought to the forefront of discussion in order to identify a potential window for early intervention with disease modifying therapy. CMR native T1 mapping has provided some insight with the ability to identify subclinical sphingolipid deposition prior to the onset of any phenotypic response. The ability to characterise the myocardium in this way has facilitated assessment of the predictive value of other clinical parameters in identifying early disease (low T1). Historical TTE studies have demonstrated that strain imaging is a reliable and sensitive marker of identifying early disease, with impaired GLS found in Fabry compared to controls (253) and also in those who are LVH negative with low T1 (121). The data presented in Chapter 5 uses CMR feature tracking to support this concept of early functional changes in FD (impaired GLS), suggesting that it may have some degree of additive value with T1 mapping in predicting earlier cardiac involvement. Furthermore, electrical changes are known to occur very early in the disease process, with some abnormalities occurring as early as childhood (34,254). More significant ECG abnormalities have been associated with more advanced cardiac disease, but novel AI techniques used to analyse resting 12-lead ECGs in greater detail have shown promise in detecting subtle electrical abnormalities that occur much earlier. Augusto et al (230) identified that specific changes in atrial depolarisation and within ventricular

repolarisation intervals are associated with subclinical disease and consequently have incorporated these parameters into the Fabry disease model. The data presented in chapter 6 supports this notion with specific QRS and T wave parameters highly predictive of low native T1 in Fabry. These individual observations raise the possibility that there is an early interaction between storage, functional change and electrical abnormalities and thus a combined predictive scoring system may further unravel the biology of Fabry cardiomyopathy.

8.3 Cardiac arrhythmia and risk prediction

The frequency of arrhythmia is variably reported within existing literature. Registry data and small single centre studies suggest that the rate of ventricular arrhythmia varies widely from 5 to 30% (42,90,91). The data presented in Chapter 7 however, demonstrated that the burden of ventricular arrhythmia appears to be much higher with 44% of the study population affected and 26% requiring therapy over a 5-year follow-up period. Although the precise mechanism for arrhythmogenesis is not fully known, certain clinical parameters have been described in the literature to confer significant arrhythmic risk (73). This has been supported by data within this thesis, all of which suggest that early intervention would be beneficial. The use of ICDs as primary prevention for life-threatening arrhythmia is well established in ischaemic cardiomyopathy, but data on ICD use in the non-ischaemic population is more variable. The evidence base for primary prevention ICD usage in the majority of infiltrative cardiomyopathies is limited to smaller retrospective studies of observational data, with no data for their use in Fabry disease. Although some parallels can be drawn between Fabry and HCM, the precise pathophysiological processes of hypertrophy, scar and arrhythmogenesis are different and thus the HCM-SCD risk score cannot be mutually applicable (96). Existing literature and data from this thesis has demonstrated that certain clinical parameters that have

been associated with arrhythmic risk in HCM are also common place in Fabry patients who have ventricular arrhythmia, suggesting that they may also confer a similar degree of arrhythmic risk in FD, but further work described later in Chapter 9 are needed to validate a risk prediction model in Fabry.

Existing literature suggests that the reported incidence of AF could be as high as 13% (90). The data from Chapter 7 found that in advanced cardiac disease the occurrence of AF was higher and interestingly often asymptomatic, thus suggesting that in addition to having a low diagnostic yield, symptom driven investigation may lead to a significant underestimation of AF in Fabry. Ischaemic stroke is common in Fabry and although its aetiology traditionally was thought to be secondary to cerebral vascular endothelial sphingolipid deposition, this thesis has highlighted that thromboembolic disease may play a more significant role. Risk factors such as left atrial dilatation, LVH and LGE were common in these patients, indicating the importance of detailed investigation in those at risk. There is currently no FD specific guidance for choice of anticoagulant therapy and the use of the CHA_2DS_2-VASc scoring system is not recommended in FD to guide its initiation (145,247). Due to the high risk of ischaemic stroke in FD, current literature and expert consensus suggests lifelong anticoagulation with warfarin in these patients (255). A small single-centre study by Liu et al (255) investigated the use of a novel Fabry-specific scoring system and compared this to the CHA_2DS_2-VASc score. *Table 8.1* highlights the individual clinical parameters within each scoring system.

Table 8.1 Clinical parameters included within the Fabry-specific and CHA_2DS_2-VASc scoring systems. Adapted from Liu et al (255).

CHA_2DS_2-VASc score		**Fabry-specific score**	
Risk factor	**Point**	**Risk factor**	**Point**
Congestive cardiac failure	1	Prior stroke/TIA	2
Hypertension	1	Angiokeratoma	1
Age ≥75 years	2	Creatinine ≥1.0mg/dL	1
Diabetes	1	LVPWd >14mm	1
Prior stroke/TIA	2	GLS <13.5%	1
Vascular disease	1		
Age 65-75 years	1		
Female sex	1		

Liu et al (255) found that although not recommended in original guidance for use in FD, the CHA_2DS_2-VASc scoring system is a feasible system that could be used as a marker of thromboembolic risk assessment in FD. Analysis of their Fabry cohort identified five specific parameters as independent predictors of AF, which were used to develop their Fabry-specific score. When comparing this with the traditionally used CHA_2DS_2-VASc scoring system, the Fabry-specific score was found to be superior in risk prediction of AF in Fabry. Further work to validate this novel scoring system in a larger Fabry cohort is crucial in the next steps of managing arrhythmic risk in FD.

8.4 Further work

This thesis has not only provided an insight into novel biomarkers supporting early detection of cardiac disease, but has also demonstrated the burden of adverse clinical outcomes in this population. Further work however, is needed to define the cardiac phenotype in greater depth, consequently aiming to improve clinical outcomes and reduce overall morbidity. The projects outlined below will be explored following on from work presented in this thesis.

8.4.1 RaILRoAD: long-term follow-up

It is anticipated that recruitment of all 164 Fabry patients will be completed in August 2022. Detailed follow-up analysis will provide a true incidence of cardiac arrhythmia from a large Fabry cohort of mixed disease severity. Real-time arrhythmic data from ILRs over a period of three years will be evaluated against baseline cardiac investigation data to provide definitive arrhythmic risk predictors and support the development of a risk stratification tool guiding treatment of arrhythmia in FD.

Hypothesis

The incidence of arrhythmia is higher than currently believed and multiple non-invasive modalities such as CMR, A-ECG, echocardiography and blood biomarkers will aid in risk stratification and prediction of arrhythmic events in FD.

8.4.2 Progression of cardiovascular disease within individual phenotypic stages

As described in Chapter 5, CMR tissue characterisation techniques have enabled the development of a proposed disease model with specific stages within the natural progression of Fabry cardiomyopathy. These include: (i) an accumulation phase, with subclinical sphingolipid storage within the myocardium; (ii) an inflammatory and myocyte hypertrophy phase, with progressive increase in myocardial mass and extent of LGE; and (iii) late fibrosis and impairment phase, with fibrosis, thinning and LV dysfunction (37). This model is based however, on cross-sectional data and there are currently no longitudinal studies evaluating changes in CMR parameters across different phenotypic time points. The rate and timing of progression between each stage is not known. Moreover, there are only limited cross-sectional data exploring the clinical characteristics of the patients at each stage, and whether there are differences that can be identified to select out those at greatest risk. These data are

crucial in improving the timing of medical intervention to prevent progressive deterioration in cardiovascular status.

Hypothesis

The aim of this follow-on study would be to define changes in cardiac structure and function that occur over time in FD. This study will identify the rate of progression within different phenotypic stages of FD and more importantly identify when patients progress through each stage.

8.4.3 The effect of oral chaperone therapy in Fabry cardiomyopathy

Migalastat is a small molecule pharmacological chaperone that reversibly binds to the active site of AGAL-A. It stabilises mutant enzyme, thus facilitating appropriate trafficking to lysosomes where AGAL-A catabolises sphingolipid (256). These mutant forms of the enzyme are termed amenable mutations and are receptive to treatment with Migalastat as a potential alternative to intravenous ERT. Use of OCT has been associated with improvements in CV disease in FD, with a number of studies showing a reduction in LV mass and wall thickness on TTE (257). Germain et al demonstrated a 6.6g/m^2 reduction in total mass following 18 months of OCT compared to only 2.0g/m^2 in those on ERT (258). The higher volume of distribution of Migalastat and consequent improved myocardial tissue penetration has been suggested as a possible mechanism for these improvements in CV parameters. Given these promising results using echocardiography, further assessment of cardiovascular disease using multiple non-invasive modalities (CMR, A-ECG, exercise testing and patient outcome markers), is crucial in assessing effectiveness of new therapies in FD.

Hypothesis

Early therapeutic intervention in patients with subclinical disease (LVH negative, low T1) with migalastat has the potential to reverse storage prior to downstream pathological changes and attenuate the development of hypertrophy and fibrosis.

8.5 Conclusion

This thesis has provided a significant insight into Fabry cardiomyopathy. The use of CMR feature tracking techniques and advanced ECG analysis has shown great promise not only in the detection of early cardiac involvement, but also in potentially predicting adverse clinical outcomes. Risk stratification and early therapy is crucial in reducing morbidity and mortality in Fabry disease and this thesis has provided a platform to provide this information and gain a better understanding of the complex pathophysiology in this rare disease.

9. Appendix

9.1 The Role of Implantable Loop Recorders in Anderson-Fabry Disease (RaILRoAD)

The data described within this thesis has highlighted the significant burden of arrhythmia in FD and in addition has demonstrated a number of clinical parameters that may confer an increased risk of arrhythmia. Prospective validation of these is essential in developing Fabry specific guidance to support the treatment of cardiac arrhythmia both medically and with device implantation. To address this, a prospective randomised controlled trial was developed and set up as part of this thesis. The initial thesis proposal aimed to incorporate this detailed cardiac rhythm follow-up data from 164 FD patients recruited prospectively, to provide a more definitive risk stratification model in Fabry cardiomyopathy. Initial delays in funding unfortunately led to a significant delay in study opening and initiation of patient recruitment. Following recruitment of 42 patients, further setbacks were encountered during the Covid-19 pandemic, where all clinical research activity was paused and consequently no further patient recruitment was possible. Thus, completed recruitment and follow-up was out of the scope of this thesis. Baseline data and some descriptive analysis of patients recruited thus far are described below.

9.1.1 Study design and set up

This is a prospective 5 year study designed to evaluate arrhythmic burden and risk in FD (105). Current standard practice for cardiac rhythm monitoring is limited to 12-lead ECGs and annual 24 hour ambulatory monitoring with further interval investigation guided by patient symptoms. ILRs are small devices subcutaneously implanted that allow continuous rhythm monitoring for a period of three years and as such these devices have the potential to provide definite evidence of arrhythmia with greater accuracy and earlier diagnosis,

particularly in asymptomatic patients. This study aims firstly to compare the diagnostic potential of ILRs to standard care ambulatory monitoring and secondly to correlate clinical cardiac parameters with real-time arrhythmic outcome data, in order to accurately risk stratify Fabry patients. A summary of the trial design can be seen in *Figure 9.1*.

Figure 9.1 RaILRoAD study timeline. Taken from Vijapurapu et al (105).

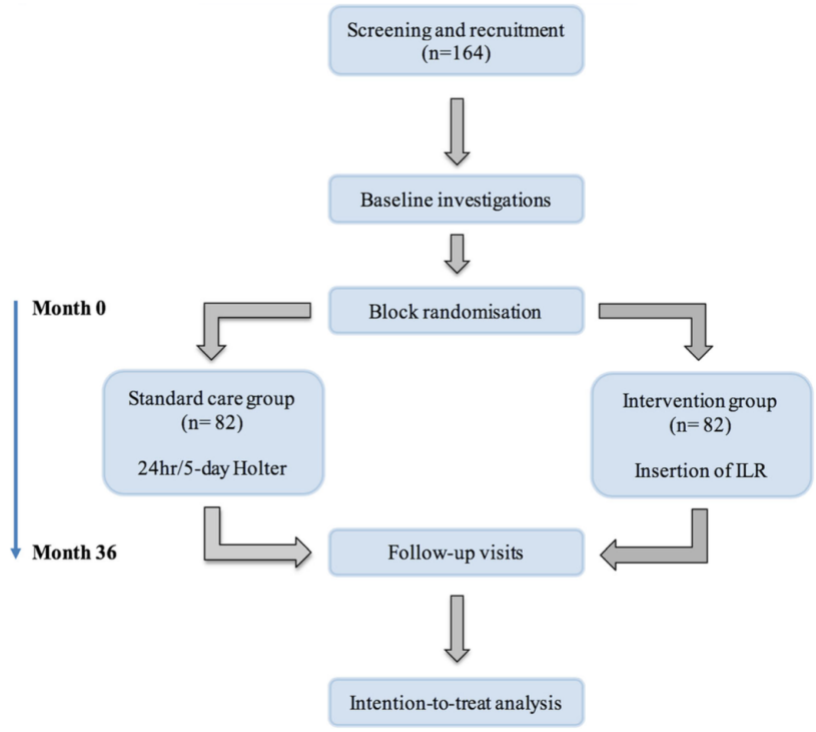

HRA and ethical approval was obtained (Integrated Research Application System project code 224749, REC reference 17/WM/0421) and the study conformed to the principles of the Helsinki Declaration. The study was registered with UHB R&D as sponsor (RRK5907) and locally at five recruiting sites within the UK and one site internationally in Australia.

The study population was enriched with certain clinical factors identified from existing literature (73) and work described in Chapter 7 (62,251) to confer a high arrhythmic risk.

Patients were block randomised to each treatment arm depending on the number of risk factors present at recruitment (*Figure 9.2*).

Figure 9.2 RaILRoAD block randomisation process. Taken from Vijapurapu et al (105).

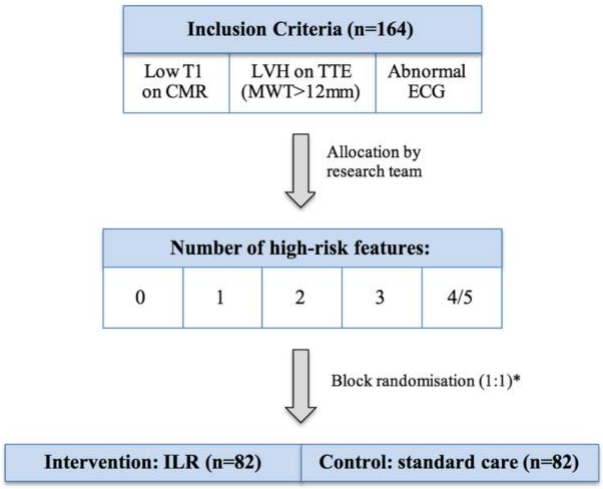

The high-risk features included LVH (defined by a MWT >12mm or an elevated LVMi), LA dilatation, elevated troponin, QRS duration >120ms, presence of LGE on CMR and a MSSI >20.

The primary outcome measures include any clinically significant arrhythmia requiring initiation or modification of therapy. These and all secondary outcome measures that will be evaluated can be seen in *Table 9.1.*

Table 9.1 Study outcome measures.

Primary outcome measures	Secondary outcome measures
AF requiring anticoagulation (defined as an episode >30 seconds)	Quantification of arrhythmia burden in those with and without LGE
Bradyarrhythmia requiring PPM implantation	Assess value of resting 12-lead ECG abnormalities in predicting arrhythmia
Supraventricular arrhythmia requiring medical therapy or ablation	Assess predictive value of A-ECG parameters in arrhythmia
NSVT requiring medical therapy, ICD	Evaluate the role of atrial size in burden of

implantation or ablation	AF
	Determine the effect of LVH on arrhythmia
	Assess the relationship of MSSI and burden of arrhythmia
	Evaluate the effects of various blood biomarkers on arrhythmia

9.1.2 Baseline demographic data

Complete baseline data for all 42 patients recruited was available. The cohort had a mean age of 49±14 years and 22 (52%) were men. A non-classical cardiac mutation was present in 50% of patients and 69% were on ERT at time of recruitment. Detailed demographic information can be seen in *Table 9.2*. The median number of high-risk features present in patients at baseline was 2.5 (IQR 1.0-4.0), with no overall difference between genders. When evaluating individual high-risk features however, a higher proportion of men had LVH and a QRS duration >120ms.

Table 9.2. Baseline demographic and high-risk feature data.

	Total	**Female**	**Male**	***p*-value***
Sample size (n, %)	42 (100)	20 (48)	22 (52)	*N/A*
Age (yrs)	49±14	48±18	50±11	*0.610*
On ERT (n, %)	29 (69)	9 (21)	20 (48)	***0.002***
Cardiac mutation (n, %)	14/28 (50)	5/11 (45)	9/17 (53)	*1.000*
BMI (kg/m^2)	29±7	29.8±7.4	27.7±7.1	*0.368*
HR (bpm)	70±13	73±13	67±13	*0.128*
SBP (mmHg)	133±17	131±16	134±18	*0.517*
DBP (mmHg)	77±9	76±7	78±11	*0.520*
Comorbidities				
CKD stage 3-5 (n, %)	3 (7)	2 (5)	1 (2)	*0.598*
HTN (n, %)	16 (38)	5 (12)	11 (26)	*0.121*
DM (n, %)	2 (5)	0 (0)	2 (5)	*0.489*
Stroke/TIA (n, %)	1 (2)	0 (0)	1 (2)	*1.000*
Smoker (n, %)	13 (31)	7 (17)	6 (14)	*0.741*
High risk features				
LVH (n, %)	28 (67)	10 (24)	18 (43)	***0.049***
LA dilatation (n, %)	27 (64)	13 (31)	14 (33)	*1.000*
Elevated troponin (n, %)	16 (38)	7 (17)	9 (21)	*0.751*
QRS >120ms (n, %)	9 (21)	1 (2)	8 (19)	***0.020***

LGE (n, %)	20 (48)	6 (14)	14 (33)	*0.056*
MSSI >20 (n, %)	12 (29)	5 (12)	7 (17)	*0.734*
Number of high risk features*	2.5 (1.0-4.0)	2.0 (1.0-3.0)	3.0 (1.75-4.25)	*0.069*

** Non-normally distributed data so presented as median and interquartile range (IQR)*

Table 9.3 demonstrates the baseline cardiac investigation and blood biomarker data. Men had a higher LVMi and MWT compared to women (LVMi: 105.0 vs. 68.9 g/m^2, p<0.001 and MWT: 15.5 vs. 9.0 mm, p=0.002). 64% of the cohort had low native T1 according to local reference ranges (men: 16/22, 73% vs. women: 11/20, 55%, p=0.336). Of the total cohort 48% had LGE (defined as visual LGE in more than two AHA segments of the LV). There was a non-significant trend towards a greater proportion in men than women (14/22, 64% vs. 6/20, 30%, p=0.056). There was no difference in hs-troponin and NT-pro BNP between genders.

Table 9.3. Cardiac investigation and blood biomarker data.

	Total	**Female**	**Male**	***p-value****
TTE				
LVEF (%)*	69 (64-73)	69 (67-75)	64 (61-68)	***0.004***
LA volume (ml)	50±27	41±14	61±35	*0.080*
ECG				
PR interval (ms)	151±19	150±18	152±20	*0.764*
QRS duration (ms)	106±22	96±15	115±23	***0.004***
T wave inversion (n, %)	24 (57)	9 (21)	15 (36)	*0.196*
CMR				
LVMi (g/m^2)*	78.4 (65.6-105.4)	68.9 (58.7-78.0)	105.0 (80.1-163.4)	***<0.001***
MWT (mm)*	11.0 (8.0-15.0)	9.0 (8.0-12.0)	15.5 (11.5-19.3)	***0.002***
LVEDVi (ml/m^2)	63±15	59±12	66±17	*0.280*
LVESVi (ml/m^2)	16±7	14±6	18±7	*0.071*
LVSVi (ml/m^2)	46±11	45±9	47±12	*0.746*
Low T1 (n, %)	27 (64)	11/20 (55)	16/22 (73)	*0.336*
LGE (n, %)	20 (48)	6/20 (30)	14/22 (64)	*0.056*
RVEDVi (ml/m^2)	61±18	58±15	65±20	*0.302*
RVESVi (ml/m^2)	19±9	17±7	21±10	*0.275*
RVSVi (ml/m^2)	42±12	40±12	44±13	*0.483*
Biomarkers				

High sensitive troponin T (ng/L)*	20.9 (7.1-45.0)	19.0 (5.0-112.5)	20.9 (8.0-40.0)	*0.813*
NT-pro BNP (ng/l)*	125 (66-612)	148 (55-452)	115 (71-1812)	*0.681*
eGFR (ml/min/1.73m^2)*	86 (65-90)	86 (56-90)	87 (72-90)	*0.775*

** Non-normally distributed data so presented as median and IQR.*

9.1.3 Descriptive follow-up data and arrhythmic risk factors

Of the 42 patients recruited to the study 18 patients were randomised to standard care ambulatory monitoring (SC) and 24 were allocated to ILR implantation in addition to standard care (men: SC 8/22, 36% vs. ILR 14/22, 64% and women: SC 10/20, 50% vs. ILR 10/20, 50%; see *Table 9.4*).

Table 9.4. Proportion of patients randomised to standard care and ILR.

	Male (n=22)	**Female (n=20)**	**p-value**
Standard care (n, %)	8 (36)	10 (50)	0.533
ILR (n, %)	14 (64)	10 (50)	

Median follow-up time of the cohort was 12 months (IQR 9.2-13.5), with no difference between genders (men: 10.3 [8.8-13.4] vs. women: 12.3 [11.0-13.4] months, p=0.080). Over this follow-up period 11 patients had arrhythmic events. All of these patients were from the ILR cohort and no events were detected within the standard care group. From the 11 patients there were 14 separate arrhythmic events, with a breakdown shown in *Table 9.6*. Of these 3 patients required treatment for arrhythmia and, following discussion with the Data, Safety and Monitoring committee, met the criteria for a primary endpoint (see *Table 9.5*). When evaluating the presence of potential risk factors within this group of 11 patients, no trends or associations were observed due to low numbers.

Table 9.5. Outcome events in the initial 42 patients recruited.

	NSVT	Pauses	Atrial fibrillation	SVT/Atrial tachycardia
Number of events	6	2	3	3
Details	All asymptomatic No treatment	All asymptomatic No treatment	One symptomatic Two required treatment	One symptomatic One required treatment

Primary endpoints			
Patient	**Clinical details**	**Arrhythmia detected**	**Treatment**
1	37M Severe LVH (LVM 213g), no LGE, normal LA size ECG: SR, RBBB, LVH with strain	Atrial tachycardia with aberrant conduction →Symptomatic	Beta blocker
2	56M Mild LVH (MWT 15mm, LVM 154g), no LGE, normal LA size ECG: SR with LVH	New AF (multiple episodes, longest 4hr 34min) → All asymptomatic	Anticoagulation and rate control
3	64M LVH (MWT 20mm, LVM 222g), LGE in basal inferolateral wall, normal LA size PMH: T2DM, COPD ECG: SR with LVH	New AF (two episodes, both >1hr) → All asymptomatic	Anticoagulation and rate control

9.2 Published work relating to this thesis

9.2.1 Oral communications

- **Vijapurapu R**. Update on the heart: Cardiovascular involvement of Fabry disease. MPS Society Focus on Fabry patient meeting. Marlow, UK, September 2018

- **Vijapurapu R**, Hawkins F, Liu B et al. A study of the different methodologies used in calculation of extra-cellular volume by CMR imaging. British Cardiovascular Imaging Annual Conference. Edinburgh, Scotland, May 2018. Short listed for Young Investigator Award.

- **Vijapurapu R**, Jovanovic A, Baig, S et al. A multicentre study of cardiac device implantation, arrhythmic burden and risk factors in Fabry cardiomyopathy. European Fabry Academy. Warsaw, Poland, October 2019. Shortlisted for Young Investigator Award.

- **Vijapurapu R**. Cardiovascular involvement of Fabry disease. MPS Society Focus on Fabry patient meeting. Marlow, UK, September 2019.

- **Vijapurapu R**, Hughes DA, Thomas M. Novel therapies in Fabry disease. Expert panellist on webinar organised by MPS Society. September 2020.

- **Vijapurapu R**, Steeds RP. Fabry disease: Epidemiology, inheritance and cardiac involvement. Expert cardiologist involved in developing and delivering E-learning module. 2020.

9.2.2 Poster communications

- **Vijapurapu R**, Hawkins F, Liu B et al. A study of the different methodologies used in calculation of extra-cellular volume by CMR imaging. British Cardiovascular Imaging Annual Conference. Edinburgh, Scotland, May 2018. Short listed for Young Investigator Award.

- **Vijapurapu R**, Nordin S, Baig S et al. Characterisation of 3D systolic strain in patients with Fabry disease. British Cardiovascular Society Annual Conference. Manchester, UK, June 2018.

- **Vijapurapu R**, Baig S, Wheeldon N et al. A national study evaluating cardiac device implantation and usage in Fabry disease. European Society of Cardiology Annual Conference. Munich, Germany, August 2018.

- **Vijapurapu R**, Baig S, Nordin S et al. The natural progression of cardiac involvement in Fabry disease. International WORLD Symposium (We're Organizing Research on Lysosomal Diseases). Florida, USA, February 2019.

- **Vijapurapu R**, Jovanovic A, Wheeldon N et al. A multicentre study of cardiac device implantation, arrhythmic burden and risk factors in Fabry cardiomyopathy. International WORLD Symposium (We're Organizing Research on Lysosomal Diseases). Florida, USA, February 2019.

- **Vijapurapu R**, Jovanovic A, Baig, S et al. A multicentre study of cardiac device implantation, arrhythmic burden and risk factors in Fabry cardiomyopathy. European Fabry Academy. Warsaw, Poland, October 2019. Shortlisted for Young Investigator Award.

- **Vijapurapu R**, Zegard A, Baig S et al. ICD implantation and device therapy Fabry vs hypertrophic cardiomyopathy. European Society of Cardiology Annual Conference. August 2020.

- **Vijapurapu R**, Maanja M, Schlegel T et al. Advanced electrocardiography predicts early cardiac involvement and incident arrhythmias in Fabry disease. European Heart Rhythm Association Annual Conference. Copenhagen, Denmark, April 2022.

9.2.3 Publications

- Baig S*, **Vijapurapu R***, Alharbi F et al. Diagnosis and treatment of the cardiovascular consequences of Fabry disease. QJM. 2019; 112(1): 3-9. *Joint first author.

- **Vijapurapu R**, Nordin S, Baig S et al. Global longitudinal strain, myocardial storage and hypertrophy in Fabry disease. Heart. 2019; 105(6): 470-476.

- **Vijapurapu R**, Kozor R, Hughes DA et al. A randomised controlled trial evaluating arrhythmia burden, risk of sudden cardiac death and stroke in patients with Fabry disease: the role of implantable loop recorders (RaILRoAD) compared with current standard practice. Trials. 2019; 20(1): 314.

- **Vijapurapu R**, Geberhiwot T, Jovanovic A et al. A study of indications for cardiac device implantation and utilisation in Fabry cardiomyopathy. Heart. 2019; 105(23).

- **Vijapurapu R**, Baig S, Nordin S et al. Longitudinal assessment of cardiovascular involvement in Fabry disease using cardiovascular magnetic resonance imaging. JACC Cardiovascular Imaging. 2020; 13(8).

- Moody WE, **Vijapurapu R**, Steeds R. Impact of myocardial contouring method on the cardiac MRI assessment of hypertrophied hearts. Radiology Cardiothoracic Imaging. 2020; 2(5).

- **Vijapurapu R**, Bradlow W, Leyva F et al. Cardiac device implantation and device usage in Fabry and hypertrophic cardiomyopathy. Orphanet Journal of Rare Diseases. 2022; 17(1).

- **Vijapurapu R**, Kotecha D, Demetriades P et al. Fabry disease and the risk of atrial fibrillation and pacemaker implantation: A systematic review. Under review in JACC EP, 2022.

- **Vijapurapu R**, Maanja M, Schlegel T et al. Advanced electrocardiography predicts early cardiac involvement and incident arrhythmia in Fabry disease. Under review in JACC CVI. 2022.

- **Vijapurapu R**, Elsayed H, Alvior AM et al. Multimodality evaluation of valve disease in Fabry disease. Under review in Canadian Journal of Cardiology. 2022.

9.2.4 Grants and awards

- Society for Mucopolysaccharide Diseases Society research grant: September 2017
- Rosetrees Trust research grant (£6,120): January 2018

9.3 Published work not directly relating to this thesis

9.3.1 Poster communications

- Augusto J, Nordin S, Kozor R, **Vijapurapu R** et al. Inflammatory Cardiomyopathy in Fabry disease. British Society of Cardiovascular Magnetic Resonance Annual Meeting. Oxford, UK, March 2019.

- Augusto J, Nordin S, Kozor R, **Vijapurapu R** et al. Inflammatory Cardiomyopathy in Fabry disease. EuroCMR Annual Congress. Venice, Italy, May 2019

- Nickander J, Nordin S, **Vijapurapu R** et al. Blood correction of native T1 increases detection of cardiac involvement in patients with Fabry disease. EuroCMR Annual Congress. Venice, Italy, May 2019

- Moon JC, Augusto J, Nordin S, **Vijapurapu R** et al. Chronic myocardial edema in Fabry disease is linked to myocardial injury and left ventricular volume/pressure overload. International WORLD Symposium (We're Organizing Research on Lysosomal Diseases). Florida, USA, February 2020.

- Price AM, Stoll V, **Vijapurapu R** et al. Myocardial tissue characterization in living kidney donors 5 years after nephrectomy. European Renal Association Annual Meeting. Milan, Italy, June 2020.

- Price AM, Moody W, Stoll V, **Vijapurapu R** et al. Cardiovascular effects of unilateral nephrectomy in living kidney donors at five years. European Renal Association Annual Meeting. Milan, Italy, June 2020.

- Price AM, Moody W, Stoll V, **Vijapurapu R** et al. Cardiovascular effects of living kidney donation: A five year long study. British Cardiovascular Society Annual Conference. Manchester, UK, June 2020.

9.3.2 Publications

- Nordin S, Kozor R, **Vijapurapu R** et al. Myocardial storage, inflammation, and cardiac phenotype in Fabry disease after one year of enzyme replacement therapy. Circulation Cardiovascular Imaging. 2019; 12(12).

- Alharbi F, Baig S, Rambhatla S, **Vijapurapu R** et al. The clinical utility of total concentration of urinary globotriaosylsphingosine plus its analogues in the diagnosis of Fabry disease. Clinica Chimica Acta. 2020; 500: 120-127.

- Augusto J, Nordin S, **Vijapurapu R** et al. Myocardial edema, myocyte injury, and disease severity in Fabry disease. Circulation Cardiovascular Imaging. 2020; 13(13).

- Baig S, Dowd R, Edwards NE, Hodson J, Fabritz L, **Vijapurapu R** et al. Prospective cardiovascular magnetic resonance imaging in adults with Alström syndrome: silent progression of diffuse interstitial fibrosis. Orphanet Journal of Rare Diseases. 2020; 15(1).

- Price AM, Moody WE, Stoll V, **Vijapurapu R** et al. Cardiovascular effects of unilateral nephrectomy in living kidney donors at 5 years. Hypertension. 2021; 77: 1273-1284.

- Augusto J, Johner N, Shah D, Nordin S, Knott K, Lau, C, Seraphim A, Hughes R, **Vijapurapu R** et al. The myocardial phenotype of Fabry disease pre-hypertrophy and pre-detectable storage. EHJ – Cardiovascular Imaging. 2021; 22: 790-799.

- Liu B, Neil DAH, Bhabra M, Patel R, Barker TA, Nikolaidis N, Billing JS, Hayer M, Baig S, Price AM, **Vijapurapu R** et al. Reverse myocardial remodelling following valve repair in patients with chronic severe primary degenerative mitral regurgitation. JACC Cardiovascular Imaging. 2021; 15(2).

10. References

1. Elliott PM. Fabry Disease: A Rare Condition Emerging From the Darkness. Circ Cardiovasc Genet 2017;10.
2. Ortiz A, Germain DP, Desnick RJ et al. Fabry disease revisited: Management and treatment recommendations for adult patients. Mol Genet Metab 2018;123:416-427.
3. Fabry Database. The Fabry Mutants List.
4. Desnick RJ, Brady R, Barranger J et al. Fabry disease, an under-recognized multisystemic disorder: expert recommendations for diagnosis, management, and enzyme replacement therapy. Ann Intern Med 2003;138:338-46.
5. Zarate YA, Hopkin RJ. Fabry's disease. Lancet 2008;372:1427-35.
6. Mehta A, Beck M, Eyskens F et al. Fabry disease: a review of current management strategies. QJM 2010;103:641-59.
7. Yousef Z, Elliott PM, Cecchi F et al. Left ventricular hypertrophy in Fabry disease: a practical approach to diagnosis. Eur Heart J 2013;34:802-8.
8. Monserrat L, Gimeno-Blanes JR, Marin F et al. Prevalence of fabry disease in a cohort of 508 unrelated patients with hypertrophic cardiomyopathy. J Am Coll Cardiol 2007;50:2399-403.
9. Nakao S, Takenaka T, Maeda M et al. An atypical variant of Fabry's disease in men with left ventricular hypertrophy. N Engl J Med 1995;333:288-93.
10. Sachdev B, Takenaka T, Teraguchi H et al. Prevalence of Anderson-Fabry disease in male patients with late onset hypertrophic cardiomyopathy. Circulation 2002;105:1407-11.
11. Spada M, Pagliardini S, Yasuda M et al. High incidence of later-onset fabry disease revealed by newborn screening. Am J Hum Genet 2006;79:31-40.

12. Burlina AB, Polo G, Salviati L et al. Newborn screening for lysosomal storage disorders by tandem mass spectrometry in North East Italy. J Inherit Metab Dis 2018;41:209-219.

13. Baig S, Vijapurapu R, Alharbi F et al. Diagnosis and Treatment of the Cardiovascular Consequences of Fabry Disease. QJM 2018.

14. Garman SC, Garboczi DN. The molecular defect leading to Fabry disease: structure of human alpha-galactosidase. J Mol Biol 2004;337:319-35.

15. Askari H, Kaneski CR, Semino-Mora C et al. Cellular and tissue localization of globotriaosylceramide in Fabry disease. Virchows Arch 2007;451:823-34.

16. Toupin A, Lavoie P, Arthus MF et al. Analysis of globotriaosylceramide (Gb3) isoforms/analogs in unfractionated leukocytes, B lymphocytes and monocytes from Fabry patients using ultra-high performance liquid chromatography/tandem mass spectrometry. Anal Chim Acta 2018;1015:35-49.

17. Boutin M, Menkovic I, Martineau T, Vaillancourt-Lavigueur V, Toupin A, Auray-Blais C. Separation and Analysis of Lactosylceramide, Galabiosylceramide, and Globotriaosylceramide by LC-MS/MS in Urine of Fabry Disease Patients. Anal Chem 2017;89:13382-13390.

18. Lavoie P, Boutin M, Auray-Blais C. Multiplex analysis of novel urinary lyso-Gb3-related biomarkers for Fabry disease by tandem mass spectrometry. Anal Chem 2013;85:1743-52.

19. Namdar M, Gebhard C, Studiger R et al. Globotriaosylsphingosine accumulation and not alpha-galactosidase-A deficiency causes endothelial dysfunction in Fabry disease. PLoS One 2012;7:e36373.

20. Vedder AC, Strijland A, vd Bergh Weerman MA, Florquin S, Aerts JM, Hollak CE. Manifestations of Fabry disease in placental tissue. J Inherit Metab Dis 2006;29:106-11.

21. Wanner C. Fabry disease model: a rational approach to the management of Fabry disease. Clin Ther 2007;29 Suppl A:S2-5.

22. Pieroni M, Moon JC, Arbustini E et al. Cardiac Involvement in Fabry Disease: JACC Review Topic of the Week. J Am Coll Cardiol 2021;77:922-936.

23. Linhart A, Germain DP, Olivotto I et al. An expert consensus document on the management of cardiovascular manifestations of Fabry disease. Eur J Heart Fail 2020;22:1076-1096.

24. Nair V, Belanger EC, Veinot JP. Lysosomal storage disorders affecting the heart: a review. Cardiovasc Pathol 2019;39:12-24.

25. Platt FM, d'Azzo A, Davidson BL, Neufeld EF, Tifft CJ. Lysosomal storage diseases. Nat Rev Dis Primers 2018;4:27.

26. Rombach SM, Twickler TB, Aerts JM, Linthorst GE, Wijburg FA, Hollak CE. Vasculopathy in patients with Fabry disease: current controversies and research directions. Mol Genet Metab 2010;99:99-108.

27. Eitzman DT, Bodary PF, Shen Y et al. Fabry disease in mice is associated with age-dependent susceptibility to vascular thrombosis. J Am Soc Nephrol 2003;14:298-302.

28. Ivanova M. Altered Sphingolipids Metabolism Damaged Mitochondrial Functions: Lessons Learned From Gaucher and Fabry Diseases. J Clin Med 2020;9.

29. Shen JS, Meng XL, Moore DF et al. Globotriaosylceramide induces oxidative stress and up-regulates cell adhesion molecule expression in Fabry disease endothelial cells. Mol Genet Metab 2008;95:163-8.

30. Chimenti C, Hamdani N, Boontje NM et al. Myofilament degradation and dysfunction of human cardiomyocytes in Fabry disease. Am J Pathol 2008;172:1482-90.

31. Brakch N, Dormond O, Bekri S et al. Evidence for a role of sphingosine-1 phosphate in cardiovascular remodelling in Fabry disease. Eur Heart J 2010;31:67-76.

32. Seydelmann N, Wanner C, Stork S, Ertl G, Weidemann F. Fabry disease and the heart. Best Pract Res Clin Endocrinol Metab 2015;29:195-204.

33. Namdar M. Electrocardiographic Changes and Arrhythmia in Fabry Disease. Front Cardiovasc Med 2016;3:7.

34. Namdar M, Steffel J, Vidovic M et al. Electrocardiographic changes in early recognition of Fabry disease. Heart 2011;97:485-90.

35. Birket MJ, Raibaud S, Lettieri M et al. A Human Stem Cell Model of Fabry Disease Implicates LIMP-2 Accumulation in Cardiomyocyte Pathology. Stem Cell Reports 2019;13:380-393.

36. Nordin S, Kozor R, Bulluck H et al. Cardiac Fabry Disease With Late Gadolinium Enhancement Is a Chronic Inflammatory Cardiomyopathy. J Am Coll Cardiol 2016;68:1707-1708.

37. Nordin S, Kozor R, Medina-Menacho K et al. Proposed Stages of Myocardial Phenotype Development in Fabry Disease. JACC Cardiovasc Imaging 2018.

38. Rozenfeld P, Feriozzi S. Contribution of inflammatory pathways to Fabry disease pathogenesis. Mol Genet Metab 2017;122:19-27.

39. Mauhin W, Lidove O, Masat E et al. Innate and Adaptive Immune Response in Fabry Disease. JIMD Rep 2015;22:1-10.

40. Linthorst GE, Vedder AC, Aerts JM, Hollak CE. Screening for Fabry disease using whole blood spots fails to identify one-third of female carriers. Clin Chim Acta 2005;353:201-3.

41. Schaefer RM, Tylki-Szymanska A, Hilz MJ. Enzyme replacement therapy for Fabry disease: a systematic review of available evidence. Drugs 2009;69:2179-205.

42. Weidemann F, Niemann M, Stork S et al. Long-term outcome of enzyme-replacement therapy in advanced Fabry disease: evidence for disease progression towards serious complications. J Intern Med 2013;274:331-41.

43. Linhart A, Elliott PM. The heart in Anderson-Fabry disease and other lysosomal storage disorders. Heart 2007;93:528-35.

44. Viggiano E, Politano L. X Chromosome Inactivation in Carriers of Fabry Disease: Review and Meta-Analysis. Int J Mol Sci 2021;22.

45. Cairns T, Muntze J, Gernert J, Spingler L, Nordbeck P, Wanner C. Hot topics in Fabry disease. Postgrad Med J 2018;94:709-713.

46. Desnick RJ, Wasserstein MP. Fabry disease: clinical features and recent advances in enzyme replacement therapy. Adv Nephrol Necker Hosp 2001;31:317-39.

47. Echevarria L, Benistan K, Toussaint A et al. X-chromosome inactivation in female patients with Fabry disease. Clin Genet 2016;89:44-54.

48. Arends M, Wanner C, Hughes D et al. Characterization of Classical and Nonclassical Fabry Disease: A Multicenter Study. J Am Soc Nephrol 2017;28:1631-1641.

49. Mahmud HM. Fabry's disease--a comprehensive review on pathogenesis, diagnosis and treatment. J Pak Med Assoc 2014;64:189-94.

50. Tuttolomondo A, Pecoraro R, Simonetta I et al. Neurological complications of Anderson-Fabry disease. Curr Pharm Des 2013;19:6014-30.

51. Tuttolomondo A, Pecoraro R, Simonetta I, Miceli S, Pinto A, Licata G. Anderson-Fabry disease: a multiorgan disease. Curr Pharm Des 2013;19:5974-96.

52. Mehta A, Clarke JT, Giugliani R et al. Natural course of Fabry disease: changing pattern of causes of death in FOS - Fabry Outcome Survey. J Med Genet 2009;46:548-52.

53. Ramaswami U, Whybra C, Parini R et al. Clinical manifestations of Fabry disease in children: data from the Fabry Outcome Survey. Acta Paediatr 2006;95:86-92.

54. Mehta A, Ricci R, Widmer U et al. Fabry disease defined: baseline clinical manifestations of 366 patients in the Fabry Outcome Survey. Eur J Clin Invest 2004;34:236-42.

55. Riccio E, Sabbatini M, Capuano I, Pisani A. Early Biomarkers of Fabry Nephropathy: A Review of the Literature. Nephron 2019;143:274-281.

56. Najafian B, Mauer M, Hopkin RJ, Svarstad E. Renal complications of Fabry disease in children. Pediatr Nephrol 2013;28:679-87.

57. Schiffmann R, Hughes DA, Linthorst GE et al. Screening, diagnosis, and management of patients with Fabry disease: conclusions from a "Kidney Disease: Improving Global Outcomes" (KDIGO) Controversies Conference. Kidney Int 2017;91:284-293.

58. Fellgiebel A, Muller MJ, Ginsberg L. CNS manifestations of Fabry's disease. Lancet Neurol 2006;5:791-5.

59. Mehta A, Ginsberg L, Investigators FOS. Natural history of the cerebrovascular complications of Fabry disease. Acta Paediatr Suppl 2005;94:24-7; discussion 9-10.

60. Vedder AC, Gerdes VE, Poorthuis BJ et al. Failure to detect Fabry patients in a cohort of prematurely atherosclerotic males. J Inherit Metab Dis 2007;30:988.

61. Feldt-Rasmussen U. Fabry disease and early stroke. Stroke Res Treat 2011;2011:615218.

62. Vijapurapu R, Geberhiwot T, Jovanovic A et al. Study of indications for cardiac device implantation and utilisation in Fabry cardiomyopathy. Heart 2019;105:1825-1831.

63. Zampetti A, Orteu CH, Antuzzi D et al. Angiokeratoma: decision-making aid for the diagnosis of Fabry disease. Br J Dermatol 2012;166:712-20.

64. van der Tol L, Sminia ML, Hollak CE, Biegstraaten M. Cornea verticillata supports a diagnosis of Fabry disease in non-classical phenotypes: results from the Dutch cohort and a systematic review. Br J Ophthalmol 2016;100:3-8.

65. Weingeist TA, Blodi FC. Fabry's disease: ocular findings in a female carrier. A light and electron microscopy study. Arch Ophthalmol 1971;85:169-76.

66. Patel V, O'Mahony C, Hughes D et al. Clinical and genetic predictors of major cardiac events in patients with Anderson-Fabry Disease. Heart 2015;101:961-6.

67. Namdar M, Kampmann C, Steffel J et al. PQ interval in patients with Fabry disease. Am J Cardiol 2010;105:753-6.

68. Eng CM, Fletcher J, Wilcox WR et al. Fabry disease: baseline medical characteristics of a cohort of 1765 males and females in the Fabry Registry. J Inherit Metab Dis 2007;30:184-92.

69. Azevedo O, Cordeiro F, Gago MF et al. Fabry Disease and the Heart: A Comprehensive Review. Int J Mol Sci 2021;22.

70. Powell AW, Jefferies JL, Hopkin RJ, Mays WA, Goa Z, Chin C. Cardiopulmonary fitness assessment on maximal and submaximal exercise testing in patients with Fabry disease. Am J Med Genet A 2018;176:1852-1857.

71. Lobo T, Morgan J, Bjorksten A et al. Cardiovascular testing in Fabry disease: exercise capacity reduction, chronotropic incompetence and improved anaerobic threshold after enzyme replacement. Intern Med J 2008;38:407-14.

72. Bierer G, Balfe D, Wilcox WR, Mosenifar Z. Improvement in serial cardiopulmonary exercise testing following enzyme replacement therapy in Fabry disease. J Inherit Metab Dis 2006;29:572-9.

73. Baig S, Edward NC, Kotecha D et al. Ventricular arrhythmia and sudden cardiac death in Fabry disease: a systematic review of risk factors in clinical practice. Europace 2018;20:f153-f161.

74. Roy A, Umar H, Ochoa-Ferraro A et al. Atherosclerosis in Fabry Disease-A Contemporary Review. J Clin Med 2021;10.

75. Chimenti C, Morgante E, Tanzilli G et al. Angina in fabry disease reflects coronary small vessel disease. Circ Heart Fail 2008;1:161-9.

76. Kampmann C, Linhart A, Baehner F et al. Onset and progression of the Anderson-Fabry disease related cardiomyopathy. Int J Cardiol 2008;130:367-73.

77. Kroman APK. Sex-specific risk assessment of sudden cardiac death. Sex and Cardiac Electrophysiology: Elsevier, 2020.

78. Mihl C, Dassen WR, Kuipers H. Cardiac remodelling: concentric versus eccentric hypertrophy in strength and endurance athletes. Neth Heart J 2008;16:129-33.

79. Hughes RK, Knott KD, Malcolmson J et al. Apical Hypertrophic Cardiomyopathy: The Variant Less Known. J Am Heart Assoc 2020;9:e015294.

80. El Dib R, Gomaa H, Carvalho RP et al. Enzyme replacement therapy for Anderson-Fabry disease. Cochrane Database Syst Rev 2016;7:CD006663.

81. Barbey F, Brakch N, Linhart A et al. Cardiac and vascular hypertrophy in Fabry disease: evidence for a new mechanism independent of blood pressure and glycosphingolipid deposition. Arterioscler Thromb Vasc Biol 2006;26:839-44.

82. Ashrafian H, Redwood C, Blair E, Watkins H. Hypertrophic cardiomyopathy:a paradigm for myocardial energy depletion. Trends Genet 2003;19:263-8.

83. Jung WI, Sieverding L, Breuer J et al. 31P NMR spectroscopy detects metabolic abnormalities in asymptomatic patients with hypertrophic cardiomyopathy. Circulation 1998;97:2536-42.

84. Elleder M, Bradova V, Smid F et al. Cardiocyte storage and hypertrophy as a sole manifestation of Fabry's disease. Report on a case simulating hypertrophic non-obstructive cardiomyopathy. Virchows Arch A Pathol Anat Histopathol 1990;417:449-55.

85. Eng CM, Germain DP, Banikazemi M et al. Fabry disease: guidelines for the evaluation and management of multi-organ system involvement. Genet Med 2006;8:539-48.

86. Linhart A, Lubanda JC, Palecek T et al. Cardiac manifestations in Fabry disease. J Inherit Metab Dis 2001;24 Suppl 2:75-83; discussion 65.

87. Nordin S, Kozor R, Baig S et al. Cardiac Phenotype of Prehypertrophic Fabry Disease. Circ Cardiovasc Imaging 2018;11:e007168.

88. Frustaci A, Morgante E, Russo MA et al. Pathology and function of conduction tissue in Fabry disease cardiomyopathy. Circ Arrhythm Electrophysiol 2015;8:799-805.

89. Linhart A, Kampmann C, Zamorano JL et al. Cardiac manifestations of Anderson-Fabry disease: results from the international Fabry outcome survey. Eur Heart J 2007;28:1228-35.

90. Acharya D, Robertson P, Kay GN et al. Arrhythmias in Fabry cardiomyopathy. Clin Cardiol 2012;35:738-40.

91. Weidemann F, Maier SK, Stork S et al. Usefulness of an Implantable Loop Recorder to Detect Clinically Relevant Arrhythmias in Patients With Advanced Fabry Cardiomyopathy. Am J Cardiol 2016;118:264-74.

92. Patel MR, Cecchi F, Cizmarik M et al. Cardiovascular events in patients with fabry disease natural history data from the fabry registry. J Am Coll Cardiol 2011;57:1093-9.

93. Galli A, Ambrosini F, Lombardi F. Holter Monitoring and Loop Recorders: From Research to Clinical Practice. Arrhythm Electrophysiol Rev 2016;5:136-43.

94. Ding EY, Marcus GM, McManus DD. Emerging Technologies for Identifying Atrial Fibrillation. Circ Res 2020;127:128-142.

95. O'Mahony C, Coats C, Cardona M et al. Incidence and predictors of anti-bradycardia pacing in patients with Anderson-Fabry disease. Europace 2011;13:1781-8.

96. Authors/Task Force m, Elliott PM, Anastasakis A et al. 2014 ESC Guidelines on diagnosis and management of hypertrophic cardiomyopathy: the Task Force for the Diagnosis and Management of Hypertrophic Cardiomyopathy of the European Society of Cardiology (ESC). Eur Heart J 2014;35:2733-79.

97. Seo J, Kim M, Hong GR et al. Fabry disease in patients with hypertrophic cardiomyopathy: a practical approach to diagnosis. J Hum Genet 2016;61:775-80.

98. Brignole M, Auricchio A, Baron-Esquivias G et al. 2013 ESC Guidelines on cardiac pacing and cardiac resynchronization therapy: the Task Force on cardiac pacing and resynchronization therapy of the European Society of Cardiology (ESC). Developed in collaboration with the European Heart Rhythm Association (EHRA). Eur Heart J 2013;34:2281-329.

99. Priori SG, Blomstrom-Lundqvist C, Mazzanti A et al. 2015 ESC Guidelines for the management of patients with ventricular arrhythmias and the prevention of sudden cardiac death: The Task Force for the Management of Patients with Ventricular Arrhythmias and the Prevention of Sudden Cardiac Death of the European Society of Cardiology (ESC). Endorsed by: Association for European Paediatric and Congenital Cardiology (AEPC). Eur Heart J 2015;36:2793-2867.

100. Linhart A, Palecek T, Bultas J et al. New insights in cardiac structural changes in patients with Fabry's disease. Am Heart J 2000;139:1101-8.

101. Weidemann F, Strotmann JM, Niemann M et al. Heart valve involvement in Fabry cardiomyopathy. Ultrasound Med Biol 2009;35:730-5.

102. Desnick RJ, Blieden LC, Sharp HL, Hofschire PJ, Moller JH. Cardiac valvular anomalies in Fabry disease. Clinical, morphologic, and biochemical studies. Circulation 1976;54:818-25.

103. Niemann M, Hartmann T, Namdar M et al. Cross-sectional baseline analysis of electrocardiography in a large cohort of patients with untreated Fabry disease. J Inherit Metab Dis 2013;36:873-9.

104. Choe WC, Passman RS, Brachmann J et al. A Comparison of Atrial Fibrillation Monitoring Strategies After Cryptogenic Stroke (from the Cryptogenic Stroke and Underlying AF Trial). Am J Cardiol 2015;116:889-93.

105. Vijapurapu R, Kozor R, Hughes DA et al. A randomised controlled trial evaluating arrhythmia burden, risk of sudden cardiac death and stroke in patients with Fabry disease: the role of implantable loop recorders (RaILRoAD) compared with current standard practice. Trials 2019;20:314.

106. Liu D, Hu K, Nordbeck P, Ertl G, Stork S, Weidemann F. Longitudinal strain bull's eye plot patterns in patients with cardiomyopathy and concentric left ventricular hypertrophy. Eur J Med Res 2016;21:21.

107. Moon JC, Messroghli DR, Kellman P et al. Myocardial T1 mapping and extracellular volume quantification: a Society for Cardiovascular Magnetic Resonance (SCMR) and CMR Working Group of the European Society of Cardiology consensus statement. J Cardiovasc Magn Reson 2013;15:92.

108. Look DCLDR. Time Saving in Measurement of NMR and EPR Relaxation Times. . Review of Scientific Instruments 1970;41:250-251.

109. Arnold JR, McCann GP. Cardiovascular magnetic resonance: applications and practical considerations for the general cardiologist. Heart 2020;106:174-181.

110. Ripley DP, Musa TA, Dobson LE, Plein S, Greenwood JP. Cardiovascular magnetic resonance imaging: what the general cardiologist should know. Heart 2016;102:1589-603.

111. Moon JC, Sachdev B, Elkington AG et al. Gadolinium enhanced cardiovascular magnetic resonance in Anderson-Fabry disease. Evidence for a disease specific abnormality of the myocardial interstitium. Eur Heart J 2003;24:2151-5.

112. Tower-Rader A, Jaber WA. Multimodality Imaging Assessment of Fabry Disease. Circ Cardiovasc Imaging 2019;12:e009013.

113. Weidemann F, Niemann M, Breunig F et al. Long-term effects of enzyme replacement therapy on fabry cardiomyopathy: evidence for a better outcome with early treatment. Circulation 2009;119:524-9.

114. Varga-Szemes AvdG, R. J; Shoepf, U. J; De Cecco, C. N; Tesche, C; Fuller, S. R; Elgavish, G. A; Suranyi, P. MRI Post-Processing Methods for Myocardial Infarct Quantification. Current Radiology Reports 2016;4:30-38.

115. Scully PR, Bastarrika G, Moon JC, Treibel TA. Myocardial Extracellular Volume Quantification by Cardiovascular Magnetic Resonance and Computed Tomography. Curr Cardiol Rep 2018;20:15.

116. Taylor AJ, Salerno M, Dharmakumar R, Jerosch-Herold M. T1 Mapping: Basic Techniques and Clinical Applications. JACC Cardiovasc Imaging 2016;9:67-81.

117. Haaf P, Garg P, Messroghli DR, Broadbent DA, Greenwood JP, Plein S. Cardiac T1 Mapping and Extracellular Volume (ECV) in clinical practice: a comprehensive review. J Cardiovasc Magn Reson 2016;18:89.

118. Kellman P, Hansen MS. T1-mapping in the heart: accuracy and precision. J Cardiovasc Magn Reson 2014;16:2.

119. Chow K, Flewitt JA, Green JD, Pagano JJ, Friedrich MG, Thompson RB. Saturation recovery single-shot acquisition (SASHA) for myocardial T(1) mapping. Magn Reson Med 2014;71:2082-95.

120. Ridgway JP. Cardiovascular magnetic resonance physics for clinicians: part I. J Cardiovasc Magn Reson 2010;12:71.

121. Pica S, Sado DM, Maestrini V et al. Reproducibility of native myocardial T1 mapping in the assessment of Fabry disease and its role in early detection of cardiac involvement by cardiovascular magnetic resonance. J Cardiovasc Magn Reson 2014;16:99.

122. Sado DM, Flett AS, Banypersad SM et al. Cardiovascular magnetic resonance measurement of myocardial extracellular volume in health and disease. Heart 2012;98:1436-41.

123. Sado DM, White SK, Piechnik SK et al. Identification and assessment of Anderson-Fabry disease by cardiovascular magnetic resonance noncontrast myocardial T1 mapping. Circ Cardiovasc Imaging 2013;6:392-8.

124. Vardarli I, Rischpler C, Herrmann K, Weidemann F. Diagnosis and Screening of Patients with Fabry Disease. Ther Clin Risk Manag 2020;16:551-558.

125. Andrade J, Waters PJ, Singh RS et al. Screening for Fabry disease in patients with chronic kidney disease: limitations of plasma alpha-galactosidase assay as a screening test. Clin J Am Soc Nephrol 2008;3:139-45.

126. Lau K, Uceyler N, Cairns T et al. Gene variants of unknown significance in Fabry disease: Clinical characteristics of c.376A>G (p.Ser126Gly). Mol Genet Genomic Med 2022;10:e1912.

127. Lee K, Jin X, Zhang K et al. A biochemical and pharmacological comparison of enzyme replacement therapies for the glycolipid storage disorder Fabry disease. Glycobiology 2003;13:305-13.

128. Hughes D. Adult Fabry Disease Standard Operating Procedure. National Institute of Clinical Excellence, 2013.

129. Poorthuis BJ, Wevers RA, Kleijer WJ et al. The frequency of lysosomal storage diseases in The Netherlands. Hum Genet 1999;105:151-6.

130. Strotmann J, Breunig F, Wanner C, Weidemann F. Progression of Fabry cardiomyopathy. Clin Ther 2007;29 Suppl A:S13-4.

131. Kampmann C, Perrin A, Beck M. Effectiveness of agalsidase alfa enzyme replacement in Fabry disease: cardiac outcomes after 10 years' treatment. Orphanet J Rare Dis 2015;10:125.

132. Hughes DA, Elliott PM, Shah J et al. Effects of enzyme replacement therapy on the cardiomyopathy of Anderson-Fabry disease: a randomised, double-blind, placebo-controlled clinical trial of agalsidase alfa. Heart 2008;94:153-8.

133. Motwani M, Banypersad S, Woolfson P, Waldek S. Enzyme replacement therapy improves cardiac features and severity of Fabry disease. Mol Genet Metab 2012;107:197-202.

134. Wyatt K, Henley W, Anderson L et al. The effectiveness and cost-effectiveness of enzyme and substrate replacement therapies: a longitudinal cohort study of people with lysosomal storage disorders. Health Technol Assess 2012;16:1-543.

135. Rombach SM, Smid BE, Bouwman MG, Linthorst GE, Dijkgraaf MG, Hollak CE. Long term enzyme replacement therapy for Fabry disease: effectiveness on kidney, heart and brain. Orphanet J Rare Dis 2013;8:47.

136. Armstrong AC, Gidding S, Gjesdal O, Wu C, Bluemke DA, Lima JA. LV mass assessed by echocardiography and CMR, cardiovascular outcomes, and medical practice. JACC Cardiovasc Imaging 2012;5:837-48.

137. Aerts JM, Groener JE, Kuiper S et al. Elevated globotriaosylsphingosine is a hallmark of Fabry disease. Proc Natl Acad Sci U S A 2008;105:2812-7.

138. Sanchez-Nino MD, Carpio D, Sanz AB, Ruiz-Ortega M, Mezzano S, Ortiz A. Lyso-Gb3 activates Notch1 in human podocytes. Hum Mol Genet 2015;24:5720-32.

139. Seydelmann N, Liu D, Kramer J et al. High-Sensitivity Troponin: A Clinical Blood Biomarker for Staging Cardiomyopathy in Fabry Disease. J Am Heart Assoc 2016;5.

140. Guerard N, Oder D, Nordbeck P et al. Lucerastat, an Iminosugar for Substrate Reduction Therapy: Tolerability, Pharmacodynamics, and Pharmacokinetics in Patients With Fabry Disease on Enzyme Replacement. Clin Pharmacol Ther 2018;103:703-711.

141. Brady RO, Schiffmann R. Possible future therapies for Fabry disease. In: Mehta A, Beck M, Sunder-Plassmann G, editors. Fabry Disease: Perspectives from 5 Years of FOS. Oxford, 2006.

142. Khan A, Barber DL, Huang J et al. Lentivirus-mediated gene therapy for Fabry disease. Nat Commun 2021;12:1178.

143. Kramer J, Bijnens B, Stork S et al. Left Ventricular Geometry and Blood Pressure as Predictors of Adverse Progression of Fabry Cardiomyopathy. PLoS One 2015;10:e0140627.

144. Lane DA, Lip GY. Use of the CHA(2)DS(2)-VASc and HAS-BLED scores to aid decision making for thromboprophylaxis in nonvalvular atrial fibrillation. Circulation 2012;126:860-5.

145. Fernandez Adrian PJ. Cardiac Manifestation of Fabry Disease: From Hypertrophic Cardiomyopathy to Early Diagnosis and Treatment in Patients Without Left Ventricular Hypertrophy. J Inborn Err Metab Scr 2016;4:1-9.

146. Kramer J, Nordbeck P, Stork S et al. Electrical Changes in Resting, Exercise, and Holter Electrocardiography in Fabry Cardiomyopathy. JIMD Rep 2015.

147. Rajagopalan N, Dennis DR, O'Connor W. Successful Combined Heart and Kidney Transplantation in Patient With Fabry's Disease: A Case Report. Transplant Proc 2019;51:3171-3173.

148. Auti OB, Bandekar K, Kamat N, Raj V. Cardiac magnetic resonance techniques: Our experience on wide bore 3 tesla magnetic resonance system. Indian J Radiol Imaging 2017;27:404-412.

149. Kramer CM, Barkhausen J, Bucciarelli-Ducci C, Flamm SD, Kim RJ, Nagel E. Standardized cardiovascular magnetic resonance imaging (CMR) protocols: 2020 update. J Cardiovasc Magn Reson 2020;22:17.

150. Schulz-Menger J, Bluemke DA, Bremerich J et al. Standardized image interpretation and post processing in cardiovascular magnetic resonance: Society for Cardiovascular

Magnetic Resonance (SCMR) board of trustees task force on standardized post processing. J Cardiovasc Magn Reson 2013;15:35.

151. Gardner BI, Bingham SE, Allen MR, Blatter DD, Anderson JL. Cardiac magnetic resonance versus transthoracic echocardiography for the assessment of cardiac volumes and regional function after myocardial infarction: an intrasubject comparison using simultaneous intrasubject recordings. Cardiovasc Ultrasound 2009;7:38.

152. Kozor R, Callaghan F, Tchan M, Hamilton-Craig C, Figtree GA, Grieve SM. A disproportionate contribution of papillary muscles and trabeculations to total left ventricular mass makes choice of cardiovascular magnetic resonance analysis technique critical in Fabry disease. J Cardiovasc Magn Reson 2015;17:22.

153. Militaru S, Ginghina C, Popescu BA, Saftoiu A, Linhart A, Jurcut R. Multimodality imaging in Fabry cardiomyopathy: from early diagnosis to therapeutic targets. Eur Heart J Cardiovasc Imaging 2018;19:1313-1322.

154. Cerqueira MD, Weissman NJ, Dilsizian V et al. Standardized myocardial segmentation and nomenclature for tomographic imaging of the heart. A statement for healthcare professionals from the Cardiac Imaging Committee of the Council on Clinical Cardiology of the American Heart Association. Circulation 2002;105:539-42.

155. Oktay AAA, H. K; Paul, T. K; O'Keefe, J. H; Ventura, H. O; Koch, C. A; Lavie, C. J. . Diabetes, Cardiomyopathy, and Heart Failure. Endotext, 2020:1-33.

156. Vijapurapu RH, F; Liu, B; Edwards, N; Steeds, R. . A study of the different methodologies used in calculation of extra-cellular volume by CMR imaging. . Heart 2018;104:A14-AA5.

157. Peguero JG, Lo Presti S, Perez J, Issa O, Brenes JC, Tolentino A. Electrocardiographic Criteria for the Diagnosis of Left Ventricular Hypertrophy. J Am Coll Cardiol 2017;69:1694-1703.

158. Khan GM. A new electrode placement method for obtaining 12-lead ECGs. Open Heart 2015;2:e000226.

159. Lidove O, Barbey F, Niu DM et al. Fabry in the older patient: Clinical consequences and possibilities for treatment. Mol Genet Metab 2016;118:319-25.

160. Hughes DA, Barba Romero MA, Hollak CE, Giugliani R, Deegan PB. Response of women with Fabry disease to enzyme replacement therapy: comparison with men, using data from FOS--the Fabry Outcome Survey. Mol Genet Metab 2011;103:207-14.

161. Liu HC, Lin HY, Yang CF et al. Globotriaosylsphingosine (lyso-Gb3) might not be a reliable marker for monitoring the long-term therapeutic outcomes of enzyme replacement therapy for late-onset Fabry patients with the Chinese hotspot mutation (IVS4+919G>A). Orphanet J Rare Dis 2014;9:111.

162. Tsuboi K, Yamamoto H. Clinical course of patients with Fabry disease who were switched from agalsidase-beta to agalsidase-alpha. Genet Med 2014;16:766-72.

163. Beck M, Hughes D, Kampmann C et al. Long-term effectiveness of agalsidase alfa enzyme replacement in Fabry disease: A Fabry Outcome Survey analysis. Mol Genet Metab Rep 2015;3:21-7.

164. Myerson SG, Montgomery HE, World MJ, Pennell DJ. Left ventricular mass: reliability of M-mode and 2-dimensional echocardiographic formulas. Hypertension 2002;40:673-8.

165. Devereux RB, Alonso DR, Lutas EM et al. Echocardiographic assessment of left ventricular hypertrophy: comparison to necropsy findings. Am J Cardiol 1986;57:450-8.

166. Reichek N, Helak J, Plappert T, Sutton MS, Weber KT. Anatomic validation of left ventricular mass estimates from clinical two-dimensional echocardiography: initial results. Circulation 1983;67:348-52.

167. Foppa M, Duncan BB, Rohde LE. Echocardiography-based left ventricular mass estimation. How should we define hypertrophy? Cardiovasc Ultrasound 2005;3:17.

168. Captur G, Manisty CH, Raman B et al. Maximal Wall Thickness Measurement in Hypertrophic Cardiomyopathy: Biomarker Variability and its Impact on Clinical Care. JACC Cardiovasc Imaging 2021;14:2123-2134.

169. Niemann M, Liu D, Hu K et al. Prominent papillary muscles in Fabry disease: a diagnostic marker? Ultrasound Med Biol 2011;37:37-43.

170. Captur G, Gatehouse P, Keenan KE et al. A medical device-grade T1 and ECV phantom for global T1 mapping quality assurance-the T1 Mapping and ECV Standardization in cardiovascular magnetic resonance (T1MES) program. J Cardiovasc Magn Reson 2016;18:58.

171. Weidemann F, Breunig F, Beer M et al. The variation of morphological and functional cardiac manifestation in Fabry disease: potential implications for the time course of the disease. Eur Heart J 2005;26:1221-7.

172. Weidemann F, Breunig F, Beer M et al. Improvement of cardiac function during enzyme replacement therapy in patients with Fabry disease: a prospective strain rate imaging study. Circulation 2003;108:1299-301.

173. Niemann M, Herrmann S, Hu K et al. Differences in Fabry cardiomyopathy between female and male patients: consequences for diagnostic assessment. JACC Cardiovasc Imaging 2011;4:592-601.

174. Vijapurapu R, Nordin S, Baig S et al. Global longitudinal strain, myocardial storage and hypertrophy in Fabry disease. Heart 2018.

175. Moody WE, Edwards NC, Chue CD et al. Variability in cardiac MR measurement of left ventricular ejection fraction, volumes and mass in healthy adults: defining a significant change at 1 year. Br J Radiol 2015;88:20140831.

176. Karamitsos TD, Hudsmith LE, Selvanayagam JB, Neubauer S, Francis JM. Operator induced variability in left ventricular measurements with cardiovascular magnetic resonance is improved after training. J Cardiovasc Magn Reson 2007;9:777-83.

177. Augusto JB, Davies RH, Bhuva AN et al. Diagnosis and risk stratification in hypertrophic cardiomyopathy using machine learning wall thickness measurement: a comparison with human test-retest performance. Lancet Digit Health 2021;3:e20-e28.

178. Germain DP, Charrow J, Desnick RJ et al. Ten-year outcome of enzyme replacement therapy with agalsidase beta in patients with Fabry disease. J Med Genet 2015;52:353-8.

179. Shah AM, Solomon SD. Myocardial deformation imaging: current status and future directions. Circulation 2012;125:e244-8.

180. Yeung DF, Sirrs S, Tsang MYC et al. Echocardiographic Assessment of Patients with Fabry Disease. J Am Soc Echocardiogr 2018;31:639-649 e2.

181. Amundsen BH, Helle-Valle T, Edvardsen T et al. Noninvasive myocardial strain measurement by speckle tracking echocardiography: validation against sonomicrometry and tagged magnetic resonance imaging. J Am Coll Cardiol 2006;47:789-93.

182. Narayanan A, Aurigemma GP, Chinali M, Hill JC, Meyer TE, Tighe DA. Cardiac mechanics in mild hypertensive heart disease: a speckle-strain imaging study. Circ Cardiovasc Imaging 2009;2:382-90.

183. Nasir K, Rosen BD, Kramer HJ et al. Regional left ventricular function in individuals with mild to moderate renal insufficiency: the Multi-Ethnic Study of Atherosclerosis. Am Heart J 2007;153:545-51.

184. Tops LF, Den Uijl DW, Delgado V et al. Long-term improvement in left ventricular strain after successful catheter ablation for atrial fibrillation in patients with preserved left ventricular systolic function. Circ Arrhythm Electrophysiol 2009;2:249-57.

185. Shanks M, Thompson RB, Paterson ID et al. Systolic and diastolic function assessment in fabry disease patients using speckle-tracking imaging and comparison with conventional echocardiographic measurements. J Am Soc Echocardiogr 2013;26:1407-14.

186. Costanzo L, Buccheri S, Capranzano P et al. Early cardiovascular remodelling in Fabry disease. J Inherit Metab Dis 2014;37:109-16.

187. Morris DA, Blaschke D, Canaan-Kuhl S et al. Global cardiac alterations detected by speckle-tracking echocardiography in Fabry disease: left ventricular, right ventricular, and left atrial dysfunction are common and linked to worse symptomatic status. Int J Cardiovasc Imaging 2015;31:301-13.

188. Obokata M, Nagata Y, Wu VC et al. Direct comparison of cardiac magnetic resonance feature tracking and 2D/3D echocardiography speckle tracking for evaluation of global left ventricular strain. Eur Heart J Cardiovasc Imaging 2016;17:525-32.

189. Erley J, Genovese D, Tapaskar N et al. Echocardiography and cardiovascular magnetic resonance based evaluation of myocardial strain and relationship with late gadolinium enhancement. J Cardiovasc Magn Reson 2019;21:46.

190. Zhao L, Zhang C, Tian J et al. Quantification of myocardial deformation in patients with Fabry disease by cardiovascular magnetic resonance feature tracking imaging. Cardiovasc Diagn Ther 2021;11:91-101.

191. Rosmini S, Bulluck H, Captur G et al. Myocardial native T1 and extracellular volume with healthy ageing and gender. Eur Heart J Cardiovasc Imaging 2018;19:615-621.

192. Bistoquet A, Oshinski J, Skrinjar O. Myocardial deformation recovery from cine MRI using a nearly incompressible biventricular model. Med Image Anal 2008;12:69-85.

193. Bistoquet A, Oshinski J, Skrinjar O. Left ventricular deformation recovery from cine MRI using an incompressible model. IEEE Trans Med Imaging 2007;26:1136-53.

194. Feher J. The Cardiac Action Potential. Quantitative Human Physiology: Elsevier, 2012.

195. Ellenbogen KAK, K. Cardiac Pacing and iCDs: WILEY Blackwell, 2014.

196. George AL, Jr. Molecular and genetic basis of sudden cardiac death. J Clin Invest 2013;123:75-83.

197. Grant AO. Cardiac ion channels. Circ Arrhythm Electrophysiol 2009;2:185-94.

198. Ganesan PS, M; Ladavich, S; Ghoraani, B. . Computer-Aided Clinical Decision Support Systems for Atrial Fibrillation. Computer-aided Technologies - Applications in Engineering and Medicine. United States of America: Intech, 2016:91-119.

199. Barold SS. Willem Einthoven and the birth of clinical electrocardiography a hundred years ago. Card Electrophysiol Rev 2003;7:99-104.

200. Meek S, Morris F. ABC of clinical electrocardiography.Introduction. I-Leads, rate, rhythm, and cardiac axis. BMJ 2002;324:415-8.

201. Abi-Saleh B, Omar B. Einthoven's triangle transparency: a practical method to explain limb lead configuration following single lead misplacements. Rev Cardiovasc Med 2010;11:33-8.

202. Koelsch S, Enge J, Jentschke S. Cardiac signatures of personality. PLoS One 2012;7:e31441.

203. Schlegel TT, Kulecz WB, Feiveson AH et al. Accuracy of advanced versus strictly conventional 12-lead ECG for detection and screening of coronary artery disease, left ventricular hypertrophy and left ventricular systolic dysfunction. BMC Cardiovasc Disord 2010;10:28.

204. Voulgari C, Pagoni S, Tesfaye S, Tentolouris N. The spatial QRS-T angle: implications in clinical practice. Curr Cardiol Rev 2013;9:197-210.

205. Gleeson S, Liao YW, Dugo C et al. ECG-derived spatial QRS-T angle is associated with ICD implantation, mortality and heart failure admissions in patients with LV systolic dysfunction. PLoS One 2017;12:e0171069.

206. Vondrak JP, M; Jurek F. . Selected transformation methods snfd their comparison for VCG leads deriving. Alexandria Engineering Journal 2022;61:3475-3485.

207. Chou TC. When is the vectorcardiogram superior to the scalar electrocardiogram? J Am Coll Cardiol 1986;8:791-9.

208. Frank E, Seiden GE. Comparison of limb and precordial vectorcardiographic systems. Circulation 1956;14:83-9.

209. Ghista DN, Acharya UR, Nagenthiran T. Frontal plane vectorcardiograms: theory and graphics visualization of cardiac health status. J Med Syst 2010;34:445-58.

210. Cortez DL, Schlegel TT. When deriving the spatial QRS-T angle from the 12-lead electrocardiogram, which transform is more Frank: regression or inverse Dower? J Electrocardiol 2010;43:302-9.

211. Dower GE, Machado HB, Osborne JA. On deriving the electrocardiogram from vectoradiographic leads. Clin Cardiol 1980;3:87-95.

212. Jaros R, Martinek R, Danys L. Comparison of Different Electrocardiography with Vectorcardiography Transformations. Sensors (Basel) 2019;19.

213. Oehler A, Feldman T, Henrikson CA, Tereshchenko LG. QRS-T angle: a review. Ann Noninvasive Electrocardiol 2014;19:534-42.

214. Yamazaki T, Froelicher VF, Myers J, Chun S, Wang P. Spatial QRS-T angle predicts cardiac death in a clinical population. Heart Rhythm 2005;2:73-8.

215. Kors JA, Kardys I, van der Meer IM et al. Spatial QRS-T angle as a risk indicator of cardiac death in an elderly population. J Electrocardiol 2003;36 Suppl:113-4.

216. Wei JJ, Chang CJ, Chou NK, Jan GJ. ECG data compression using truncated singular value decomposition. IEEE Trans Inf Technol Biomed 2001;5:290-9.

217. Priori SG, Mortara DW, Napolitano C et al. Evaluation of the spatial aspects of T-wave complexity in the long-QT syndrome. Circulation 1997;96:3006-12.

218. Okin PM, Devereux RB, Fabsitz RR, Lee ET, Galloway JM, Howard BV. Principal component analysis of the T wave and prediction of cardiovascular mortality in American Indians: the Strong Heart Study. Circulation 2002;105:714-9.

219. Rautaharju PM, Kooperberg C, Larson JC, LaCroix A. Electrocardiographic abnormalities that predict coronary heart disease events and mortality in postmenopausal women: the Women's Health Initiative. Circulation 2006;113:473-80.

220. Maanja M, Wieslander B, Schlegel TT et al. Diffuse Myocardial Fibrosis Reduces Electrocardiographic Voltage Measures of Left Ventricular Hypertrophy Independent of Left Ventricular Mass. J Am Heart Assoc 2017;6.

221. Maanja M, Schlegel TT, Kozor R et al. The electrical determinants of increased wall thickness and mass in left ventricular hypertrophy. J Electrocardiol 2020;58:80-86.

222. Ball RL, Feiveson AH, Schlegel TT, Starc V, Dabney AR. Predicting "heart age" using electrocardiography. J Pers Med 2014;4:65-78.

223. Ladejobi AOM-I, J. R; Shelly Cohen, M; Attia, Z. I; Scott, C; G; LeBrasseur, N. K; Gersh, B. J; Noseworthy, P. A; Friedman, P. A; Kapa, S; Lopez-Jimenez, F. . The 12-lead electrocardiogram as a biomarker of biological age. . European Heart Journal - Digital Health 2021;2:379-389.

224. Lindow TP-L, I; Schlegel, T; Ugander, M. . Heart age estimated using explained advanced electrocardiography. . MedRxiv 2022.

225. Lundin MH, E.; Nordlund, D.; Gyllenhammar, T.; Steding Ehrenborg, K.; Engblom, H.; Carlsson, M.; Atar, D.; vanderPals, J.; Erlinge, D. Left ventricular global wall thickness is easily calculated, detects and characterizes hypertrophy, and has prognostic utility. 20th Cardiovascular Spring Meeting. Gothenburg, Sweden, 2019.

226. Bacharova L, Estes HE, Schocken DD et al. The 4th Report of the Working Group on ECG diagnosis of Left Ventricular Hypertrophy. J Electrocardiol 2017;50:11-15.

227. Kardys I, Kors JA, van der Meer IM, Hofman A, van der Kuip DA, Witteman JC. Spatial QRS-T angle predicts cardiac death in a general population. Eur Heart J 2003;24:1357-64.

228. Potter SL, Holmqvist F, Platonov PG et al. Detection of hypertrophic cardiomyopathy is improved when using advanced rather than strictly conventional 12-lead electrocardiogram. J Electrocardiol 2010;43:713-8.

229. Lindow T, Palencia-Lamela I, Schlegel TT, Ugander M. Heart age estimated using explainable advanced electrocardiography. Sci Rep 2022;12:9840.

230. Augusto JB, Johner N, Shah D et al. The myocardial phenotype of Fabry disease pre-hypertrophy and pre-detectable storage. Eur Heart J Cardiovasc Imaging 2021;22:790-799.

231. Christopoulos G, Graff-Radford J, Lopez CL et al. Artificial Intelligence-Electrocardiography to Predict Incident Atrial Fibrillation: A Population-Based Study. Circ Arrhythm Electrophysiol 2020;13:e009355.

232. Attia ZI, Noseworthy PA, Lopez-Jimenez F et al. An artificial intelligence-enabled ECG algorithm for the identification of patients with atrial fibrillation during sinus rhythm: a retrospective analysis of outcome prediction. Lancet 2019;394:861-867.

233. Sanz-Garcia A, Cecconi A, Vera A et al. Electrocardiographic biomarkers to predict atrial fibrillation in sinus rhythm electrocardiograms. Heart 2021;107:1813-1819.

234. Sweda R, Sabti Z, Strebel I et al. Diagnostic and prognostic values of the QRS-T angle in patients with suspected acute decompensated heart failure. ESC Heart Fail 2020;7:1817-1829.

235. Yogasundaram H, Nikhanj A, Putko BN et al. Elevated Inflammatory Plasma Biomarkers in Patients With Fabry Disease: A Critical Link to Heart Failure With Preserved Ejection Fraction. J Am Heart Assoc 2018;7:e009098.

236. Glikson M, Nielsen JC, Kronborg MB et al. 2021 ESC Guidelines on cardiac pacing and cardiac resynchronization therapy. Eur Heart J 2021;42:3427-3520.

237. Saini A, Ellenbogen KA, Tan A, Kaszala K, Huizar JF. "Train tracks" and "step ladders" on implantable cardioverter defibrillator interval plot in a patient with dual tachycardia: Putting the dots together. Pacing Clin Electrophysiol 2017;40:1298-1301.

238. Fields AVM, N. N; Simson, M. B; Lin, D. . Recurrent Ventricular Tachycardia Associated with Vasospastic Angina Effectively Managed with Implantable Cardioverter Defibrillator. Journal of Cardiology and Clinical Research 2015;3:1043.

239. Waldek S, Patel MR, Banikazemi M, Lemay R, Lee P. Life expectancy and cause of death in males and females with Fabry disease: findings from the Fabry Registry. Genet Med 2009;11:790-6.

240. Wilson HC, Hopkin RJ, Madueme PC et al. Arrhythmia and Clinical Cardiac Findings in Children With Anderson-Fabry Disease. Am J Cardiol 2017;120:251-255.

241. Kramer J, Niemann M, Stork S et al. Relation of burden of myocardial fibrosis to malignant ventricular arrhythmias and outcomes in Fabry disease. Am J Cardiol 2014;114:895-900.

242. Shah JS, Hughes DA, Sachdev B et al. Prevalence and clinical significance of cardiac arrhythmia in Anderson-Fabry disease. Am J Cardiol 2005;96:842-6.

243. Pichette M, Serri K, Page M, Di LZ, Bichet DG, Poulin F. Impaired Left Atrial Function in Fabry Disease: A Longitudinal Speckle-Tracking Echocardiography Study. J Am Soc Echocardiogr 2017;30:170-179 e2.

244. Sene T, Lidove O, Sebbah J et al. Cardiac device implantation in Fabry disease: A retrospective monocentric study. Medicine (Baltimore) 2016;95:e4996.

245. Di LZ, Pichette M, Nadeau R, Bichet DG, Poulin F. Severe bradyarrhythmia linked to left atrial dysfunction in Fabry disease-A cross-sectional study. Clin Cardiol 2018;41:1207-1213.

246. Mishra V, Banerjee A, Gandhi AB et al. Stroke and Fabry Disease: A Review of Literature. Cureus 2020;12:e12083.

247. Kirchhof P, Benussi S, Kotecha D et al. 2016 ESC Guidelines for the management of atrial fibrillation developed in collaboration with EACTS. Eur Heart J 2016;37:2893-2962.

248. Sharif ZI, Lubitz SA. Ventricular arrhythmia management in patients with genetic cardiomyopathies. Heart Rhythm O2 2021;2:819-831.

249. Maron BJ, Gardin JM, Flack JM, Gidding SS, Kurosaki TT, Bild DE. Prevalence of hypertrophic cardiomyopathy in a general population of young adults. Echocardiographic analysis of 4111 subjects in the CARDIA Study. Coronary Artery Risk Development in (Young) Adults. Circulation 1995;92:785-9.

250. Ommen SR, Mital S, Burke MA et al. 2020 AHA/ACC Guideline for the Diagnosis and Treatment of Patients With Hypertrophic Cardiomyopathy: Executive Summary: A Report of the American College of Cardiology/American Heart Association Joint Committee on Clinical Practice Guidelines. Circulation 2020;142:e533-e557.

251. Vijapurapu R, Bradlow W, Leyva F et al. Cardiac device implantation and device usage in Fabry and hypertrophic cardiomyopathy. Orphanet J Rare Dis 2022;17:6.

252. Kober L, Thune JJ, Nielsen JC et al. Defibrillator Implantation in Patients with Nonischemic Systolic Heart Failure. N Engl J Med 2016;375:1221-30.

253. Gruner C, Verocai F, Carasso S et al. Systolic myocardial mechanics in patients with Anderson-Fabry disease with and without left ventricular hypertrophy and in comparison to nonobstructive hypertrophic cardiomyopathy. Echocardiography 2012;29:810-7.

254. Havranek S, Linhart A, Urbanova Z, Ramaswami U. Early cardiac changes in children with anderson-fabry disease. JIMD Rep 2013;11:53-64.

255. Liu D, Hu K, Schmidt M et al. Value of the CHA2DS2-VASc score and Fabry-specific score for predicting new-onset or recurrent stroke/TIA in Fabry disease patients without atrial fibrillation. Clin Res Cardiol 2018;107:1111-1121.

256. Benjamin ER, Flanagan JJ, Schilling A et al. The pharmacological chaperone 1-deoxygalactonojirimycin increases alpha-galactosidase A levels in Fabry patient cell lines. J Inherit Metab Dis 2009;32:424-40.

257. Hughes DA, Nicholls K, Shankar SP et al. Oral pharmacological chaperone migalastat compared with enzyme replacement therapy in Fabry disease: 18-month results from the randomised phase III ATTRACT study. J Med Genet 2017;54:288-296.

258. Germain DP, Hughes DA, Nicholls K et al. Treatment of Fabry's Disease with the Pharmacologic Chaperone Migalastat. N Engl J Med 2016;375:545-55.